THESIS

INFERRING EARLY STONE AGE TOOL TECHNOLOGY AND RAW MATERIAL FROM CUT MARK MICROMORPHOLOGY USING HIGH-RESOLUTION 3-D SCANNING WITH APPLICATIONS TO MIDDLE BED II, OLDUVAI GORGE, TANZANIA

Submitted by

Trevor L. Keevil

Department of Anthropology

In partial fulfillment of the requirements

For the Degree of Master of Arts

Colorado State University

Fort Collins, Colorado

Spring 2018

Master's Committee:

Advisor: Michael C. Pante

Mica Glantz
Michael Lacy

ABSTRACT

INFERRING EARLY STONE AGE TOOL TECHNOLOGY AND RAW MATERIAL FROM CUT MARK MICROMORPHOLOGY USING HIGH-RESOLUTION 3-D SCANNING WITH APPLICATIONS TO MIDDLE BED II, OLDUVAI GORGE, TANZANIA

The appearance of cut marked bones in the archaeological record 2.6 million years ago roughly coincides with the emergence of simple Oldowan core and flake tools in the East African archaeological record. This development is associated with the dietary shift in Early Stone Age hominins to carnivory and numerous morphological changes in the genus *Homo,* including larger brain sizes. Approximately 1.7 million years ago, *Homo erectus*, a new species of hominin, emerges alongside a technological transition in the East African archaeological record from the simple core and flake technology of the Oldowan to the more advanced bifacially flaked large cutting tools of the Acheulean tradition. However, the function of these Acheulean handaxes remains uncertain. To fully appreciate the relationship between evolutionary changes in the hominin lineage and the development of different stone tool traditions, experimental models capable of identifying how different tool forms were used by early hominins when butchering large mammal carcasses must be established.

Previous macromorphological studies of bone surface modifications have shown that cut marks on bones can be accurately differentiated from tooth, trample, and rodent gnaw marks. However, studies relating cut mark micromorphology to the specific technological form or raw material type of the tool that made the mark have been limited due to poorly defined analytical methodologies that use subjective and qualitative observations to describe mark morphology.

The lack of a standardized approach for diagnosing tool technology from cut mark morphology has limited the development of models capable of effectively interpreting the dynamic butchery and lithic behaviors of Early Stone Age hominins during the Oldowan-Acheulean transition.

This thesis presents an objective and replicable approach for quantitatively modeling micromorphological characteristics of experimentally created cut marks to examine whether different stone tool types leave unique and quantifiable patterns in the cut marks they create. Experimental cut marks were created using Oldowan flake tools and Acheulean biface tools. Both tool types were made from four different raw material types commonly found in Early Stone Age archaeological assemblages from Olduvai Gorge, Tanzania: quartzite, basalt, chert, and phonolite. Experimental marks were scanned using a Nanovea white-light confocal profilometer and analyzed using Digital Surf's Mountains Software to generate multivariate discriminant models capable of categorizing cut marks based on the form of the tool that created them. These models were used to classify the tool forms that created 1.6 million year old archaeological trace marks recovered from a site in Middle Bed II, Olduvai Gorge, Tanzania.

The results from this thesis indicate that when the morphological features of a cut mark are analyzed and modeled using high-resolution 3-D scanning, the Early Stone Age tool technology and raw material type that made the mark can be accurately identified. Identifying the causal connections between cut mark morphology and properties of the stone tool that created the mark has important applications for further understanding the evolutionary trends in morphology, behavior and cognition of Early Stone Age hominins.

ACKNOWLEDGEMENTS

I would like to thank my advisor, Dr. Michael Pante, for providing me with guidance throughout this degree and offering me multiple opportunities to study in Olduvai Gorge. I would also like to thank my committee members, Dr. Mica Glantz and Dr. Michael Lacy, for their support on this thesis. The encouragement and direction of Dr. Ann Magennis was also influential to the completion of this thesis. I would like to acknowledge the Colorado State University Anthropology Department for funding my studies and conference travel throughout the entirety of my degree.

I am grateful to Dr. Jason LaBelle and Kristen Welch, who provided me with the initial lithic tools used to complete a pre-thesis exploratory project. I would like to thank Dr. Jay Reti, who graciously manufactured and provided me with all the lithic tools used in this thesis. I would also like to thank Dr. Ignacio de la Torre for providing me with the opportunity to work in and use fossil materials from Olduvai Gorge. I must also thank Olekipa, who bravely saved me from an "ant" while working in Olduvai.

This thesis would not have been possible without the support of my family and friends. My parents, Heather and Norman, have always provided endless support and encouragement in all my pursuits. I have to thank my brother Rory, who was always on call for any technical support questions regarding the engineering portion of this project. My good friend Leddy offered both the moral and statistical help necessary to complete this thesis. And finally, I would like to thank my friends/editors/late-night lab mates, Emily Orlikoff and Matthew Muttart, who provided necessary academic and emotional support throughout the entirety of this degree.

TABLE OF CONTENTS

LIST OF TABLES

LIST OF FIGURES

CHAPTER 1 INTRODUCTION

1.1) Research Problem

The appearance and persistence of cut marked fossils throughout Early Stone Age faunal assemblages supports the hypothesis that early members of the genus *Homo* were capable of foraging and processing large mammal carcasses. These Early Stone Age faunal assemblages are often preserved in direct association with Oldowan stone tools, further supporting the characterization of early *Homo* as a butcher (Berthelet and Chavaillon, 2001; Bishop et al., 2006; Bunn, 1981). Experimental research has recognized that the sharp cutting edge characteristic of Oldowan flake tools is effective for butchering and processing large animal carcasses (Key and Lycett, 2011; McCall, 2005; Toth, 1985). However, over time this successful flake-based tool tradition is slowly supplemented with complex bifacially flaked tools, leading to the advent of the Acheulean tool tradition (Beyene et al., 2013; de la Torre et al., 2008). This technological shift from the Oldowan to the Acheulean is characterized by a long transitional period, represented by archaeological assemblages containing both flake and biface stone tool technologies (de la Torre and Mora, 2014).

The slow emergence and limited extent of Acheulean bifaces during the transitional Oldowan-Acheulean period has led to the question of whether these two stone tool traditions were used for similar functions. It has been proposed that the earliest Acheulean biface technologies were not primarily used for the same butchery purpose as Oldowan flakes, instead serving other functional or symbolic purposes (Domínguez-Rodrigo et al., 2001; Gamble, 1998; Kohn and Mithen, 1999; Pope et al., 2015). These hypotheses are supported by a lack of cut marked bones in direct archaeological association with numerous early Acheulean archaeological sites (Beyene et al., 2013; Lepre et al., 2011). As well, there is experimental phytolith evidence that indicates that at least some Acheulean handaxes may have been used to process plant and wood materials (Domínguez-Rodrigo et al., 2001; Keeley and Toth, 1981; Schick and Toth, 1993). However, the impact of the technological transition to the Acheulean culture on hominin evolution cannot be fully understood without specific knowledge of how Acheulean tools were used. This research seeks to establish criteria for recognizing traces of butchery produced with Acheulean technology on fossil bones.

Past research has shown that broad morphological analyses of different bone surface modifications, such as cut marks, tooth marks, and percussion marks, can effectively identify and differentiate the presence of past actors in the archaeological record (Blumenschine, 1995; Fisher, 1995; Njau and Blumenschine, 2006; Olsen and Shipman, 1988; Potts and Shipman, 1981; Shipman and Rose, 1983). Previous research using hominin induced bone surface modifications are often based on qualitative descriptions and patterns of fossilized cut marks to interpret Early Stone Age hominin butchery behaviors, such as scavenging and hunting (Blumenschine, 1995; Bunn and Kroll, 1986; Capaldo, 1998; Domínguez-Rodrigo and Barba, 2006; Domínguez-Rodrigo et al., 2014; Merritt, 2015; Pante et al., 2012; 2015; Shipman, 1986). These behavioral interpretations are primarily based on the presence, location, and frequency of cut marks and other bone surface modifications created by different actors in a fossil assemblage. However, these studies are unable to incorporate information regarding specific characteristics of the effector (e.g. stone tool/tooth) or actor (e.g. hominin/carnivore) that made each mark. This limitation inhibits a complete characterization of Early Stone Age hominin butchery and tool behaviors, particularly during the Oldowan-Acheulean transition when tools that characterize both of these stone tool industries are found with archaeological sites.

Recently, high-resolution bone surface modification modelling techniques using micro-photogrammetry and confocal scanning have been employed in an effort to surpass broad descriptions of archaeological actors (e.g. hominin, carnivore, rodent) and instead recognize specific characteristics of these actors (Aramendi et al., 2017; Arriaza et al., 2017; Bello and Soligo, 2008; Bello et al., 2009; Boschin and Crezzini, 2012; de Juana et al., 2010; Maté-Gonzalez et al, 2015; 2016; 2017; Pante et al., 2017; Yravedra et al., 2017b). Some bone surface modification research is currently focused on identifying the relationship between cut mark micromorphology and features of the stone tool that made the mark, such as technological form or raw material type (Bello et al., 2009; Maté-Gonzalez et al, 2015; 2016; 2017; Yravedra et al., 2017b). However, a lack of control over experimental variables, such as force and angle of tool impact, and low-resolution analytical methodologies limit the interpretations and validity of these studies.

Studies using high-resolution 3-D laser scanning have recently highlighted the effectiveness of using this methodology to reproduce and quantitatively analyze the micromorphological characteristics of cut marks (Pante et al., 2017). This thesis employs this new methodological approach to measure and characterize the micromorphological features of cut marks created by Early Stone Age tools that differ in technological form and raw material type and has three main objectives:

1. To create a comprehensive cut mark measurement database that identifies and models the micromorphological features representative of cut marks made by Early Stone Age tools of varying technological form.

2. To create a comprehensive cut mark measurement database that identifies and models the micromorphological features representative of cut marks made by Early Stone Age tools of varying raw material type.
3. To use the results from an experimentally created cut mark databases to classify archaeological cut marks recovered from a Middle Bed II, Olduvai Gorge site to a specific Early Stone Age tool technology and raw material type category.

1.2) Establishing a Taphonomic Theoretical Framework

The goal of this thesis is to identify replicable and theoretically grounded causal connections between cut mark micromorphology and the structural characteristics of a stone tool in an effort to better understand hominin butchery behaviors in the archaeological record. Therefore, the research conducted in this thesis primarily employs a middle-range theoretical approach, which calls for empirical and observable experimentation in the present to identify dynamic behaviors in the past (Binford, 1981; Raab and Goodyear 1984). This approach is achieved through actualistic experimentation, which establishes direct cause and effect relationships between a dynamic behavior and its resulting observable and preservable trace (Gifford-Gonzalez, 1991). Only when the observable result of a specific behavior is understood in the contemporary, can that same observable trace be understood when it is recovered in the archaeological record. This study seeks to integrate these perspectives by modeling the observable and measurable micromorphological features of cut marks experimentally created by known stone tool behaviors in the present to understand hominin tool use behaviors in the past.

The theoretical approach of this thesis is grounded in the theoretical principals of uniformitarianism, a principle that originated through geological interpretations of natural processes (Hutton, 1795). The theoretical principles of Uniformitarianism state that geologic and natural laws behave and remain constant throughout time and space, allowing natural and observable processes in the present to be considered analogous to similar processes in the past (Gould, 1965). This theory can be expanded to paleoanthropology through the actualistic method, which suggests that the dynamic and unobservable actions of past archaeological agents can be understood effectively only through analogous and causal relationships of experimentally tested observations in the present (Binford, 1981; Gifford, 1981). The uniformitarian aspect of this thesis relies upon the assumption that experimentally created cut marks are justifiably similar to cut marks created by early hominins during butchery events in the archaeological record.

A fundamental analytical objective in taphonomic research is to understand the relationship between static trace marks recovered from the fossil record and the unobservable and dynamic behavior that created them. As such, Gifford-Gonzalez (1991) developed a theoretical paradigm using a nested system of relational analogies to link six taphonomic contextual categories together. This method emphasizes the use of empirical and experimentally tested causal relationships to successionally connect a static trace first to its causal agent, then effector, actor and finally to its broader behavioral and ecological contexts (Gifford-Gonzalez, 1991). Under this model, specific behaviors associated with a trace mark can only be fully understood when the causal agent, effector and actor that made the mark are also understood. This relational approach provides a logical theoretical chain to connect an observable mark to its broader and unobservable behaviors and limits the probability that the behavioral inference of a trace mark is based on unfounded and flawed assumptions. This thesis defines a methodology capable of establishing a causal connection between a static trace mark and its effector, which is the tool technology and raw material that created the cut mark. When an empirical and replicable relationship between a cut mark and its tool effector is understood, broader inferences higher up Gifford-Gonzalez (1991) nested hierarchy of hominin behavior and ecological contexts can be related to the mark.

Recognizing the causal connection between the action of an archaeological agent and its resulting trace establishes a foundation for identifying and isolating the dynamic behaviors of agents in the archaeological record. However, these hominin behavioral and environmental interaction reconstructions are often restricted due to equifinalities and a lack of fundamental biological and behavioral laws that lead to morphologically typical trace marks (Gifford-Gonzalez, 1991). Bone surface modification equifinalities occur when the morphological characteristics of a fossilized trace mark can realistically be attributed to multiple different actors in the archaeological record (Gifford-Gonzalez, 1991). This concern highlights the need for an objective, replicable, and accurate methodology to identify and interpret trace marks.

The aim of this thesis is to analyze and interpret specific patterns of cut mark micromorphology using a middle-range and actualistic theoretical framework. This approach aims to build upon previous studies that use a similar theoretical and analytical framework to establish causal links between the micromorphological characteristics of experimentally created bone surface modifications and hominin butchery behaviors in the past.

1.3) Chapter Summaries

This study will first quantitatively define the variable morphological patterns of cut marks experimentally created by different Early Stone Age tools of varying technological form and raw material type. Patterns of experimental cut mark micromorphology are then used to identify the technological form and raw material type of tools that created fossilized cut marks in a faunal assemblage recovered from Olduvai Gorge, Tanzania.

Chapter 2 of this thesis summarizes the relevant literature necessary for understanding trends in Early Stone Age tool technologies and butchery practices. The development of relevant bone surface modification analytical methods and technologies will also be described in this chapter. Chapter 3 defines the experimental procedures and statistical analysis used in this thesis. Chapter 4 will provide an overview of the statistical results from this experiment. And finally, chapters 5 and 6 will describe and summarize the overall findings of this project.

CHAPTER 2 BACKGROUND

Early Stone Age faunal assemblages that preserve fossils with cut and percussion marks provide the earliest and most direct evidence of hominin carnivory in the archaeological record. These assemblages are often preserved in direct association with Early Stone Age stone tools, providing evidence for an expanded hominin ecological niche during this period into tool-assisted carnivory. Taphonomic studies have previously focused on developing models capable of using the frequency, patterning, and morphology of these marks to provide behavioral interpretations of Early Stone Age hominins (Capaldo, 1998; Domínguez-Rodrigo and Barba, 2006; Domínguez-Rodrigo and Pickering, 2003; Domínguez-Rodrigo et al., 2014; Merritt, 2015; Pante et al., 2012; 2015; Shipman, 1986). However, much still remains to be understood regarding the utilization of Early Stone Age tools by early hominins when butchering large mammal carcasses.

This chapter provides an overview of the development of stone tool traditions in the archaeological record, methods of cut mark identification and analysis, behavioral interpretations from cut mark analysis, and the applications of using high-resolution 3-D scanning to model bone surface modifications.

2.1) Early Stone Age Tool Traditions

One of the most significant innovations during the evolution of Early Stone Age hominins is the advent and utilization of stone tools that possess sharp cutting edges to process large mammal carcasses. This technological innovation can be identified in the Early Stone Age archaeological record by the appearance of stones knapped by hominins and fossils bearing trace marks inferred to have been created by these stone tools (de Heinzelin et al., 1999; Leakey, 1966; 1971; Semaw et al., 1997; 2003). These tool forms are often correlated with the expansion of the hominin foraging niche to begin including meat resources from large mammal carcasses, likely leading to numerous morphological changes in the evolutionary history of the genus *Homo* (Aiello and Wheeler, 1995; Isler and van Schaik, 2009; Leonard et al., 2007). To fully appreciate the evolutionary benefits that stone tools and an expanded dietary breadth into carnivory provided early hominins, trends in the emergence, distribution, and utilization of Early Stone Age tool forms must be assessed.

The earliest hominin modified tool forms can be separated into two technological traditions, the Oldowan and the Acheulean, based on tool complexity, morphology, and temporal period it was recovered in. These two cultures are described in detail below.

2.1.1) Oldowan Tool Industry

The Oldowan tool tradition represents the first evidence of Early Stone Age hominins expanding their ecological niche to begin consistently including meat resources from large mammals in their diets, a significant step in the evolution of the hominin lineage. The Oldowan tool tradition is predated only by the technologically rudimentary 3.3 million-year-old Lomekwian culture, recovered from a single site in West Turkana, Kenya (Harmand et al., 2015; Lewis and Harmand, 2016). However, these Lomekwian tool forms are not preserved in direct association with cut marked fossils, limiting the interpretation of these tools as butchery instruments. Although, the nearby 3.39 million-year-old Dikika, Ethiopia assemblage preserves bone surface modifications that have been suggested to be the earliest evidence of cut marks; this interpretation remains controversial with others arguing the marks were inflicted by animal trampling (McPherron et al., 2010; Thompson et al., 2015; but see: Domínguez-Rodrigo et al., 2010; 2011; 2012). Therefore, the slightly later Oldowan tool tradition is currently the first evidence of stone tools that can be unequivocally connected to hominin carnivory (Domínguez-Rodrigo and Alcalá, 2016; Domínguez-Rodrigo et al., 2005; Ferraro et al., 2013).

The initial defining characteristic of the Oldowan Industry was archaeological assemblages containing chopper tool forms, which were originally considered to be the primary butchery tool of this tradition (Leakey, 1966; 1971). However, later actualistic studies now propose that the main butchery tool form during the Oldowan were simple and sharp-edged flakes knapped from the choppers (Toth, 1985). Other tools often found in Oldowan assemblages include anvils, hammerstones, knapping debitage, and unmodified manuports (Leakey, 1966; 1971). Together, these tools define the simplistic and diverse hominin toolkit representative of Oldowan archaeological assemblages.

The earliest evidence of Oldowan tools in the archaeological record comes from the 2.6 million-year-old site in Gona, Ethiopia, which is associated with one cut marked fossil (Domínguez-Rodrigo et al., 2005; Semaw et al., 1997; 2003). A nearby 2.5 million-year-old site from Bouri, Ethiopia also preserves early evidence of cut marked fossils, but with no Oldowan tools associated with the assemblage (de Heinzelin et al., 1999); however, the origin of these marks has recently been questioned (Sahle et al., 2017). Researchers have used the presence of cut marked fossils in the Gona and Bouri assemblages to propose that Oldowan hominins were using stone tools for butchery related activities as early as 2.6 million years ago (Domínguez-Rodrigo et al., 2005). Other early East African Oldowan sites include the 2.34 million-year-old Lokalalei, West Turkana, Kenya site (Roche et al., 1999), 2.33 million-year-old Hadar, Ethiopia site (Kimbel et al., 1996), 2.0 million-year-old Kanjera South, Kenya site (Bishop et al., 2006; Plummer et al.,1999), 2.0 million-year-old Fejej, Ethiopia site (Barsky et al., 2011), 1.9 to 1.6 million-year-old Koobi Fora, Kenya sites (Bunn, 1981; Isaac, 1997), and 1.8 million-year-old

Olduvai Gorge, Tanzania site (Bunn and Kroll, 1986; Leakey, 1971). However, Oldowan sites prior to 2.0 million years ago rarely preserve cut marked fossils, establishing doubt as to the function of these tools as being exclusively for butchery (Delagnes and Roche, 2005; Domínguez-Rodrigo et al., 2005). Following the initial development of Oldowan tools in East Africa there is a rapid diffusion of Oldowan tool forms after 2.0 million years ago to numerous localities throughout Africa and Eurasia (e.g. Kuman, 1994; Kuman and Clarke, 2000; Sahnouni and de Heinzelin, 1998; Mgeladze et al., 2011). The wide spread and well-documented history of Oldowan tools in East Africa and Eurasia provides the framework for the hypothesis that these tool forms provided an important and useful function to Early Stone Age hominins.

Experimental studies replicating the possible functions of Oldowan stone tools emphasize the diversity of behaviors that these tools can be used for. Modern experiments using Oldowan tools highlight the effectiveness of using Oldowan tool forms to process animal carcasses, organic materials such as wood, animal hides, and crack both nuts and bones (McCall, 2005; Plummer, 2004; Toth, 1985). These functionality experiments are further supported by use-wear analyses of Oldowan stone tools, which indicate that these tools were used to process both plant and animal resources (Lemorini et al., 2014).

Cut marked bones recovered from Oldowan archaeological assemblages provide direct evidence for understanding and modeling the possible uses of stone tools for butchering large mammal carcasses. Archaeological analyses of Oldowan faunal assemblages identify a pattern of early hominins having consistent access to medium sized bovid carcasses, and a wide range of aquatic resources, including fish, crocodiles and turtles (Blumenschine and Pobiner, 2007; Braun et al., 2010; Ferraro et al., 2013). These interpretations are primarily based on fossils bearing cut marks, which provide direct causal links between stone tool use and butchery behaviors.

However, which Oldowan tool forms (e.g. flakes, choppers, or scrappers) created cut marks has never been established, preventing interpretations of how Oldowan hominins used distinct tool forms when butchering.

2.1.2) Acheulean Tool Industry

The defining characteristic of the Acheulean tool tradition is the inclusion of bifacial handaxes knapped from large cores and flakes into the Early Stone Age hominins toolkit (Debénath and Dibble, 1994; Lycett, 2008; Semaw et al., 2009; Shea, 2007). Other tool forms that originate throughout the Acheulean, but are less defining and prolific than the characteristic bifacial handaxe, include stone cleaver and pick tools (Shea, 2007). The hominin species often credited with creating these new Acheulean tool forms is *Homo erectus*, who first appears in the archaeological record approximately 1.9 million years ago, slightly before the earliest Acheulean stone tools (Antón, 2003; Antón et al., 2014). This study uses the characteristic bifacially knapped handaxe to represent stone tools from the Acheulean tradition.

The characteristic feature of early Acheulean sites, particularly during the transition from the Oldowan to the Acheulean, are lithic assemblages containing a large proportion of handaxe tools relative to other tool forms (Kleindienst, 1961; Leakey, 1971). Although, de la Torre (2011) has recently suggested that any site with handaxes should be classified as Acheulean, as the presence of a handaxe tool implies that the associated hominins had the mental and physical capacity to produce these complex tools. However, some lithic assemblages during the Acheulean lack handaxe tool forms and are still considered Acheulean; these sites are interpreted as having unique ecological or site-related functions that did not necessitate, allow, or lead to the accumulation and production of characteristic Acheulean handaxes (Ashton et al., 1994; de la Torre, 2016).

The earliest Acheulean lithics come from two 1.76 million-year-old sites located in Kokiselei 4, West Turkana, Kenya (Lepre et al., 2011) and Konso, Ethiopia (Beyene et al., 2013), and a 1.7 million-year-old site in Olduvai Gorge, Tanzania (Diez-Martín et al., 2015), which all contain crudely made unifacial and bifacial handaxe tool forms. Interestingly, temporally and geographically similar sites are still being classified as Oldowan during this time, highlighting this period as transitional between Early Stone Age tool traditions (Lepre et al., 2011). Following the initial appearance of Acheulean tools, there is a rapid dispersion of this technological tradition to other areas in Africa and Eurasia. By 1.6 million years ago, there are numerous Acheulean sites throughout Africa, including other Olduvai Gorge, Tanzania sites (Leakey, 1971), Peninj, Tanzania (de la Torre et al., 2008; Isaacs and Curtis, 1974), and Lower Vaal River, South Africa (Gibbon et al., 2009). Important and early Acheulean sites outside Africa include the 1.4 million-year-old assemblages from Ubeidiya, Israel (Bar-Yosef, 1994) and Southern India (Pappu et al., 2011), and a 1.0 million-year-old site from Northeast Spain (Mosquera et al., 2016; Vallverdú et al., 2014).

Similar to the Oldowan tool technology, the commonly inferred function of Acheulean stone tools are related to foraging and subsistence, including butchering and skinning animal carcasses (Mitchell, 1995; Rabinovich et al., 2008; Schick and Toth, 1993; Solodenko et al., 2015; Yravedra et al., 2017a), and processing wood and plant materials (Binneman and Beaumont, 1992; Domínguez-Rodrigo et al., 2001; Schick and Toth, 1993). Alternative, but more controversial, theories have also been proposed as the original function of handaxe tools, including the “Killer Frisbee” hypothesis, where handaxes were used as projectiles to hunt (O’Brien, 1981; Shea, 2007), and the “Sexy Handaxe” hypothesis, which suggests that handaxes provided a sexually selective advantage for tool making hominins (Kohn and Mithen, 1999).

Both of the earliest Acheulean sites in West Turkana and Konso are not directly associated with any hominin-modified faunal remains, limiting interpretations of these tools as being used for a butchery function (Beyene et al., 2013; Lepre et al., 2011). However, the slightly later FLK West, Olduvai Gorge, Tanzania Acheulean assemblage preserves four cut marked fossils, which may indicate that Acheulean tools were used for a similar butchery purpose as Oldowan tools (Diez-Martín et al., 2015; Yravedra et al., 2017a). Significantly later Acheulean assemblages throughout the Old World often preserve *in situ* evidence of Acheulean tools and cut marked bones together (e.g. Bello et al., 2009; Rabinovich et al., 2008; Yravedra et al., 2010). These observations of cut marked bones provide support for the hypothesis that Acheulean tools were used for butchering related tasks. However, the sparsity of assemblages containing cut marked fossils during the initial emergence and diffusion of the Acheulean begs the question of whether these tools originated to be used for butchering large mammal carcasses.

2.1.3) Oldowan-Acheulean Technological Transition

The transition from simple Oldowan core and flake tools to a more complex Acheulean bifacial technology represents a significant technological advance during the Early Stone Age. However, the exact environmental, behavioral or social catalysts that caused Early Stone Age hominins to change their preferred lithic technology during this period is not well understood. Furthermore, whether these two tool traditions were used for the same butchery purposes is not clear, as the flake tool forms characteristic of the Oldowan occur throughout the Acheulean.

Current paradigms modeling the transition from the Oldowan to Acheulean often relate this transition to the emergence and disappearance of hominin species in the archaeological record. Generally, the emergence of a new Lower Paleolithic hominin species is correlated with significant increases in brain and body size, which increase daily metabolic demands (Foley and

Lee, 1991; Isler and van Schaik, 2009). It has been suggested that Acheulean tool forms are generally more efficient for processing larger, more calorie dense meat resources in comparison to Oldowan flake tools (Galán and Domínguez-Rodrigo, 2014; Key and Lycett, 2017; Jones, 1980; Mitchell, 1995; Schick and Toth, 1993). This idea supports the hypothesis that Acheulean tools may have been produced to overcome the daily metabolic demands of increased brain size in Early Stone Age hominins by providing a way to more efficiently obtain meat resources.

Fluctuations in environmental conditions during the Oldowan-Acheulean transition may have also been a significant driving force provoking hominins to develop more advanced stone tool technologies. Archaeological analyses of Oldowan faunal assemblages indicate that *Homo habilis* likely scavenged meat resources, obtaining scraps of flesh and bone marrow left on carcasses killed by other carnivores (Blumenschine, 1986; Cavallo and Blumenschine, 1989; Pante et al., 2012). Scavenging behaviors provide consistent access to meat resources; however, depending on the environmental and competitive conditions, provide significantly less resources compared to hunting (Blumenschine et al., 1987). Behavioral reconstructions of faunal assemblages associated with the Oldowan-Acheulean transition indicate that during this period hominins began using a hunting foraging strategy (Pante, 2013; Pickering et al., 2004; Pobiner et al., 2008). Being the primary consumer of a carcass provides significantly more consumable and nutritious meat resources compared to scavenging (Blumenschine, 1986). The development of these hunting behaviors can possibly be attributed to a significant climatic shift in Africa during the early Acheulean period, characterized by an increase in open grassland environments and a reduction in wooded habitats (Bobe and Behrensmeyer, 2004; Cerling et al., 1988; 2011; Magill et al., 2013). Wooded habitats represent low competition and danger environments abundant with scavengeable carcasses, while open grassland environments tend to have more competition and fewer scavengeable carcasses (Blumenschine, 1989). Therefore, the rise of open habitats may have limited the scavenging opportunities of early hominins, leading to environmental conditions favoring the development of Acheulean tools to hunt and more efficiently deflesh large mammal carcass.

An alternative hypothesis for the emergence of Acheulean handaxes could be that early Acheulean tools were not used for the same purposes as Oldowan flakes. Instead, it is possible that during the Oldowan-Acheulean transitionary period Acheulean tools provided an alternative benefit, either socially or behaviorally (Gamble, 1998; Kohn and Mithen, 1999; Pope et al., 2015). This could explain the presence of Acheulean tools in earlier assemblages and the sparsity of handaxe tool forms in some later assemblages, or why early Acheulean assemblages often contain handaxes, but few or no cut marked fossils. Use-wear analyses of Acheulean handaxes show that hominins did use handaxes for some butchery behaviors (Solodenko et al., 2015). However, the extent and temporal consistency of hominins using handaxes throughout the Early Stone Age for carcass processing behaviors is not fully understood. From this uncertainty in tool use behaviors, this thesis aims to establish an alternative method capable of connecting Early Stone Age butchery behaviors with specific lithic technological forms to better understand how different tool forms were used.

2.2) East African Early Stone Age Raw Material Sources

A trend noted throughout both the Oldowan and Acheulean Industries is variability in the raw materials used for creating stone tools. Whether stone tools of differing raw material type were used for the same or different butchery purposes is not currently well understood.

The lithic raw material types represented in most early Oldowan sites suggests that hominins preferentially selected raw materials that were available locally or within a short distance to them (Blumenschine et al., 2003; Braun et al., 2008; Semaw et al., 2003). This localized selectivity is characteristic of most East African Oldowan lithic assemblages, where tools are primarily made from local quartz, basalts and high-quality lava cobbles (Stout et al., 2005). Following the transition to the Acheulean in East Africa, tools are being made from similar raw materials as those from the Oldowan, but also include raw materials sourced from more distant sources, often including basalt, quartz, quartzite, chert, obsidian, phonolites, and other silicic volcanics (e.g. Asfaw et al., 1992; Diez-Martín et al., 2015; Jones, 1979; Piperno et al., 2009).

The diversity of raw material procurement strategies documented throughout Early Stone Age archaeological assemblages highlights the geographic variability and adaptability of early hominins. However, this diversity also leads to the question of whether some raw materials were being used preferentially for different purposes. One way the usage of different raw materials can be identified in the archaeological record is through the morphological analysis of cut marked fossils (de Juana et al., 2010; Greenfield, 2006; Yravedra et al., 2017b). The physical and structural characteristics of different stone raw material types, such as elasticity, hardness, and brittleness, can create tools with unique cutting edge shapes (Eren et al., 2014; Goldman-Neuman and Hovers, 2011). It has also been reported that certain Oldowan tools were knapped differently depending on the raw material they are made from, which would also lead to tool forms having distinct cutting edges (Gurtov and Eren, 2014). Comparatively, analyses of Acheulean tools note that handaxes created from different raw materials tend to not vary in morphology or size (Eren et al., 2014; Sharon, 2008). Overall, these observations suggest that some Early Stone Age tools may have distinct cutting edges unique to the raw material type used to create them and will therefore leave distinct cut marks relative to their form. A primary goal of this thesis is to provide a means to connect specific raw materials to fossilized cut mark morphologies in the archaeological record to better understand hominin raw material preferences for butchery behaviors.

2.3) Previous Methods Modeling Cut Mark Morphology

Modeling the morphological patterns of various bone surface modifications is a significant focus in paleoanthropological research, as these marks often represent the only direct evidence of hominin butchery in the archaeological record. As such, a frequent analytical focus within taphonomy is concentrated on establishing standardized criteria to define and identify marks based on the archaeological actors that created them. Identifying the various carnivorous actors represented in a faunal assemblage allows for broader inferences to be made regarding early hominin environmental interactions and carnivory.

One line of inference for identifying and interpreting bone surface modifications is macroscopic studies of trace mark morphology. This approach primarily uses qualitative descriptions of the relative length, width, and profile shape of a mark to differentiate between archaeological actors, such as hominins, carnivores, rodents, or trampling (e.g. Blumenschine and Selvaggio, 1988; Blumenschine et al., 1996; Bunn, 1981; Domínguez-Rodrigo et al., 2009). Blumenschine et al. (1996) note that trained analysts are able to macroscopically distinguish between these bone surface modifications with 97% accuracy. However, it also been proposed that the lack of a discipline-wide approach for macroscopically identifying bone surface modifications limits the replicability and comparative nature of studies using this method (Domínguez-Rodrigo and Barba, 2006; Lupo and O'Connell, 2002). Therefore, establishing an objective and replicable method to describe and identify the actors associated with different trace marks if of the utmost importance to this field.

Modeling cut marks using Scanning Electron Microscopy (SEM) has previously been employed as a high-resolution trace mark modeling technique to overcome the limitations of macroscopic trace mark analysis. In particular, SEM analyses have noted that cut marks tend to leave internal striations while tooth marks tend to lack striations and be flat or rounded (Potts and Shipman, 1981). However, this approach is again based on qualitative and subjective observations of cut mark morphology. Other SEM studies have also attempted to establish morphological criteria to distinguish the physical properties of a tool effector from cut mark morphology, but are similarly limited by qualitative and subjective trace mark descriptions (Bartelink et al., 2001; Greenfield, 1999; 2006). Critics of SEM analysis also note that this method is only able to create 2-D images from a 3-D object, preventing quantitative volumetric measurements from being measured, is destructive to archaeological fossils, and tends to be inaccurate (Bartelink et al. 2001; Bello, 2011; Bello and Soligo, 2008; Boschin and Crezzini, 2012; Gilbert and Richards, 2000; Schroettner et al., 2006).

Similar to SEM analysis, other bone surface modification analyses have employed various technologically assisted modelling methodologies in an attempt to identify the relationship between cut mark morphology and tool effector. These approaches include using Micro-CT scanners (Thali et al., 2003) and Digital Imaging Techniques (Gilbert and Richards, 2000) to model and interpret the unique micromorphology of a cut mark. However, these studies all encounter similar issues as SEM analysis due to the lack of clearly defined, replicable, and quantitative methods.

Micro-photogrammetry is a recent modeling technique being implemented in numerous studies that attempt to quantitatively relate the micromorphological features of a trace mark to the archaeological agent that created it (Arriaza et al., 2017; Maté-González et al., 2015; 2016;

Yravedra et al., 2017a; 2017b). This method works by combining multiple photos of a cut mark taken from various angles to reconstruct and model marks in 3-D (Maté-González et al., 2015). From these reconstructions, quantifiable measurements, such as width along the cut mark, opening angle, and cut mark depth, can be recorded (Maté-González et al., 2015). This method has recently been applied to distinguish between experimental cut marks made by stone tools of differing raw material types, with interesting results (Maté-González et al., 2016; Yravedra et al., 2017b). However, this approach is currently associated with numerous methodological and technical limitations when modeling trace marks.

The current analytical methodology used for modeling cut marks with micro-photogrammetry is primarily based on the experimental protocol put forth by Maté-Gonzalez et al. (2015). However, the capability of this methodology to effectively classify tool effector from cut mark morphology is unknown due to a lack of inter-observer studies assessing whether micro-photogrammetric measurements and results are replicable between analysts. This method is also limited by its need to take numerous “approximate” measurements, which introduce observer bias into the analysis and results of this method (Maté-Gonzalez et al., 2015). This methodology calls for analysts to take a cross-sectional profile across a cut mark at approximately 50% of its length, or, if the researchers do not care about analytical replicability, at least between 30% and 70% of the cut marks length (Maté-Gonzalez et al., 2015). However, Pante et al. (2017) recently demonstrated that analyzing the central cross-sectional profile of a cut mark is neither replicable between researchers, nor is it representative of the entire cut mark. As well, two of seven cross-sectional profile landmarks the micro-photogrammetric method uses when measuring cut marks are instructed to be placed at “approximately” 10% above either side of the deepest point of the mark (Maté-Gonzalez et al., 2015). Using multiple approximate measurements when evaluating the morphological features of a cut mark likely limits the replicability of this method and prevents researchers from using this data to draw any informative conclusions regarding patterns in cut mark micromorphology. This methodology is also restricted by its analytical technique, which is only able to reconstruct and analyze 2-D cross-sectional profiles from a cut mark. This limitation prevents this methodology from recording and measuring any unique information or explanatory trends from the entirety of a 3-D cut mark.

Modeling cut marks using micro-photogrammetry is also associated with significant levels of experimental error when reconstructing and analyzing cut mark micromorphology. The average total model error of the 13 cut marks that Maté-Gonzalez et al. (2015) analyzed in their fundamental micro-photogrammetry study was ± 22.1 µm. This large error rate is a significant obstacle when measuring the micromorphological features of relatively small bone surface modifications, such as cut marks. Other studies that analyze bone surface modifications using micro-photogrammetry record similarly large levels of average total model error when reconstructing and analyzing trace marks (Arriaza et al., 2017; Maté-González et al., 2016; Yravedra et al., 2017a; 2017b). The significant model error rates associated with micro-photogrammetry limits the overall analytical power of this methodology and makes any attempt to identify tool effector from trace mark morphology ineffective.

2.4) Application of High-Resolution 3-Dimensional Laser Scanning to Model Cut Marks

Using 3-D laser scanning to model and reconstruct cut mark micromorphology has recently allowed trace mark modeling research to surpass previous 2-D limitations, establishing the framework for a quantitative approach to effectively analyze the micromorphological features of a cut mark (Bello and Soligo, 2008; Bello et al., 2009; 2013; Pante et al., 2017). This technology presents an objective method for measuring the linear and volumetric features of cut marks, and is preferential to other trace mark modelling techniques, as it is not inhibited by artifact size or destructive to fragile artifacts (Kaiser and Katterwe, 2001; Kuzminsky and Gardiner, 2012). However, for analyses using 3-D scanning to be capable of interpreting past hominin butchery behaviors, a standardized methodology must be established that is accessible, accepted and understood by the general paleoanthropological discipline.

Until recently, studies using high-resolution 3-D scanning have not established a clear and discipline-wide methodology for analyzing the micromorphological features of various trace marks. A fundamental 3-D scanning study by Bello and Soligo (2008) identified six quantitative measurements capable of recognizing tool effector from cut mark morphology, including cut mark slope angle, opening angle, bisector angle, shoulder height, floor radius, and depth. Later studies based off this initial approach used these measurements to model the relationship between cut mark morphology and lithic tool technology, but ultimately failed due to a limited methodology (Bello et al., 2009; 2013). Critics of this specific scanning methodology question the accuracy and informative capacities of slope angle, bisector angle and shoulder height measurements, suggesting that these variables are too influenced by the force and angle with which a researcher holds a tool when cutting a bone, not due to the variable cutting edge of a stone tool (Boschin and Crezzini, 2012). Furthermore, previous 3-D modelling studies have never addressed whether their methods are reproducible between analysts, preventing any meaningful or informative trends in the micromorphological characteristics of cut marks from being identified.

Recently, Pante et al. (2017) addressed the lack of a defined and replicable high-resolution 3-D scanning methodology by detailing a standardized and quantitative approach to reconstruct and measure the micromorphological features of a cut mark. The replicability of this methodology has been tested using an inter-observer approach, where the morphological features of trace marks were independently analyzed by three observers, which showed that this techniques methodology is both replicable and precise (Pante et al., 2017). This replicable and easily learned methodology is also able to distinguish cut marks from tooth marks with 97.5% accuracy, a value slightly higher than that obtained in the macroscopic study undertaken by Blumenschine et al. (1996). This thesis aims to expand upon this methodology by identifying and interpreting the relationship between cut mark micromorphology and the physical and structural properties of a tool.

2.5) Application of Cut Marks for Understanding Early Stone Age Butchery and Lithic Behaviors

Interpreting the dynamic carnivorous behaviors that emerge with and characterize early genus *Homo* are primarily limited to the analysis of fossilized trace marks and stone tools in the archaeological record. Of the numerous taphonomic marks that are left on fossils, cut and percussion marks preserve the most direct traces for identifying past hominin carnivory. Past actualistic studies modeling patterns of cut, percussion, and tooth marks establish the framework for identifying how hominins accessed large mammal carcasses and the interactions between hominins and other mammalian carnivores in the archaeological record (Binford, 1981; Blumenschine, 1995; Capaldo, 1998; Domínguez-Rodrigo, 1999; Domínguez-Rodrigo and Pickering, 2003; Oliver, 1994; Pante et al., 2012; Selvaggio, 1998; Shipman, 1986). These models rely on the ability of researchers to accurately use macroscopic trace mark analysis techniques to differentiate between bone surface modifications based on the carnivorous actor that created each mark represented in a faunal assemblage.

Feeding trace models document one methodology that use patterns of bone surface modifications in an archaeological assemblage to model and interpret the presence, interactions, and behaviors of Early Stone Age hominins. These behavioral models document ecological scenarios using the relative proportion of different bone surface modifications throughout a faunal assemblage to propose who the associated actors were and how they interacted (Blumenschine, 1995; Capaldo, 1998; Pante et al., 2012; Selvaggio, 1998). These scenarios include carnivore-only, hammerstone-only, hammerstone-to-carnivore, carnivore-to-hominid, carnivore-to-hominid-to-carnivore, whole-bone-to-carnivore, and vulture-to-hominin-to-carnivore models (Blumenschine, 1995; Capaldo, 1998; Pante et al., 2012; Selvaggio, 1998). Fossil assemblages associated with only one carnivorous actor tend to be characterized by a high percentage of bone surface modifications made by that carnivorous actor, either cut and percussion marks or tooth marks (Blumenschine, 1995). Fossil assemblages with multiple carnivorous agents are identified based on the relative frequency of different bone surface modifications produced by numerous actors, with each multi-agent model predicting a different frequency of each trace mark. These models provide an actualistic and theoretically ground method to identify instances of hominin-carnivore interactions in the archaeological record; however, these models can only be employed when trace marks can be identified accurately and consistently between researchers.

Critics of feeding trace models propose that they underemphasize the importance of cut marks, rely too heavily on tooth and percussion mark frequencies, and are supported by inconsistent bone surface modification identification methods (Domínguez-Rodrigo, 1997; Domínguez-Rodrigo and Barba, 2006; Domínguez-Rodrigo et al., 2014). Other studies have similarly proposed that taphonomic equifinalities limit the capacity of feeding trace models to effectively identify the influence of different carnivorous agents in an assemblage (Domínguez-Rodrigo and Barba, 2006; 2007). These critiques highlight the need to establish an unbiased, replicable, and consistent methodology for identifying trace marks in the archaeological record in order to make broader behavioral and environmental inferences of Early Stone Age hominins.

2.6) Conclusion

The appearance of Oldowan stone tools in the archaeological record documents one of the most important technological innovations during the evolution of Early Stone Age hominins. However, over time, this successful tool tradition is supplemented by Acheulean bifacial handaxes and it is currently unclear whether there these new tool forms were used for a similar butchery purposes as earlier Oldowan tools. This uncertainty arises due to the persistence of Oldowan flake tools long into the Acheulean transitionary period, which has led some researchers to propose that Acheulean tools may have originated for other, non-butchery related functions (Kohn and Mithen, 1999; Pope et al., 2015). One method for recognizing the use of different tool forms in an archaeological butchery event is through the morphological analysis of fossilized cut marks (Bello et al., 2009; 2013; Greenfield, 1999; 2006; Maté-González et al., 2016; Yravedra et al., 2017b). Recently, high-resolution 3-D scanning has been employed as an objective, replicable, and quantitative method to reconstruct and measure the micromorphological characteristics of cut marks (Pante et al., 2017). This high-resolution scanning approach provides the methodological foundation for future research to begin analyzing the specific micromorphological features of cut marks created by Early Stone Age tools of varying technological form and raw material type. When these informed connections are made, new information can be identified from cut marks in the archaeological record to better model hominin butchery behaviors.

CHAPTER 3 MATERIAL AND METHODS

The purpose of this study is to systematically characterize variations in the micromorphological features of cut marks created by lithic tools that differ in techno-complex and raw material type. The experimental protocols detailed in this thesis were developed to minimize the influence of extrinsic variation on cut mark production and analysis by maximizing inter-analyst comparability and result reproducibility. When the external factors of tool impact angle and pressure are controlled for between cutting trials, distinct patterns in cut mark morphology can be directly related to the cutting edge of the tool that made the mark. Detailed explanations of raw material sources, experimental methodology, data collection protocol, and 3-dimensional cut mark analysis are outlined below.

3.1) Experimental Bone Sample

The bones used in this study were collected with an emphasis on keeping bone surface and materials as consistent as possible. Sectioned bovid femur and tibia midshafts were obtained from Beaver's Market, a local butcher in Fort Collins, Colorado. Bones were sectioned transversely across the bone shaft using a mechanized bone saw. Only hind limb long bone midshafts were used in this study in order to keep cortical bone density consistent throughout all cutting trials, allowing for better cut mark comparability and experimental control (Braun et al., 2016; Lam and Pearson, 2005). All analyzed bones were assumed to have come from size four bovids, which includes all animals that weigh between 750 and 2000 pounds (based on animal size class definitions established by Bunn (1982)). Any remaining flesh was removed from the surface of each bone using plastic knives and wooden skewers as to not alter the bone surface, leaving only the periosteum intact and preventing unintentional bone surface markings. All bone surfaces were thoroughly inspected before proceeding with the study to identify pre-experimental bone surface marks. The location of these marks was noted to ensure that any pre-study bone surface modifications were not confused with experimentally created cut marks. Tibia and femur bones were randomly assigned to each tool class during the cutting trial portion of this experiment (Table 3.1).

Table 3.1) Number and type of hind limb bones used in this study for each cut mark group.

Cut Mark Group	ID	Bone	Cut Mark Group	ID	Bone
Quartzite Biface	1	Tibia	Quartzite Flake	1	Tibia
	2	Femur		2	Tibia
	3	Tibia		3	Femur
				4	Femur
Basalt Biface	1	Femur	Basalt Flake	1	Tibia
	2	Tibia		2	Femur
	3	Tibia		3	Femur
Chert Biface	1	Tibia	Chert Flake	1	Tibia
	2	Tibia		2	Tibia
	3	Tibia		3	Femur
Phonolite Biface	1	Tibia	Phonolite Flake	1	Tibia
	2	Tibia		2	Femur
				3	Tibia

3.2) Early Stone Age Tool Sample

The modern tool sample used in this study was experimentally produced with a focus on creating accurately replicated tool shapes and cutting edges that are comparable to stone tools recovered in Early Stone Age archaeological contexts. All tools were manufactured by Dr. Jay Reti, University of California Santa Cruz, an expert on the production and formation of East African Early Stone Age tools, using raw materials he collected from the modern outcrops in Olduvai Gorge, Tanzania. Two Early Stone Age tool technologies were created for this study: bifacially flaked handaxes and unretouched flakes. Both tool classes were produced using four different raw materials that are commonly found in Early Stone Age Olduvai Gorge archaeological sites: quartzite, basalt, chert and phonolite (Figure 3.1). One biface tool was made from each raw material and was used to create all biface cut marks for that cut mark grouping. Five flake tools were made from each raw material type and all were used equally to create flake cut marks in this study.

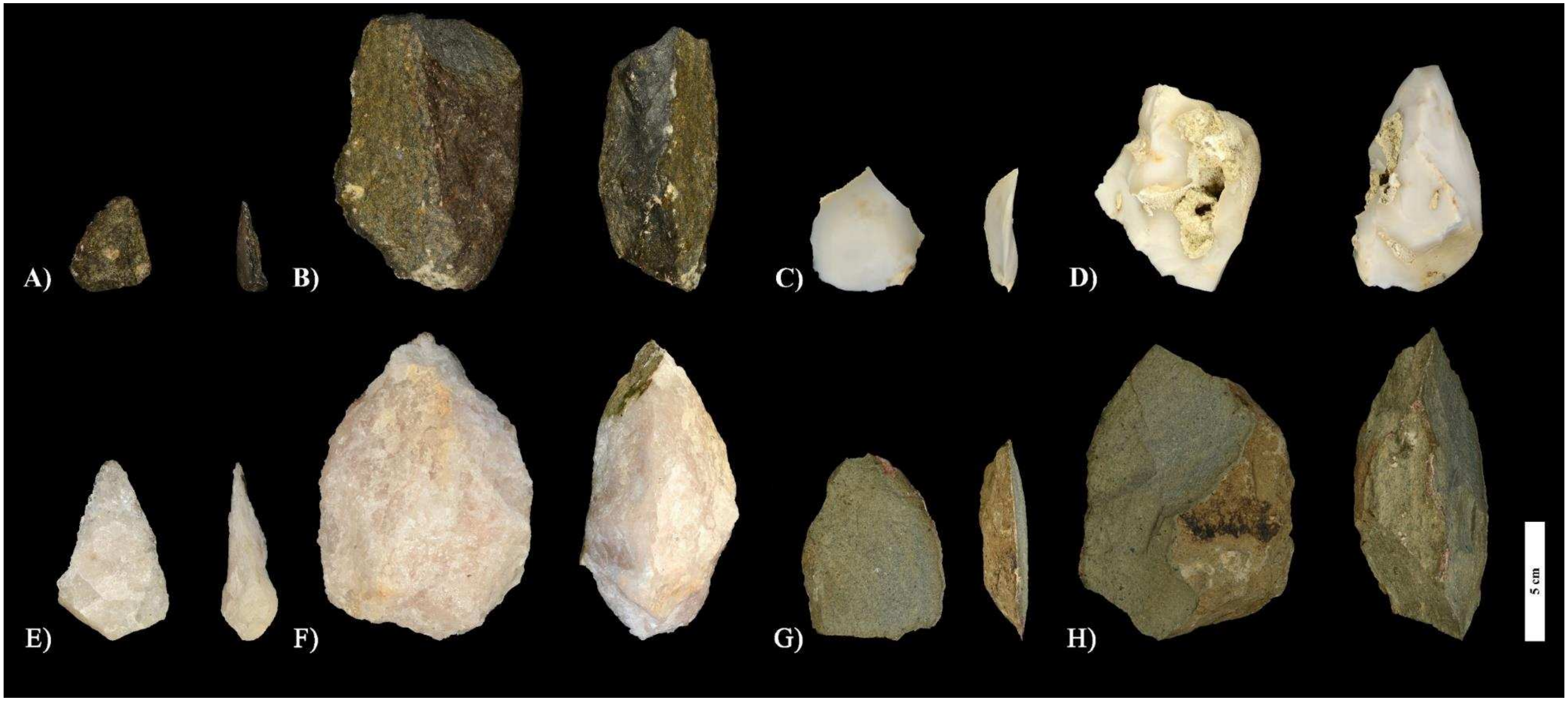

Figure 3.1) Sample image of different tool technological forms and raw material types used in this study. All tools are shown in a ventral and a use edge profile view. (A) Basalt Flake; B) Basalt Biface; C) Chert Flake; D) Chert Biface; E) Quartzite Flake; F) Quartzite Biface; G) Phonolite Flake; H) Phonolite Biface).

3.3) Standardization of Cut Mark Creation

Experimental cut marks were created for this study with a focus on maximizing experimental control between cutting trials. Specifically, all cut marks were created with the goal of keeping the applied force and impact angle of each tool relative to the bone surfaces constant. This methodological approach was accomplished by designing a cutting machine that allowed for both variables to be controlled for throughout this study, isolating the effects of the independent variables, tool technology and raw material, on cut mark micromorphology (Figure 3.2).

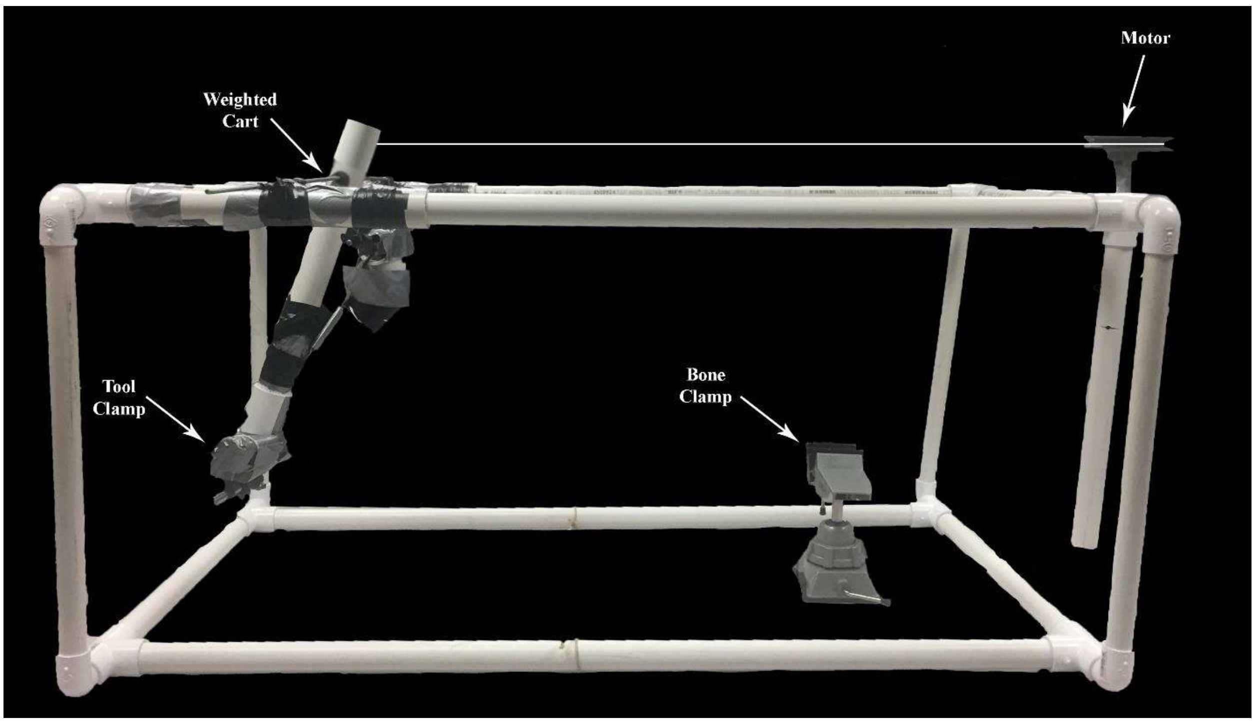

Figure 3.2) Schematic of motorized cutting machine used to create standardized cut marks.

The frame of the standardized cutting machine was made using 1-inch diameter PVC pipes. This frame was 1.0 meter long, 0.6 meters wide, and 0.45 meters tall. The weighted cart portion of the machine was connected to the frame using two 0.3 meter long pieces of 1-1/4 inch PVC pipe that slid along the length of the upper frame. These two sliding cart PVC pipes were connected across the width of the frame using a metal rod. A mobile arm clamp made from a

0.45-meter-long PVC pipe was attached to the center of this transverse metal rod at an angle of approximately 60 degrees. An adjustable metal clamp was attached to the bottom of this mobile arm to hold stone tools, which allowed for the angle and area of tool impact on bone surfaces to be controlled. Due to differences in the weight of each tool form, an adjustable weighted bag was attached to the cart to keep the applied force constant between all trials. Each tool was standardized to a weight of 1.2 kg (*m*), the weight of the largest tool without any additional weight. This weighted cart was then connected to an 11.43 cm diameter pulley driven by a 30-rpm battery operated motor by high strength fishing line. This pulley and motor setup allowed the weighted cart to be moved along the frame of the cutting machine at a constant speed throughout all cutting trials. Bones to be cut were placed in a fixed clamp 0.75 meters away from the starting location of the tool. The height of the bone clamp and machine were adjusted for each cutting trial to ensure that the stone tool always met each bone at a consistent height, regardless of bone or tool size.

The acceleration and force exerted by the cart on the bone was kept constant throughout this study. This was achieved by keeping all adjustable variables constant, allowing for a general calculation of the force applied by the cart on a bone for each cutting trial. The force of the arm was determined by first calculating the force of friction between the cart and frame (Equation 3.1) and the force exerted by the pulley on the cart (Equation 3.2). These forces were determined to be 3.532 N and 20.997 N, respectively. The coefficient of friction (μ) between two PVC pipes was determined to be 0.3, as documented by the PVC pipe manufacturer. The torque (τ) of the motor was determined to be 1.2 N•m, as documented by the manufacturer of the motor. The force of gravity was assumed to be 9.81 m/s^2 (*g*).

$$F_{friction} = \mu \times m \times g \qquad \text{[Equation 3.1]}$$

$$F_{pulley} = \frac{\tau}{pulley\ radius} \quad \text{[Equation 3.2]}$$

Following these calculations, the force exerted by the arm was calculated by subtracting the force of friction from the force exerted by the pulley (Equation 3.3).

$$F_{cart} = F_{pulley} - F_{friction} \quad \text{[Equation 3.3]}$$

The total force exerted by the arm was determined to be 17.465 N, or approximately 3.92 pounds of force. This force would be slightly higher than the actual force applied to the bone due to a reduction in speed when the tool contacts the bone. However, this reduction would be consistent for all cutting trials.

All bones were cut on each useable surface five times. A useable surface was defined as one side of a bone that had no pre-experimental surface markings, protrusions, or grooves. Each bone was cut on a maximum of two different useable surfaces present on the cortical surface of the bone. When cutting bones, the cart was placed at the end of the PVC frame and was pulled completely over the surface of the bone, representing one cut mark trial. In some instances, patches of cut marks were created during a single cutting trial due to different sections of the same tools cutting edge encountering the bone in multiple locations. Cut marks analyzed from these patches were treated as independent marks when the marks were not touching and had no overlapping portions. The decision to treat these marks independently was made to keep the results of this experiment as comparable to archaeological cut marks as possible, where patches of adjacent cut marks cannot necessarily be attributed to a single cutting stroke or behavior. Patches of multiple cut marks were primarily noted during cutting trails with larger bifacial stone tools, which tend to have considerably broader and more uneven cutting edges.

3.4) Cleaning Bones

All cut marked bones were cleaned following the cutting trials in order to remove any remaining tissue, grease or marrow present on the bone to allow for unobstructed scanning of cut marks. Removing the grease from a bone also serves to make the experimental bones used in this thesis more comparable to fossil bones, which no longer contain grease or soft tissue matter. All bones were placed in a simmering solution of water and hydrogen peroxide until thoroughly degreased. Any ligaments or tissues that remained after boiling were removed using a plastic knife and wooden skewer to avoid altering the morphology of any cut marks that were near the remaining ligaments. Bones were then dried and labeled.

3.5) Archaeological Sample of Fossil Trace Marks

Archaeological trace marks were collected off fossils recovered from a Middle Bed II site in Olduvai Gorge, Tanzania. This site is dated to approximately 1.6 million years old. This period was selected for this study because it represents the Oldowan-Acheulean transition in Olduvai Gorge. This time frame is of interest to this study, as cut marks made by both flake and biface tools are expected to be represented in the assemblage. All marks were previously identified as cut marks by Dr. Michael Pante using the trace mark identification protocols put forth by Blumenschine et al. (1996). Trace marks were scanned from 14 different fossils, amounting to 22 total marks analyzed (Table 3.2). All marks were molded using 3M ESPE Express STD Firmer Set, a vinyl polysiloxane impression material putty. Molds were created by mixing a putty base with a hardening catalyst, firmly applying this mixture to the surface of a cut marked fossils surface, and allowing the mixture to harden for approximately one minute. Molds were individually bagged and brought to the Colorado State University Zooarchaeology and Paleoanthropology Lab for analysis.

Table 3.2) Fossilized trace marks analyzed in this study.

ID	Skeletal Element	Cut Mark Location	Fossil Taxa	Body Size	Number of Marks
119	Phalanx	Body	Bovid	3	1
928	Tibia	Midshaft	Indeterminate	3	2
952	Atlas	Dorsal Arch	Bovid	3	2
1062	Tibia	Midshaft	Indeterminate	3	1
1300	Cervical Vertebrae	Body	Bovid	3	1
1418	Mandible	Horizontal Ramus	Suid	3	1
1601	Phalanx	Body	Bovid	3	1
1751	Tibia	Midshaft	Equid	3	1
2135	Humerus	Midshaft	Indeterminate	2	4
2226	Mandible	Vertical Ramus	Bovid	3	2
2537	Innominate	Acetabulum	Equid	3	1
2784	Long Bone	Midshaft	Indeterminate	2	2
3025	Femur	Near Epiphysis	Hippo	5	2
3132	Ulna	Midshaft	Bovid	3	1

3.6) Scanning Procedure

Experimental and archaeological cut marks were scanned following the experimental methodology outlined by Pante et al. (2017). This systematic and replicable methodology allows for the database defined in this study to be comparable to future bone surface modification analyses using a similar methodological approach.

All experimental and fossil cut marks were scanned using a Nanovea ST400 white-light confocal profilometer and its associated software. A 3-mm optical pen with a z-axis resolution of 40 nm was used for all scans to maximize analytical accuracy. Cut marks were scanned at a step-distance of 5 µm in the x-direction and 10 µm in the y-direction. These step-distance values instruct the scanner to generate cross-sectional profiles every 10 µm along the length of a cut mark and to record a depth data point every five µm along these cross-sectional profiles. These step-distance values were selected to minimize data collection time, while still providing accurate and detailed representations of the studied mark. The scanner was set at a dual frequency rate of 300 Hz and 1000 Hz. Setting a dual frequency is necessary when the surface being scanned has variable reflectivity, such as the surface of a bone. Areas of low reflectivity are scanned using the lower frequency and areas of high reflectivity are scanned using the higher frequency.

Cut marks were manually oriented and levelled underneath a camera before scanning. Foam bone holders were used to manually level cut marks so they were as flat as possible in their z-axis relative to the scanner. Manually levelling cut marks is a necessary step, as the 3-mm optical pen equipped on the scanner is only able to scan depths up to 3000 μm. When a section of a cut mark is angled outside this 3000 μm range the optical pen will not record depth data from that area. Levelled cut marks were oriented with their longest axis perpendicular to the x-axis of the scanner. A rectangular area was then drawn around the cut mark using the camera provided by the Nanovea profilometer software, which defines the specific section of bone surface to be scanned. Non-cut marked bone surfaces surrounding the mark in all directions were included in each scan; including this external surface ensured that the Nanovea scanner captured the entirety of the mark and is mandatory for later analytical procedures.

3.7) Data Analysis

Scanned cut marks and archaeological molds were digitally analyzed according to the procedures outlined by Pante et al. (2017). Marks were processed and measured using Digital Surf's Mountains Software version 7.4.

<u>3.7.1) Data Processing</u>

Scanned cut mark surface files generated by the Nanovea scanner were uploaded and processed using Digital Surf's Mountains software (Figure 3.3A). First, any non-measured data points present on the unmodified scan were filled. Non-measured data points occur on scans with variable reflectivity and were only filled when the missing data point did not occur in the cut mark itself. Missing data points were filled using a function from the Mountains software that takes the mean of all data points immediately surrounding the non-measured point and estimates the expected depth value of the missing data point. Following this step, the form of the bone surface was removed from the scan by levelling the non-cut marked surface portion of the scan. This process works by excluding the cut mark data from the levelling algorithm, producing a scanned surface that contains a flat and unmodified cut mark (Figure 3.3B). Once the marks were leveled, any large peaks or holes present on the non-cut marked portions of the scan were retouched and removed. Due to the topographical nature of the raster images produced by this methodology, this step is necessary to prevent non-informative and extreme data points outside the cut mark from obscuring cut mark morphology. Finally, when more than one cut mark was present on the same scanned surface, the scan was divided so each mark could be analyzed independently.

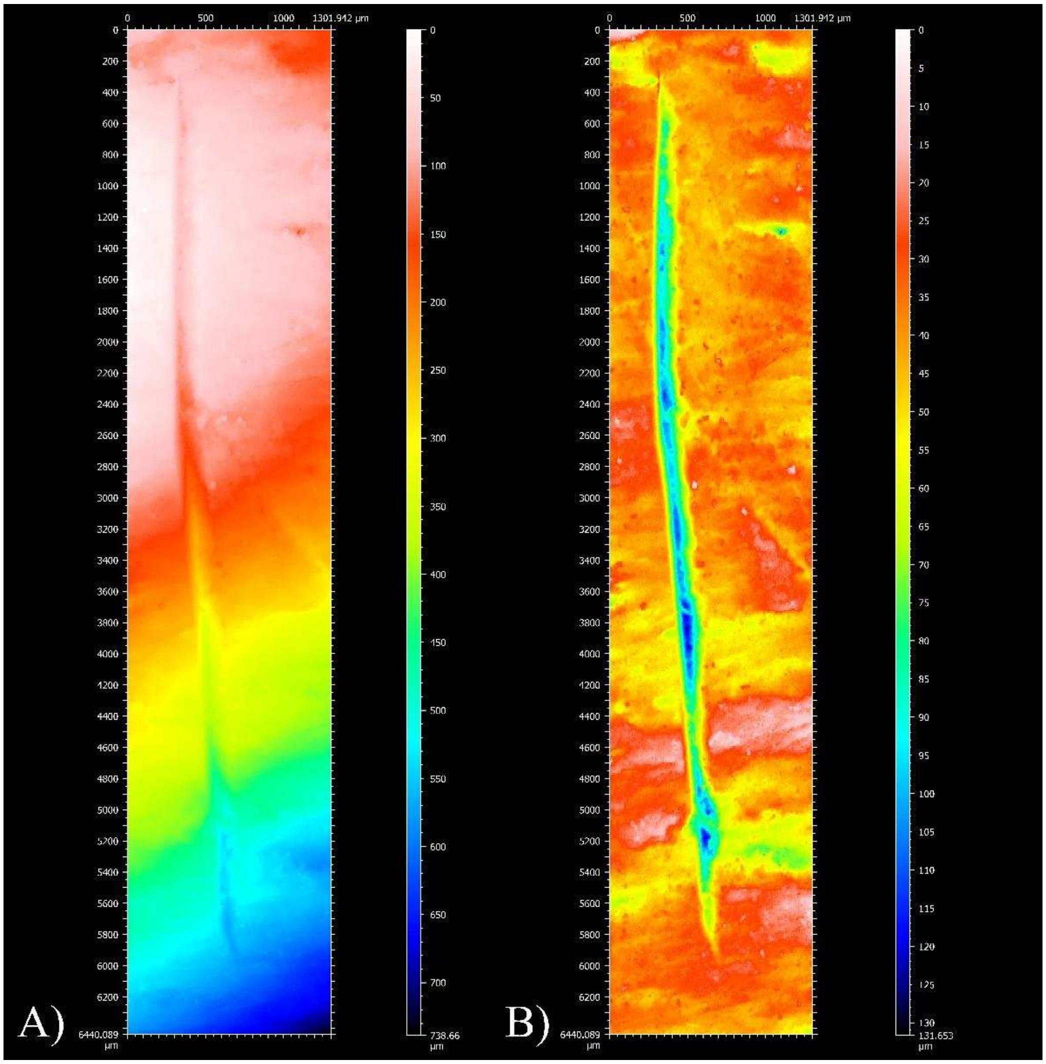

Figure 3.3) Unmodified bone surface produced by the Nanovea scanning software (A) and the bone surface after having non-measured points filled in, the form removed and retouched (B). Color scales next to each surface represent depth.

3.7.2) 3-Dimensional Cut Mark Measurements

Once the cut mark files were processed, measurements were taken from the 3-D reconstruction of each mark. Maximum length (µm) and width measurements (µm) were recorded using the “distance” tool provided by the Digital Surf’s Mountains software (Figure 3.4A). Length was taken as the maximum distance from one end of a cut mark to the other and could be measured in multiple increments if the cut mark was not straight. Width was recorded perpendicular to this length measurement and was taken along the widest part of the entire cut mark. Volume (µm^3), surface area (µm^2), maximum depth (3-D) (µm), and mean depth (µm) measurements were recorded using the “volume of a hole” function provided by the software. This tool allows users to manually outline the boundary of a mark using a series of interconnected points and records the measurements from within this defined area (Figure 3.4B). This tool uses a least squares plane parameter to create a covering overtop of the cut mark, which represents an estimation of the pre-cut mark bone surface and allows 3-D volume measurements to be recorded from within this enclosure.

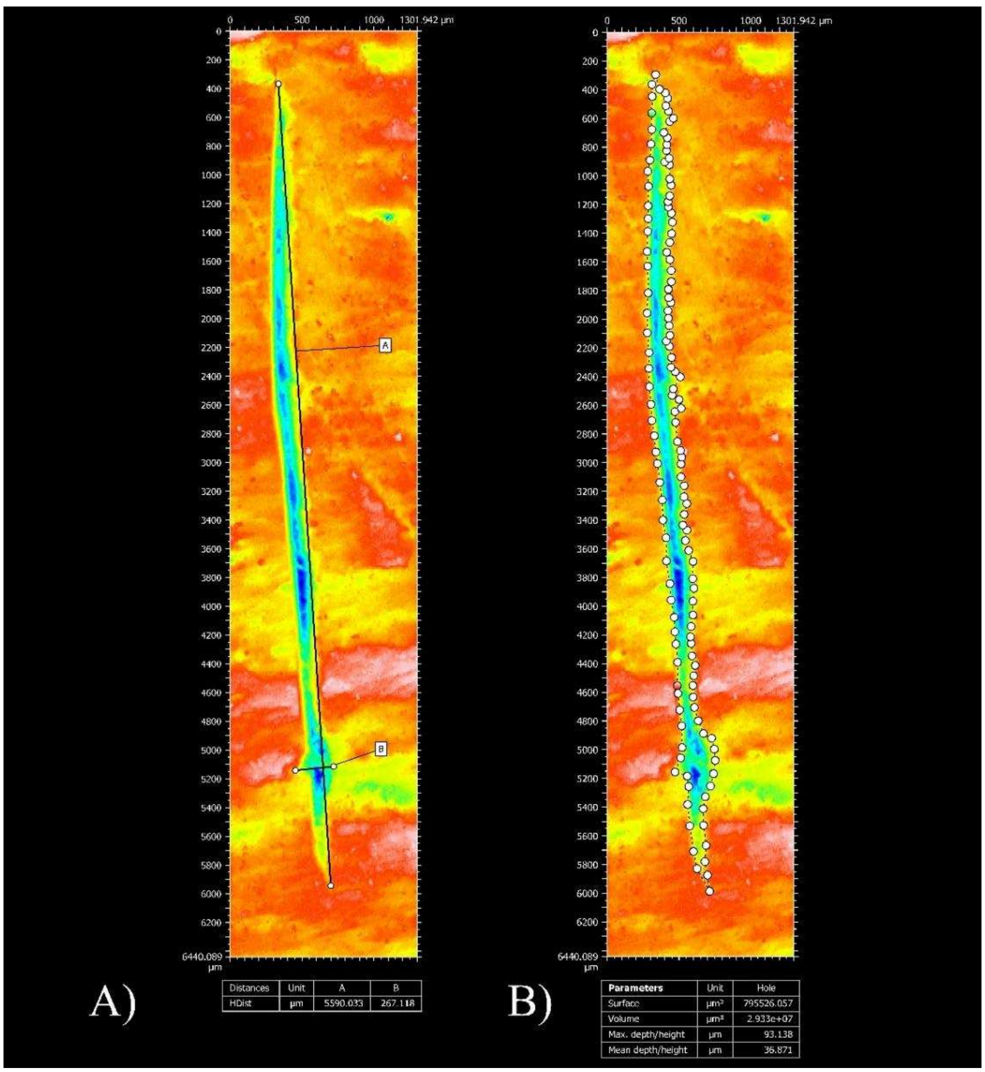

Figure 3.4) Example of cut mark length and width measurements (A), and volume, surface area, maximum depth (3-D), and mean depth measurements (B). Parameter boxes underneath each scan record the specific values associated with each of the six measurements.

3.7.3) 2-D Cross-Sectional Profile Measurements

A 2-D cross-sectional profile was taken and analyzed from each cut mark across the deepest point of the entire mark (Figure 3.5). Profiles were extracted perpendicular to the long axis of the cut mark, which in some instances was oblique to the scanned surface. The deepest cross-sectional profile was identified using the "extract profile" function provided by the Mountains software. The deepest profile was chosen for analysis as it is thought to be the most reliably identified profile between different scans of the same cut mark (Pante et al., 2017). As well, having the software automatically select the cross-sectional profile to be analyzed limits selection bias and increases the comparability of scanned data between researchers.

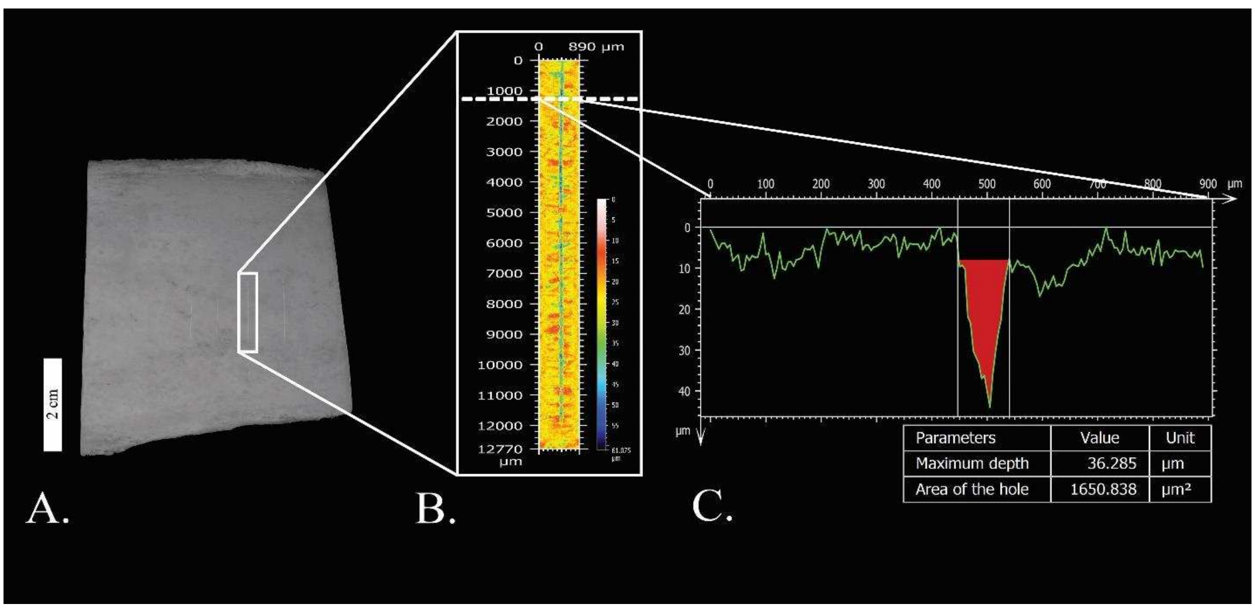

Figure 3.5) Example of the cut mark cross-sectional profile extraction process. (A) represents a cut marked bone, (B) depicts the profile containing the deepest point of this cut mark, and (C) represents the extracted profile with the "area of a hole" function applied.

The total cut mark area (µm^2) and maximum depth (profile) (µm) of each cross-sectional profile was recorded using the Mountains software "area of a hole" function with an "under the water" measurement setting. This function allows users to manually define the leftmost and rightmost boundaries of a cut mark in the cross-sectional profile and measures within the selected area (Figure 3.6). The "under the water" measurement setting limits the height of the area measured from a cut mark profile to be under the height of the lowermost edge of the cut mark. From the area selected using this function, the left-most and right-most x-axis coordinates of the cut mark can be identified on the cross-sectional profile containing both the mark and external bone surface (Figure 3.6). These two boundary coordinates can then be used to excise the cut mark from the entire cross-sectional profile that includes unmodified bone surface, creating a new 2-D profile containing only the cut mark.

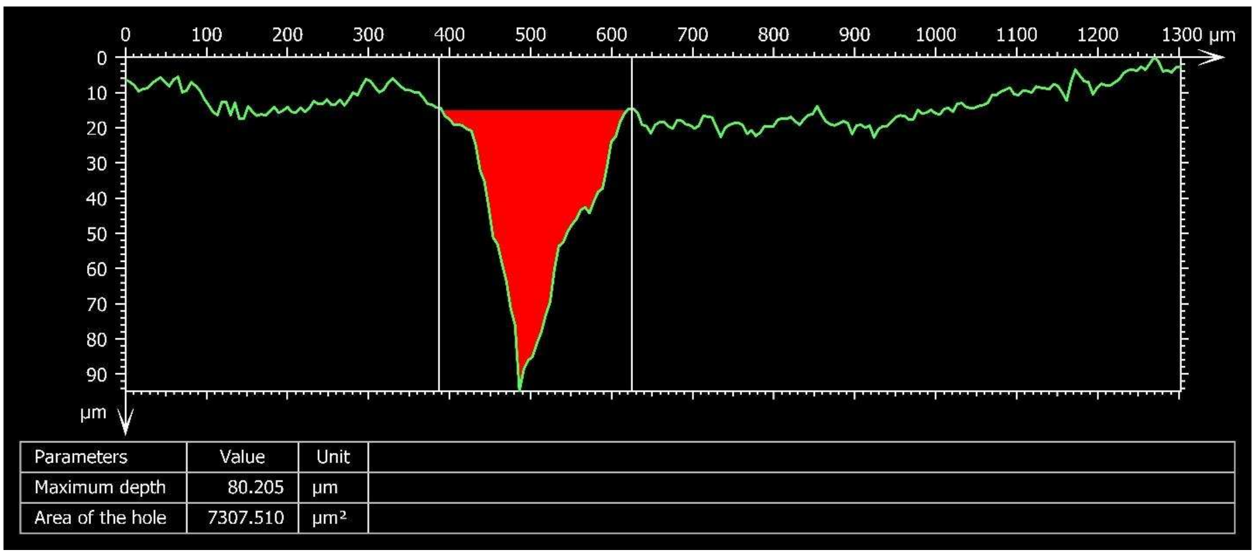

Figure 3.6) 2-D cross-sectional profile of a cut mark taken at its deepest point. The red section depicts the area of the cut mark used to measure the variables located in the parameters table. The vertical white lines represent the user defined leftmost and rightmost boundaries of this cut mark.

The profile width (µm) of the cut mark was recorded from the extracted 2-D cross-sectional profile containing only the mark. The roughness (R_a) of this extracted cut marks profile was recorded using the "parameters table" function, which provides a variety of surface texture measurements. The opening angle (^{o}) and radius (µm) of the cut mark were also calculated from this extracted profile using the "contour analysis" function provided by the associated software. Cut mark opening angle was calculated by measuring the angle between two best fit lines extending from each side of the cut mark profile to the deepest point (Figure 3.7). Cut mark radius was calculated by measuring the radius of a best fit arc extending between the leftmost and rightmost sides of the cut mark profile (Figure 3.8).

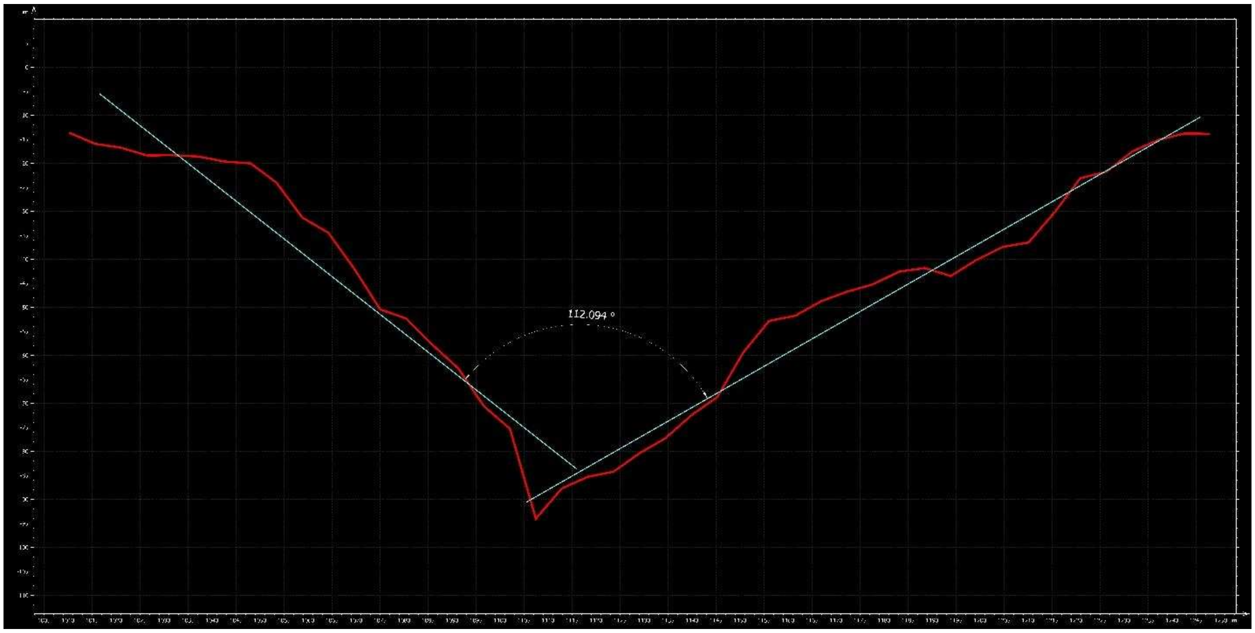

Figure 3.7) Cut mark opening angle measurement. Red line represents the cut mark; blue lines represent best fit lines from each side of the profile to the deepest point.

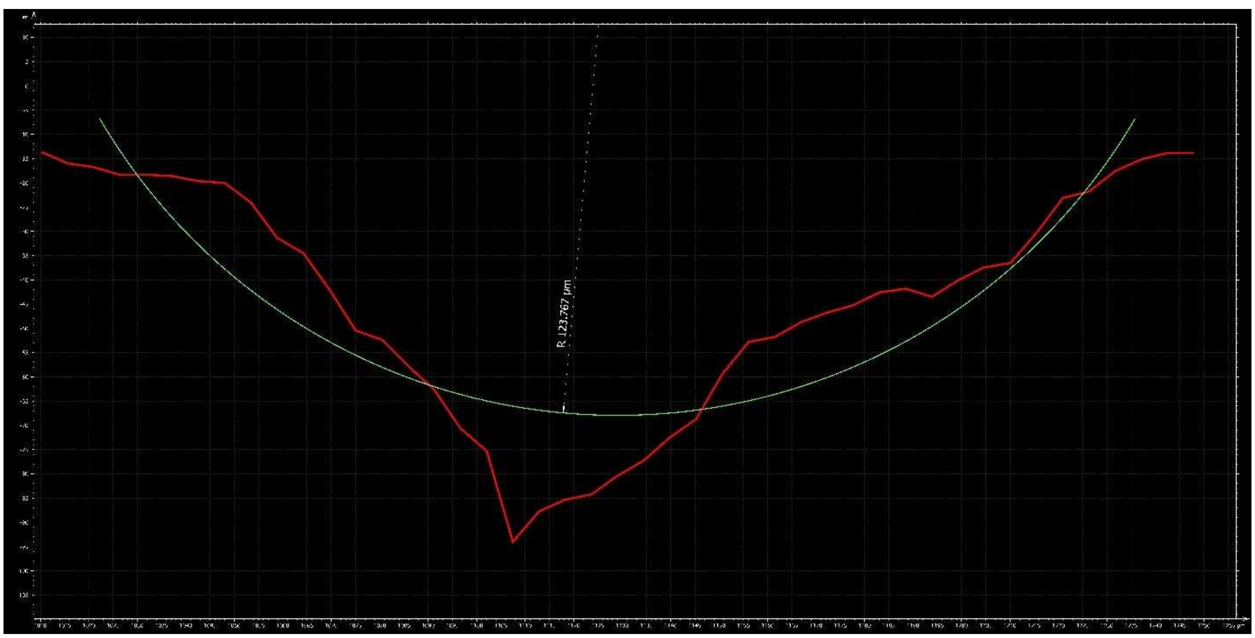

Figure 3.8) Cut mark radius measurement. Red line represents the cut mark; green line represents the best fit arc of the entire mark.

3.8) Statistical Analysis

Statistical analyses were performed using Microsoft Excel, PAST-Paleontological Statistics Software Package 3.16 (Hammer et al., 2001), and R 3.4.2 (R Core Team, 2017).

<u>3.8.1) Univariate Analysis</u>

The cut mark data used in this analysis was initially grouped into eight categories based on the technological form and raw material of the tool that created each mark (Table 3.1). Shapiro-Wilks tests were first used to identify whether each recorded measurement was normally distributed for all cut mark groups. These tests were conducted using the statistical PAST 3.16 software. Measurements indicating the presence of at least one non-normally distributed group were corrected using Box-Cox transformations. Optimal lambda values for the Box-Cox transformations were calculated using a preprogramed function found in the PAST software. However, non-parametric tests were still used for all following univariate analyses due to the presence of a minimal number of cut mark groups that remained not normally distributed following the Box-Cox transformations for some measurements. A Kruskal-Wallis test was performed on each measurement using the R "dunn.test" package (Dinno, 2017). This test indicates whether a statistically significant pairwise relationship is present in the distribution of data between cut mark groups. Following the indication of a statistically significant result (*p*-value less than 0.05), a *post hoc* unadjusted two-tailed Dunn's test from the R package "dunn.test" (Dinno, 2017) was applied to each measurement. Dunn's tests were not adjusted using a multiple comparisons adjustment procedure due to the foundational and exploratory nature of this project (Rothman, 1990). However, as this database is expanded future analyses should consider using adjustments for multiple comparisons.

3.8.2) Multivariate Analysis

Multivariate normality was first determined using a Mardia's Test of Multivariate Skewness and Kurtosis for each grouping of cut marks. Mardia's Tests were performed using the "mardiaTest" function from the R "MVN" package (Korkmaz et al., 2016). Normalized data is an important quality for multivariate discriminant analysis models and, therefore, all data was transformed to provide the most normalized distribution possible (McLachlan, 2004). Quadratic discriminant analyses (QDA) using all 12 of the measured variables were applied to a variety of cut mark groupings to test the accuracy of using multivariate statistics to classify cut marks. QDA were used in lieu of the linear discriminant analyses performed by Pante et al. (2017) due to the lack of homogenous variance-covariance matrices across groups, as determined by Box's M tests. Box's M tests were performed using the "boxM" function found in the R "biotools" package (da Silva, 2017). QDA were performed using the "qda" function found in the R "MASS" package (Ripley et al., 2017). QDA creates discriminatory models capable of categorizing unknown multivariate data points into groups using a quadratic dimensionality reduction technique. Discriminant analysis expands upon the theoretical principals defined in Bayes' Theorem to identify and estimate predicted multivariate distributions of cut mark groups using posterior information from the experimental multivariate data (McLachlan, 2004). The output of QDA are posterior probability estimates for each cut mark data point, which demonstrate the certainty of the discriminant model when classifying data into each of the predefined cut mark groups of the model (Ripley et al., 2017). QDA were created in this thesis for numerous subgroupings of cut marks based on various similarities in the technological form and raw material of the tool that made each mark. Sliced average variance estimation (SAVE) tests were performed on each discriminant model in this study to identify the first two discriminatory dimensions. This test was performed using the “dr” and “dr.direction” functions found in the R “dr” package (Weisberg, 2015). This step is necessary as quadratic discriminant analysis in the R “MASS” package do not provide canonical variables that can be plotted; however, the distribution of variables is considered to be the same between QDA and SAVE tests when visually representing data (Cook and Yin, 2001; Pardoe et al., 2007). The numerous QDA models created in the experimental portion of this thesis were used to classify archaeological cut marks that were created by tools of unknown technological form and raw material type. All archaeological trace mark data was first transformed using the same Box-Cox transformation methods used on the experimental data in order to be comparable. Archaeological cut marks were assigned to a cut mark group based on all their recorded measurement distributions in comparison to the experimentally created cut mark data.

CHAPTER 4 RESULTS

4.1) Assessment of Univariate Normality

Box plots were created for each studied metric to visualize and document instances of non-normalized data for each of the 12 cut mark measurements recorded in this thesis (Appendix A). Shapiro-Wilk tests of normality were conducted individually on all measurements for each cut mark group. All analyzed measurements indicated a non-normal distribution for at least one cut mark group and were transformed using a Box-Cox transformation. Optimal lambda values for each variable were automatically obtained using the PAST Statistical software (Table 4.1).

Table 4.1) Optimal lambda values applied for each Box-Cox measurement transformation.

	Measurement	**Optimal Lambda**
3-D Measurements	Surface Area	0.1177
	Volume	-0.0429
	Maximum Depth	-0.5017
	Mean Depth	-0.4521
	Maximum Length	0.4047
	Maximum Width	-0.3086
Profile Measurements	Maximum Depth	-0.2012
	Area	-0.0652
	Width	-0.069
	Roughness	-0.0731
	Angle	2.1549
	Radius	-0.1983

4.2) Univariate Differences in Cut Mark Micromorphology

Kruskal-Wallis tests were conducted between each tool technology group for all measured variables. Kruskal-Wallis tests were used for all variables due to the presence of non-normalized data within tool technology groups for some of the measured variables. Instances of significant differences were noted when a *p*-value of less than or equal to 0.05 was reported. All

12 measurements analyzed indicated the presence of at least one statistically significant relationship in the multiple pairwise comparisons of cut mark groupings (Table 4.2).

Table 4.2) Kruskal-Wallis test comparisons for each univariate measurement between cut mark groupings based on the tool form and raw material that made the mark. Bolded *p*-values indicate a significant result.

	Measurement	*df*	*H*	*p*-value
3-D Measurements	Surface Area	7	19.06	**0.008**
	Volume	7	17.22	**0.016**
	Maximum Depth	7	17.83	**0.013**
	Mean Depth	7	21.28	**0.003**
	Maximum Length	7	20.65	**0.004**
	Maximum Width	7	25.06	**<0.001**
Profile Measurements	Maximum Depth	7	23.27	**0.002**
	Area	7	16.65	**0.020**
	Width	7	23.52	**0.001**
	Roughness	7	23.81	**0.001**
	Opening Angle	7	34.97	**<0.001**
	Radius	7	23.76	**0.001**

Following the rejection of the Kruskal-Wallis tests, *post hoc* Dunn's test were applied to each measurement variable to identify pairs of cut mark groupings with statistically significant relationships. Dunn's tests were used for all *post hoc* tests in lieu of other multiple pairwise comparison tests due to the presence of some measurement groups having non-normalized data. Instances of statistically significant relationships were noted when a *p*-value of less than 0.05 was recorded. Each test identified at least one statistically significant pairwise relationship between tool groups for the studied variable (Tables 4.3-4.14). Surface area taken from the 3-D cut mark reconstruction and cross-sectional profile area measurements noted the fewest significant relationships, with only 6 out of 28 pairs having a significant difference (Table 4.3 and Table 4.10). The Dunn's Test comparing 3-D cut mark width measurements noted the greatest number of statistically significant relationships, with 12 of 28 cut mark pairs indicating a statistical difference. Twenty-five out of the 28 tool pairs reported a statistically significant relationship for at least one measurement variable. Tool group pairs that indicated no statistically significant relationships between any of the 12 measurement variables were basalt and phonolite flakes, basalt and chert flakes, and chert flakes and bifaces.

Table 4.3) Dunn's Multiple Comparison Test for cut mark surface area measurements (3-D) between all studied cut mark groups. Statistically significant relationships are bolded.

	Quartzite Biface	**Quartzite Flake**	**Basalt Biface**	**Basalt Flake**	**Chert Biface**	**Chert Flake**	**Phonolite Biface**
Quartzite Flake	0.099						
Basalt Biface	**0.008**	0.329					
Basalt Flake	0.790	0.157	**0.015**				
Chert Biface	**0.003**	0.193	0.726	**0.006**			
Chert Flake	0.056	0.805	0.462	0.093	0.286		
Phonolite Biface	0.245	0.627	0.141	0.358	0.074	0.461	
Phonolite Flake	0.972	0.107	**0.009**	0.818	**0.004**	0.061	0.260

Table 4.4) Dunn's Multiple Comparison Test for cut mark volume measurements (3-D) between all studied cut mark groups. Statistically significant relationships are bolded.

	Quartzite Biface	Quartzite Flake	Basalt Biface	Basalt Flake	Chert Biface	Chert Flake	Phonolite Biface
Quartzite Flake	0.284						
Basalt Biface	**<0.001**	**0.015**					
Basalt Flake	0.249	0.951	**0.015**				
Chert Biface	**0.012**	0.146	0.338	0.156			
Chert Flake	0.168	0.767	**0.031**	0.810	0.241		
Phonolite Biface	0.230	0.898	**0.021**	0.945	0.185	0.868	
Phonolite Flake	0.514	0.675	**0.004**	0.625	0.061	0.471	0.584

Table 4.5) Dunn's Multiple Comparison Test for cut mark maximum depth (3-D) measurements between all studied cut mark groups. Statistically significant relationships are bolded.

	Quartzite Biface	Quartzite Flake	Basalt Biface	Basalt Flake	Chert Biface	Chert Flake	Phonolite Biface
Quartzite Flake	0.699						
Basalt Biface	**0.001**	**0.003**					
Basalt Flake	**0.016**	**0.043**	0.313				
Chert Biface	0.070	0.153	0.119	0.569			
Chert Flake	0.185	0.350	**0.036**	0.275	0.613		
Phonolite Biface	**0.011**	**0.031**	0.417	0.859	0.463	0.212	
Phonolite Flake	0.088	0.187	0.095	0.497	0.915	0.691	0.400

Table 4.6) Dunn's Multiple Comparison Test for cut mark mean depth (3-D) measurements between all studied cut mark groups. Statistically significant relationships are bolded.

	Quartzite Biface	**Quartzite Flake**	**Basalt Biface**	**Basalt Flake**	**Chert Biface**	**Chert Flake**	**Phonolite Biface**
Quartzite Flake	0.972						
Basalt Biface	**0.010**	**0.009**					
Basalt Flake	**0.011**	**0.010**	0.984				
Chert Biface	0.972	0.999	**0.009**	**0.010**			
Chert Flake	0.652	0.678	**0.002**	**0.002**	0.677		
Phonolite Biface	0.827	0.800	**0.019**	**0.020**	0.801	0.502	
Phonolite Flake	0.184	0.172	0.222	0.229	0.173	0.073	0.267

Table 4.7) Dunn's Multiple Comparison Test for cut mark maximum length (3-D) measurements between all studied cut mark groups. Statistically significant relationships are bolded.

	Quartzite Biface	**Quartzite Flake**	**Basalt Biface**	**Basalt Flake**	**Chert Biface**	**Chert Flake**	**Phonolite Biface**
Quartzite Flake	0.292						
Basalt Biface	0.149	0.711					
Basalt Flake	0.114	**0.008**	**0.002**				
Chert Biface	0.804	0.420	0.233	0.067			
Chert Flake	0.204	**0.020**	**0.006**	0.762	0.129		
Phonolite Biface	0.251	0.924	0.784	**0.006**	0.368	**0.015**	
Phonolite Flake	0.232	**0.025**	**0.008**	0.716	0.149	0.950	**0.019**

Table 4.8) Dunn's Multiple Comparison Test for cut mark maximum width (3-D) measurements between all studied cut mark groups. Statistically significant relationships are bolded.

	Quartzite Biface	**Quartzite Flake**	**Basalt Biface**	**Basalt Flake**	**Chert Biface**	**Chert Flake**	**Phonolite Biface**
Quartzite Flake	**0.005**						
Basalt Biface	0.641	**0.018**					
Basalt Flake	**<0.001**	0.505	**0.002**				
Chert Biface	**0.017**	0.692	**0.049**	0.284			
Chert Flake	**0.005**	0.995	**0.017**	0.496	0.694		
Phonolite Biface	0.264	0.096	0.501	**0.018**	0.204	0.094	
Phonolite Flake	**0.001**	0.644	**0.004**	0.845	0.391	0.636	**0.033**

Table 4.9) Dunn's Multiple Comparison Test for cut mark maximum depth (profile) measurements between all studied cut mark groups. Statistically significant relationships are bolded.

	Quartzite Biface	**Quartzite Flake**	**Basalt Biface**	**Basalt Flake**	**Chert Biface**	**Chert Flake**	**Phonolite Biface**
Quartzite Flake	0.420						
Basalt Biface	**<0.001**	**0.001**					
Basalt Flake	**0.010**	0.077	0.099				
Chert Biface	**0.044**	0.226	**0.031**	0.594			
Chert Flake	0.183	0.604	**0.004**	0.210	0.482		
Phonolite Biface	**0.007**	0.057	0.148	0.862	0.488	0.161	
Phonolite Flake	**0.031**	0.178	**0.044**	0.693	0.892	0.401	0.577

Table 4.10) Dunn's Multiple Comparison Test for cut mark area (profile) measurements between all studied cut mark groups. Statistically significant relationships are bolded.

	Quartzite Biface	**Quartzite Flake**	**Basalt Biface**	**Basalt Flake**	**Chert Biface**	**Chert Flake**	**Phonolite Biface**
Quartzite Flake	0.991						
Basalt Biface	0.692	0.683					
Basalt Flake	0.061	0.059	0.131				
Chert Biface	**0.048**	**0.046**	0.105	0.887			
Chert Flake	0.194	0.190	0.356	0.567	0.482		
Phonolite Biface	0.647	0.639	0.945	0.158	0.128	0.403	
Phonolite Flake	**0.003**	**0.003**	**0.008**	0.248	0.320	0.088	**0.012**

Table 4.11) Dunn's Multiple Comparison Test for cut mark width (profile) measurements between all studied cut mark groups. Statistically significant relationships are bolded.

	Quartzite Biface	**Quartzite Flake**	**Basalt Biface**	**Basalt Flake**	**Chert Biface**	**Chert Flake**	**Phonolite Biface**
Quartzite Flake	0.125						
Basalt Biface	0.494	**0.025**					
Basalt Flake	**0.011**	0.321	**0.001**				
Chert Biface	0.104	0.928	**0.019**	0.369			
Chert Flake	**0.043**	0.633	**0.006**	0.606	0.700		
Phonolite Biface	0.788	0.206	0.338	**0.023**	0.175	0.079	
Phonolite Flake	**0.004**	0.171	**<0.001**	0.687	0.201	0.365	**0.008**

Table 4.12) Dunn's Multiple Comparison Test for cut mark roughness (profile) measurements between all studied cut mark groups. Statistically significant relationships are bolded.

	Quartzite Biface	Quartzite Flake	Basalt Biface	Basalt Flake	Chert Biface	Chert Flake	Phonolite Biface
Quartzite Flake	0.844						
Basalt Biface	**<0.001**	**0.001**					
Basalt Flake	**0.014**	**0.024**	0.229				
Chert Biface	0.428	0.551	**0.005**	0.098			
Chert Flake	**0.044**	0.069	0.105	0.666	0.224		
Phonolite Biface	**0.011**	**0.019**	0.295	0.894	0.080	0.579	
Phonolite Flake	0.466	0.595	**0.004**	0.086	0.949	0.201	0.069

Table 4.13) Dunn's Multiple Comparison Test for cut mark opening angle (profile) measurements between all studied cut mark groups. Statistically significant relationships are bolded.

	Quartzite Biface	Quartzite Flake	Basalt Biface	Basalt Flake	Chert Biface	Chert Flake	Phonolite Biface
Quartzite Flake	0.252						
Basalt Biface	**0.003**	**<0.001**					
Basalt Flake	0.501	0.621	**<0.001**				
Chert Biface	0.542	0.592	**<0.001**	0.959			
Chert Flake	0.208	0.920	**<0.001**	0.547	0.521		
Phonolite Biface	0.051	**0.002**	0.308	**0.008**	**0.010**	**0.001**	
Phonolite Flake	0.457	0.687	**<0.001**	0.933	0.894	0.612	**0.007**

Table 4.14) Dunn's Multiple Comparison Test for cut mark radius (profile) measurements between all studied cut mark groups. Statistically significant relationships are bolded.

	Quartzite Biface	**Quartzite Flake**	**Basalt Biface**	**Basalt Flake**	**Chert Biface**	**Chert Flake**	**Phonolite Biface**
Quartzite Flake	0.236						
Basalt Biface	**0.010**	**<0.001**					
Basalt Flake	0.283	0.893	**<0.001**				
Chert Biface	0.890	0.295	**0.007**	0.352			
Chert Flake	0.465	0.642	**0.001**	0.735	0.554		
Phonolite Biface	0.234	**0.018**	0.175	**0.022**	0.184	0.053	
Phonolite Flake	0.509	0.600	**0.001**	0.689	0.602	0.949	0.064

The cut mark group made by basalt biface tools had the greatest number of statistically significant relationships for all 12 measurements analyzed in this univariate analysis. Of the 104 pairwise relationships that noted a significant relationship, basalt biface cut marks were included in 52. The quartzite biface cut mark group noted 30 statistically significant relationships, the second most out of all eight cut mark groups. Alternatively, chert flake and chert bifaces reported the fewest number of statistically significant univariate relationships, with only 16 and 17 significant relationships respectively.

Univariate Dunn's tests between each of the 12 individual measurements of the two quartzite cut mark groups noted minimal variation. The only statistically significant measurement between quartzite biface and flake cut marks was maximum width taken from a 3-D reconstruction of the cut mark. Further examination of this relationship reveals that quartzite bifaces tend to have significantly larger cut mark widths compared to quartzite flake cut marks (Figure 4.1).

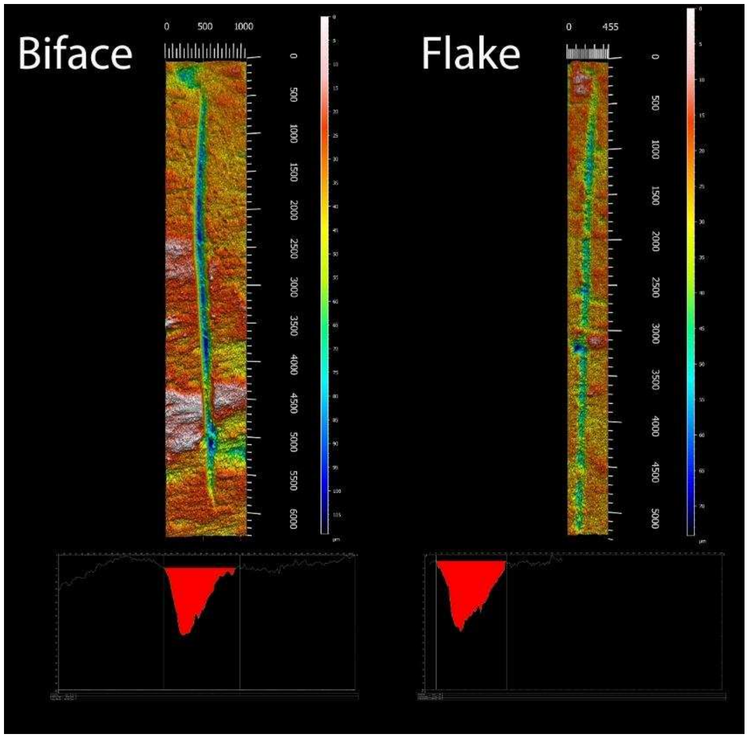

Figure 4.1) Example of 3-D top view and deepest cross-sectional profile of cut marks made by quartzite biface and flake tools. Both cross-sectional profiles are standardized to be 100 µm deep and 1000 µm long to enhance visual comparability.

A detailed examination of the 12 univariate measurement reported by each basalt cut mark group shows that multiple measurements are statistically distinct between cut marks made by basalt biface and basalt flake tools. Univariate Dunn's tests show that basalt bifaces tend to have statistically larger cut mark surface area, width, opening angle, and radius measurements compared to cut marks made by basalt flakes. These tests also indicate that cut marks made by basalt flake tools tend to have significantly larger cut mark volume and length measurements compared to basalt biface cut marks (Figure 4.2).

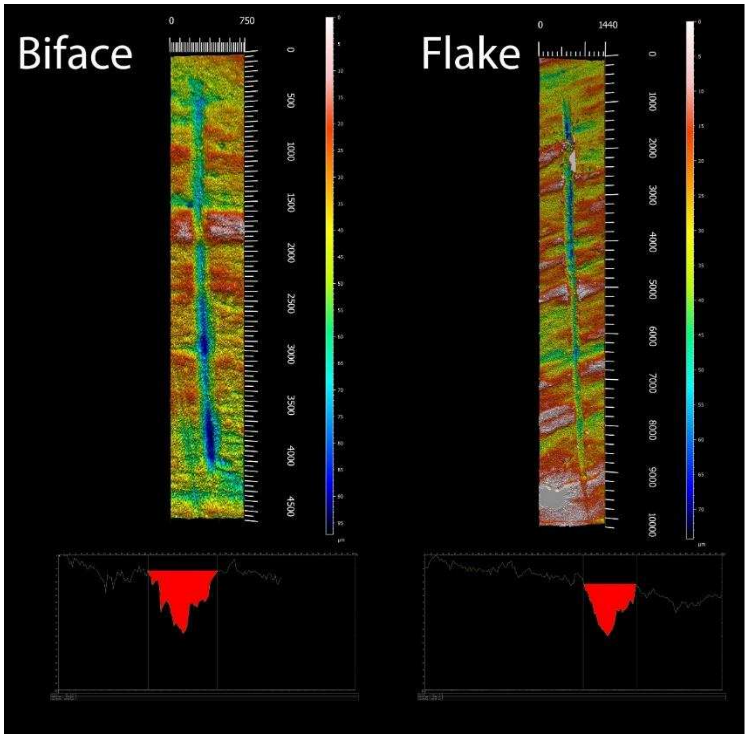

Figure 4.2) Example of 3-D top view and deepest cross-sectional profile of cut marks made by basalt biface and flake tools. Both cross-sectional profiles are standardized to be 100 µm deep and 1000 µm long to enhance visual comparability.

Univariate Dunn's test of all 12 cut mark measurements studied in this thesis noted no statistically significant pairwise relationships between cut marks made by chert biface and chert flake tools (Figure 4.3). Macroscopic and empirically untested observations of the chert biface and flake tool edges used for this thesis suggests that both chert tool forms tend to have similarly narrow and sharp cutting edges. Similarities in tool cutting edge would likely produce cut marks that share similar micromorphological characteristics.

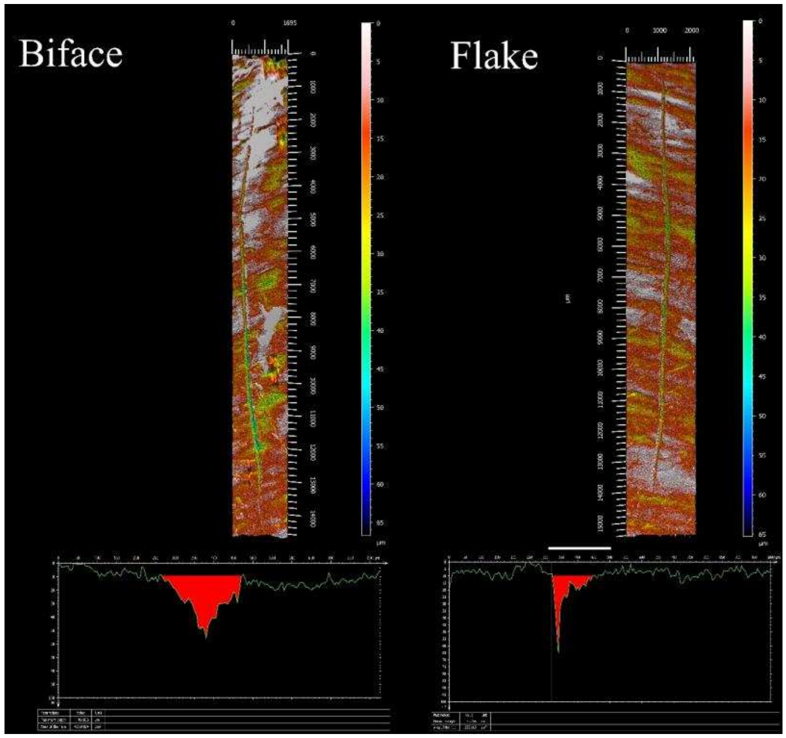

Figure 4.3) Example of 3-D top view and deepest cross-sectional profile of cut marks made by chert biface and flake tools. Both cross-sectional profiles are standardized to be 100 µm deep and 1000 µm long to enhance visual comparability.

Further examination of the univariate Dunn's tests performed on each of the 12 measurements identified numerous statistically significant differences between cut marks made by phonolite biface and flake tools. In particular, these tests noted that phonolite biface cut marks tend to have larger cut mark widths, cross-sectional area and opening angle compared to phonolite flake cut marks. These same univariate analyses noted that phonolite flake cut marks tend to be significantly longer than phonolite biface cut marks (Figure 4.4).

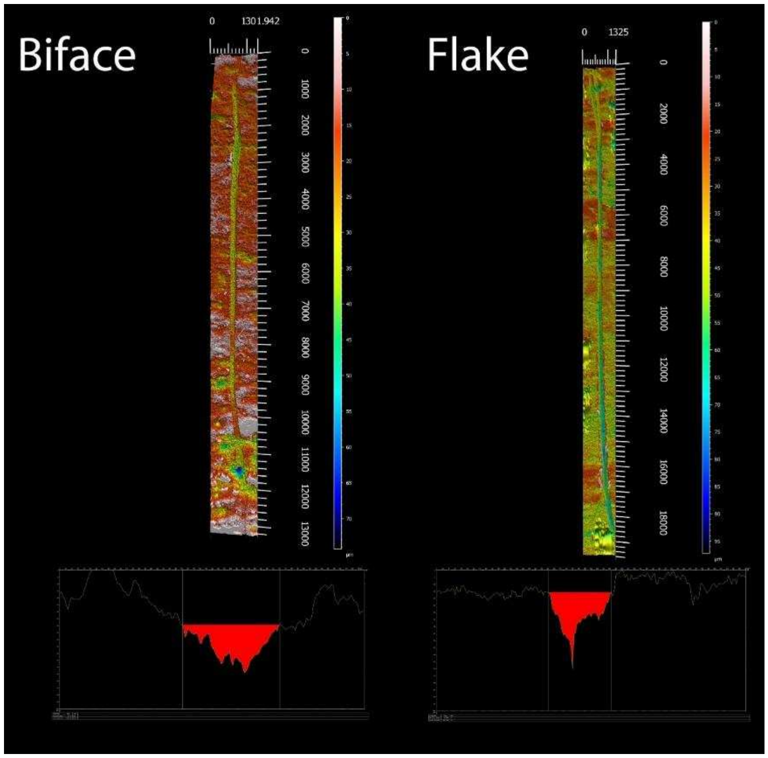

Figure 4.4) Example of 3-D top view and deepest cross-sectional profile of cut marks made by phonolite biface and flake tools. Both cross-sectional profiles are standardized to be 100 µm deep and 1000 µm long to enhance visual comparability.

4.3) Multivariate Analysis: Creating Predictive Discriminant Models

Mardia's Tests of Multivariate Normality were performed on each of the eight cut mark groupings to determine multivariate normality (Table 4.15). The basalt biface cut mark group was the only group to indicate a statistically significant deviation from multivariate normality. A *p*-value of 0.001 indicated a minimal degree of multivariate skewness in the distribution of the basalt biface cut mark data. However, it has been noted that discriminant analyses are robust enough to handle slight deviations from parametric assumptions when data is not significantly skewed (Clarke et al., 1979).

Table 4.15) *P*-values reported by Mardia's tests of Multivariate Normality for the eight cut mark groupings. Bolded values indicate statistically significant results.

Cut Mark Grouping	**Skewness**	**Kurtosis**
Quartzite Biface	0.205	0.504
Quartzite Flake	0.238	0.558
Basalt Biface	**0.001**	0.289
Basalt Flake	0.613	0.312
Chert Biface	0.107	0.590
Chert Flake	0.654	0.203
Phonolite Biface	0.470	0.273
Phonolite Flake	0.553	0.262

Box's M tests were performed on each discriminant model tested by this thesis to determine whether their variance-covariance matrices were equal between the multivariate data of the cut mark groupings (Table 4.16). Covariance matrices were considered significantly unequal when a *p*-value of less than 0.05 was identified and thus supported the use of a quadratic discriminant analysis. Eight of the nine discriminant models indicated instances of cut mark groupings lacking equal covariance matrices (Table 4.16). The Box's M test comparing the variance-covariance matrix of cut marks created by phonolite flake and biface tools noted a statistically insignificant difference. However, a quadratic discriminant model was still used to characterize this relationship in order to maintain a comparative relationship between all discriminant models described in this thesis.

Table 4.16) Box's M *p*-values reported for the different quadratic models tested in this thesis. Bolded *p*-values indicate models with statistically significant differences between the variance-covariance matrices of the cut mark groupings.

Quadratic Discriminant Groupings of Cut Marks based on Tool Effector Characteristics	**Box's M *p*-value**
Technology and Raw Material Model	**<0.0001**
Technology Only Model	**0.0283**
Raw Material Only Model	**<0.0001**
Quartzite Tool Model	**<0.0001**
Basalt Tool Model	**<0.0001**
Chert Tool Model	**0.0105**
Phonolite Tool Model	0.2123
Biface Tools by Raw Material Model	**<0.0001**
Flake Tools by Raw Material Model	**<0.0001**

Nine different discriminant models were developed in this thesis by categorizing cut mark data points into various subgroupings, based on similarities in the technological form and raw material type of the tool that created each mark. The confusion matrices created by these nine discriminant models recorded a wide range of classification accuracies, depending on how the cut mark data was subcategorized. Discriminant model accuracies ranged between 71.22% when cut marks were discriminated based only on the raw material of the tool that created them to 100% classification accuracy when cut marks created only by quartzite tools or basalt tools were compared. Sliced average variance estimation (SAVE) analyses were also conducted for each model to identify the first two and most important discriminatory dimensions created from the multivariate data reduction of all 12 measurements. These dimensions were used to graphically represent each model to better interpret and visualize the multivariate data reduction procedures executed by the quadratic discriminant analysis.

The confusion matrix created by the quadratic discriminant model classifying cut marks made by tools of all raw material and technological types classified 166 of 205 cut marks accurately (Table 4.17). The quartzite biface cut mark group was the most accurately classified group in this model, with 24 of 25 marks correctly identified as being made by a quartzite biface tool. Alternatively, the quartzite flake cut mark group was the most incorrectly classified group, having only 17 of 25 cut marks correctly classified. The discriminatory power and variable classification accuracy of this quadratic model can be assessed through the analysis and visual representation of the model's dimensional reduction generated by a SAVE analysis. Therefore, all 205 cut marks analyzed in this discriminant model were plotted along the first two SAVE dimensions of this model (Figure 4.5).

Table 4.17) Confusion matrix for the quadratic discriminant analysis classifying cut mark data based on both the technology and raw material of the tool that made each mark. The classification accuracy of this model is 80.97%. Bolded values indicate the number of correctly classified cut marks for each cut mark grouping.

		Given Group								
		Quartzite Biface	Quartzite Flake	Basalt Biface	Basalt Flake	Chert Biface	Chert Flake	Phonolite Biface	Phonolite Flake	Total
Predicted Group	Quartzite Biface	**24**	0	0	0	1	1	1	1	28
	Quartzite Flake	0	**17**	0	2	0	1	1	1	22
	Basalt Biface	1	1	**22**	0	0	0	1	1	26
	Basalt Flake	0	2	0	**22**	1	1	1	0	27
	Chert Biface	0	0	0	0	**18**	0	0	0	18
	Chert Flake	0	2	0	2	1	**21**	0	0	26
	Phonolite Biface	0	3	4	0	2	1	**20**	0	30
	Phonolite Flake	0	0	1	1	2	1	1	**22**	28
	Total	25	25	27	27	25	26	25	25	**205**

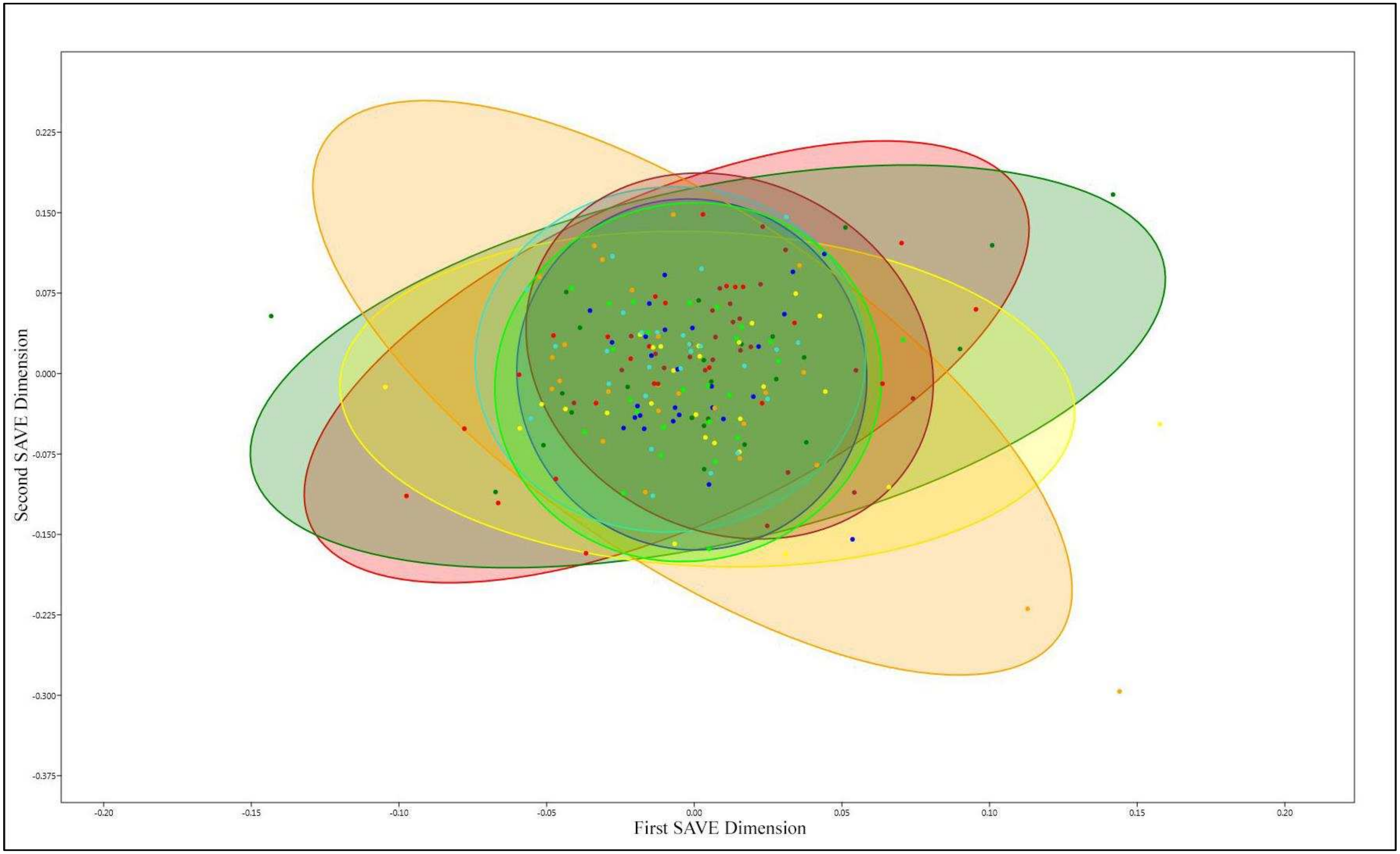

Figure 4.5) Graph showing the distribution of cut mark data points based on the results from a discriminant analysis between all eight cut mark groupings. Ellipses represent 95% confidence intervals for each cut mark group. Red dots represent quartzite biface cut marks, green dots represent quartzite flake cut marks, yellow dots represent basalt biface cut marks, blue dots represent basalt flake cut marks, orange dots represent chert biface cut marks, turquoise dots represent chert flake cut marks, brown dots represent phonolite biface cut marks, and lime-green dots represent phonolite flake cut marks.

In total, 39 of 205 cut marks misclassified in the quadratic discriminant model classifying the raw material type and technological form of the tool that made each mark. Twenty-three of the 39 incorrectly classified cut marks misclassified as being part of another cut mark group of the same tool technological form, but different raw material type. Only two of the 39 misclassified cut marks incorrectly classified in a group that was created by a tool of the same raw material, but different technological type.

Bayesian posterior probabilities provided by the tool technology and raw material quadratic discriminant model can be used to identify and interpret trends in cut mark misclassification rates in this discriminant model. Posterior probabilities provide an assessment of the discriminant models confidence when classifying a cut mark into the eight predefined tool groups of the model. The first posterior probability represents the predicted group with the largest classification percentage associated with it and is therefore the most probable tool classification for that mark in this model. When considering the 166 correctly classified data points in this tool technology and raw material model, the average first probability for these data points was 89%, with a median value of 98%. When considering the 39 incorrectly classified data points in this same model, the average first probability for these cut marks was only 62%, with a median first probability of 60%. When the first posterior probability percentages of the correctly and incorrectly classified data sets are compared using a *t*-test, a *p*-value of <0.001 is recorded, indicating a significant difference in the confidence of this model when correctly and incorrectly classifying data. The first posterior probability percentages of correctly classified data are significantly larger than the first posterior probability percentages of incorrectly classified data in this quadratic discriminant model. These values may provide insight into establishing an acceptable range of first posterior probability percentage values when classifying the unknown tool effector of an archaeological cut mark. Archaeological marks that have a first posterior probability percentage substantially less than the average 89% noted by the 166 correctly classified marks might indicate an instance of problematic classification.

The second posterior probabilities for each cut mark similarly provide insight into the effectiveness of the technology and raw material discriminant model. The second posterior probability of a cut mark represents the group classification that recorded the second largest posterior percentage, and is therefore, the second most probable tool group for that mark. Of the 39 cut marks that did not correctly classify in the tool technology and raw material discriminant model at the first posterior probability level, 27 correctly classified at the second posterior level, six at the third posterior level, three at the fourth posterior level, two at the fifth posterior level, and one at the sixth posterior level (Table 4.18). When considering the 27 misclassified cut marks that correctly classified at the second posterior probability level, the average correct posterior probability is 27.4%. Comparatively, when the second posterior probabilities of the 166 correctly classified cut marks in this model are analyzed, the average second posterior probability is 9%. When the distribution of second posterior probabilities are compared using a *t*-test between correctly and incorrectly classified cut marks, it is indicated that the second probability distribution of incorrectly classified data points is significantly larger. This comparison implies that when classifying data points of unknown origin that both the first and second posterior probabilities should be considered when evaluating the classification. If the first posterior probability is relatively small and the second posterior probability is large, then the tool classification of the unknown mark should be reevaluated, as it may be incorrect.

Table 4.18) Posterior probabilities for the 39 incorrectly classified data points from the tool technology and raw material quadratic discriminant model. (QBF = Quartzite biface, QNR = Quartzite Flake, BBF = Basalt Biface, BNR = Basalt Flake, CBF = Chert Biface, CNR = Chert Flake, PBF = Phonolite Biface, PNR = Phonolite Flake).

Actual Tool Group	1st Probability Class	1st Probability Percentage	2nd Probability Class	2nd Probability Percentage	Correct Probability Percentage	Correct Probability Level
QBF	BBF	58%	QBF	42%		
QNR	CNR	75%	QNR	25%		
QNR	PBF	36%	QNR	24%		
QNR	PBF	96%	QNR	3%		
QNR	BNR	60%	QNR	40%		
QNR	CNR	62%	QNR	19%		
QNR	BNR	71%	QNR	22%		
QNR	BBF	98%	QNR	2%		
QNR	PBF	59%	BBF	27%	27%	4
BBF	PBF	58%	BBF	42%		
BBF	PBF	60%	PNR	19%	19%	3
BBF	PBF	50%	BBF	34%		
BBF	PBF	86%	BBF	13%		
BBF	PNR	85%	BBF	14%		
BNR	CNR	49%	BNR	28%		
BNR	QNR	59%	BNR	32%		
BNR	PNR	40%	BNR	35%		
BNR	CNR	77%	QNR	8%	8%	3
BNR	QNR	86%	BNR	14%		
CBF	PBF	79%	PNR	10%	4%	5
CBF	PBF	68%	BBF	18%	2%	6
CBF	PNR	68%	CBF	18%		
CBF	BNR	65%	CNR	31%	31%	3
CBF	CNR	34%	QNR	30%	30%	3
CBF	PNR	77%	CBF	21%		
CBF	QBF	43%	CBF	29%		
CNR	QBF	36%	CNR	26%		
CNR	BNR	51%	CNR	47%		
CNR	PBF	60%	QBF	17%	5%	5
CNR	QNR	56%	CNR	42%		
CNR	PNR	49%	CNR	39%		
PBF	BNR	34%	PNR	24%	24%	4
PBF	QNR	47%	QBF	22%	21%	4
PBF	BBF	71%	QNR	10%	10%	3
PBF	QBF	60%	PBF	39%		
PBF	PNR	53%	PBF	41%		
PNR	BNR	62%	PNR	38%		
PNR	QBF	84%	QNR	10%	10%	3
PNR	QNR	50%	PNR	36%		

Third to eighth posterior probabilities were also recorded for each cut mark in this discriminant model, providing posterior probability estimations for each mark in all eight cut mark groups. However, the majority of cut marks analyzed in this thesis recorded third to eighth posterior probabilities significantly less than 0.001%. Therefore, the examination of these posterior probabilities was considered uninformative and were not analyzed further.

The confusion matrix created by a quadratic discriminant model classifying cut marks based on tool technological form, ignoring raw material, classified 161 of 205 cut marks correctly (Table 4.19). The flake cut mark group was the most accurately classified group in this model, with 83 of 103 cut marks correctly classified. The biface cut mark group classification accuracy was marginally lower than the flake cut mark group, with 78 of 102 cut marks correctly classified. A SAVE analysis was performed on this technology only discriminant model in an effort to identify and visualize the multivariate distribution of biface and flake cut marks along the two most explanatory discriminatory dimensions of this model (Figure 4.6).

Table 4.19) Confusion matrix for the quadratic discriminant analysis classifying biface and flake cut marks made by tools of all raw material types. The accuracy of this model is 78.54%. Bolded values indicate the number of correctly classified cut marks for each group.

		Given Group		
		Biface	Flake	Total
Predicted Group	Biface	**78**	20	98
	Flake	24	**83**	107
	Total	102	103	205

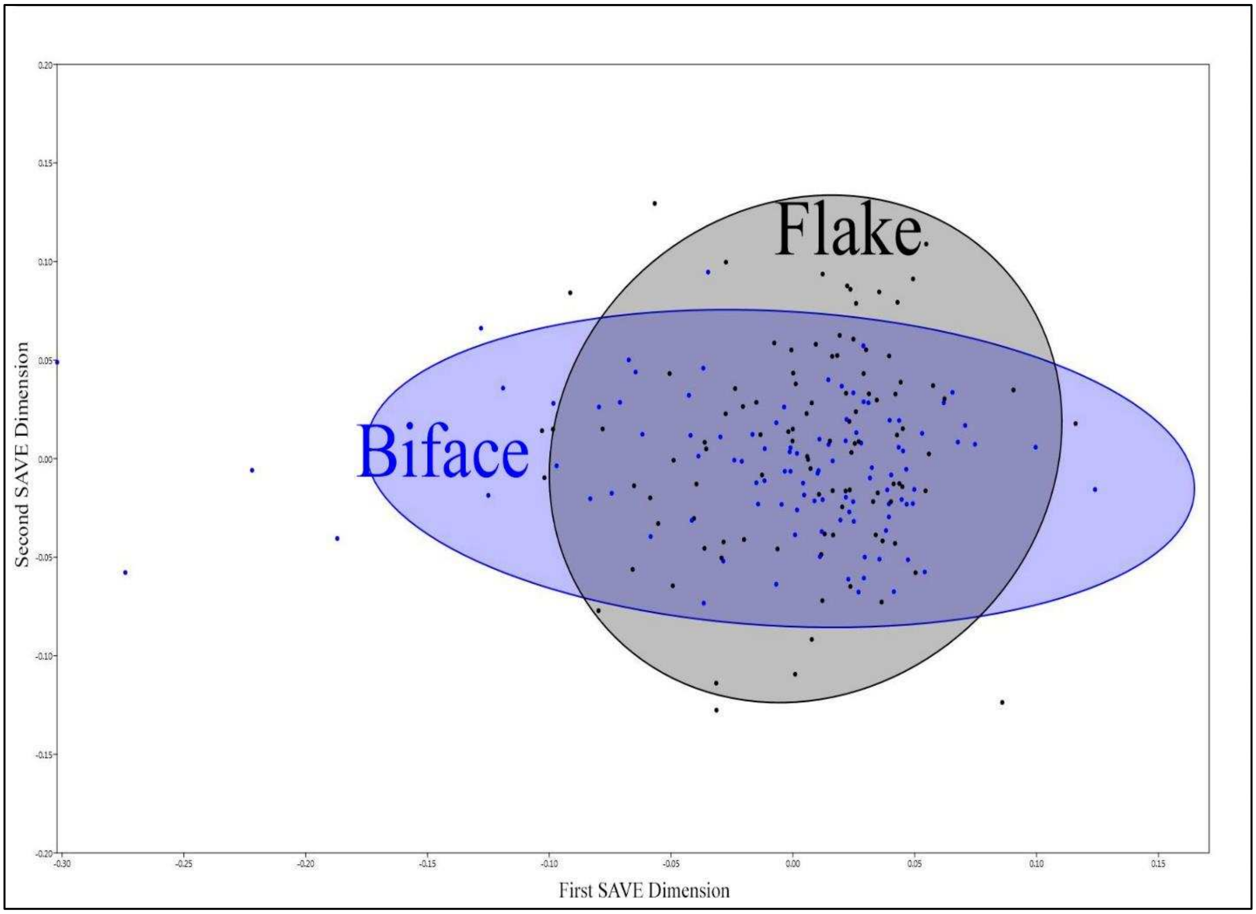

Figure 4.6) Graph showing the distribution of cut mark data points based on the results from a discriminant analysis between cut marks made by biface and flake tools. Ellipses represent 95% confidence intervals for each cut mark group. Blue dots represent biface cut marks and black dots represent flake cut marks.

The technology only discriminant model can be better understood by dividing the two technology cut mark classes back into the eight original cut mark groups that separate marks based on tool effector technological form and raw material (Table 4.20). This new confusion matrix shows that cut marks made by basalt flakes were the most accurately classified group in the technology only model, with 25 of 27 cut marks correctly identified as being made by a flake tool. Alternatively, cut marks made by chert biface and phonolite biface tools were the two most misclassified cut mark groups in this model. Both groups incorrectly classified eight of 25 cut marks, accounting for over 36% of the misclassified marks. Interestingly, the classification accuracies for the eight cut mark groups in the tool technology only discriminant model do not correlate to the classification accuracies recorded in the tool technology and raw material discriminant model when the same cut mark groupings are compared (Table 4.17). For example, the tool technology and raw material model correctly classified 22 of 27 basalt flake cut marks, much less than the 25 of 27 correctly classified basalt flake cut marks in the tool technology only model. The only two cut mark groups that had relatively similar classification accuracies in both discriminant models were the chert biface and basalt biface cut mark groups.

Table 4.20) Confusion matrix for a quadratic discriminant model classifying cut marks made by different tool technologies. Original cut mark classifications are subdivided based on tool raw material type and technological form to better recognize differences in classification accuracy between cut mark groups. Bolded values indicate the number of correctly classified cut marks for each of the eight cut mark groupings

		Original Cut Mark Grouping							
		Quartzite Biface	Basalt Biface	Chert Biface	Phonolite Biface	Quartzite Flake	Basalt Flake	Chert Flake	Phonolite Flake
Predicted	Biface	**21**	**23**	**17**	**17**	5	2	8	5
	Flake	4	4	8	8	**20**	**25**	**18**	**20**

Posterior probabilities for the tool technology only discriminant model were also recorded, providing first and second posterior probability for all 205 cut marks. This model provided only two posterior probability levels, as only two possible cut mark group classifications were considered. When considering the 161 cut marks that correctly classified in this model, the average first posterior probability was 84%, with a median probability of 89%. When considering the 44 cut marks that incorrectly classified in the tool technology only model, the average first posterior probability was 69%, with a median classification probability of 66%. Similar to the discriminant model classifying cut marks based on both tool technology and raw material, when the correct and incorrect first posterior probability distributions are compared using a *t*-test, a *p*-value of <0.001 is recorded. Again, this *p*-value suggests that this discriminant model records statistically distinct posterior probabilities when correctly and incorrectly classifying cut marks.

The average second posterior probabilities for the 161 data points correctly classified in the tool technology only discriminant model was 16.4%. Comparatively, the average second posterior probability for the 44 cut marks that incorrectly classified in this discriminant model was 31.4%. When the distribution of these two second posterior probability groups are compared using a *t*-test, it is reported that the second posterior probabilities of incorrectly classified cut marks are significantly larger than the second posterior probabilities of correctly classified cut marks. This observation supports the inference that all posterior probability percentages should be considered when classifying cut marks of unknown origin. If the first and second posterior probabilities associated with an archaeological cut mark are relatively low, then the tool classification of that mark should be evaluated further.

The effectiveness and classification accuracy of the tool technology only model can be further investigated when the variable of raw material is completely removed from the discriminant analysis. This is achieved by creating new discriminant models that only compare cut marks made by tools of differing technology of one raw material type. The classification accuracy of these models ranges between 100% when classifying cut marks based on technological form of quartzite or basalt tools, 96% when discriminating the tool form of phonolite tools, and 93% when discriminating chert tool forms (Table 4.21).

Table 4.21) Classification accuracies of tool technology only quadratic discriminant models that include tools made of only one raw material type.

Cut Mark Grouping	Classification Accuracy (%)
Quartzite Tools	100
Basalt Tools	100
Chert Tools	92.16
Phonolite Tools	96

The confusion matrix created by a quadratic discriminant analysis classifying cut marks based only on tool raw material type correctly classified 146 out of 205 cut marks (Table 4.22). The most accurately classified cut mark group in this model are cut marks made by phonolite tools, with 40 of 50 cut marks classified correctly. Cut marks made by quartzite tools are the least accurately classified cut mark group in this model, with only 30 of 50 cut marks correctly classified. A SAVE analysis was performed on this discriminant model to identify and visualize the distribution of the four cut mark groups along the two most important and explanatory dimensions of the model (Figure 4.7).

Table 4.22) Confusion matrix for a quadratic discriminant analysis classifying cut marks by tool raw material type. The accuracy of this model is 71.22%. Bolded values indicate the number of correctly classified cut marks for each cut mark grouping.

		Given Group				
		Quartzite	Basalt	Chert	Phonolite	Total
Predicted Group	Quartzite	**30**	4	3	2	39
	Basalt	7	**39**	4	4	54
	Chert	3	4	**37**	4	48
	Phonolite	10	7	7	**40**	64
	Total	50	54	51	50	205

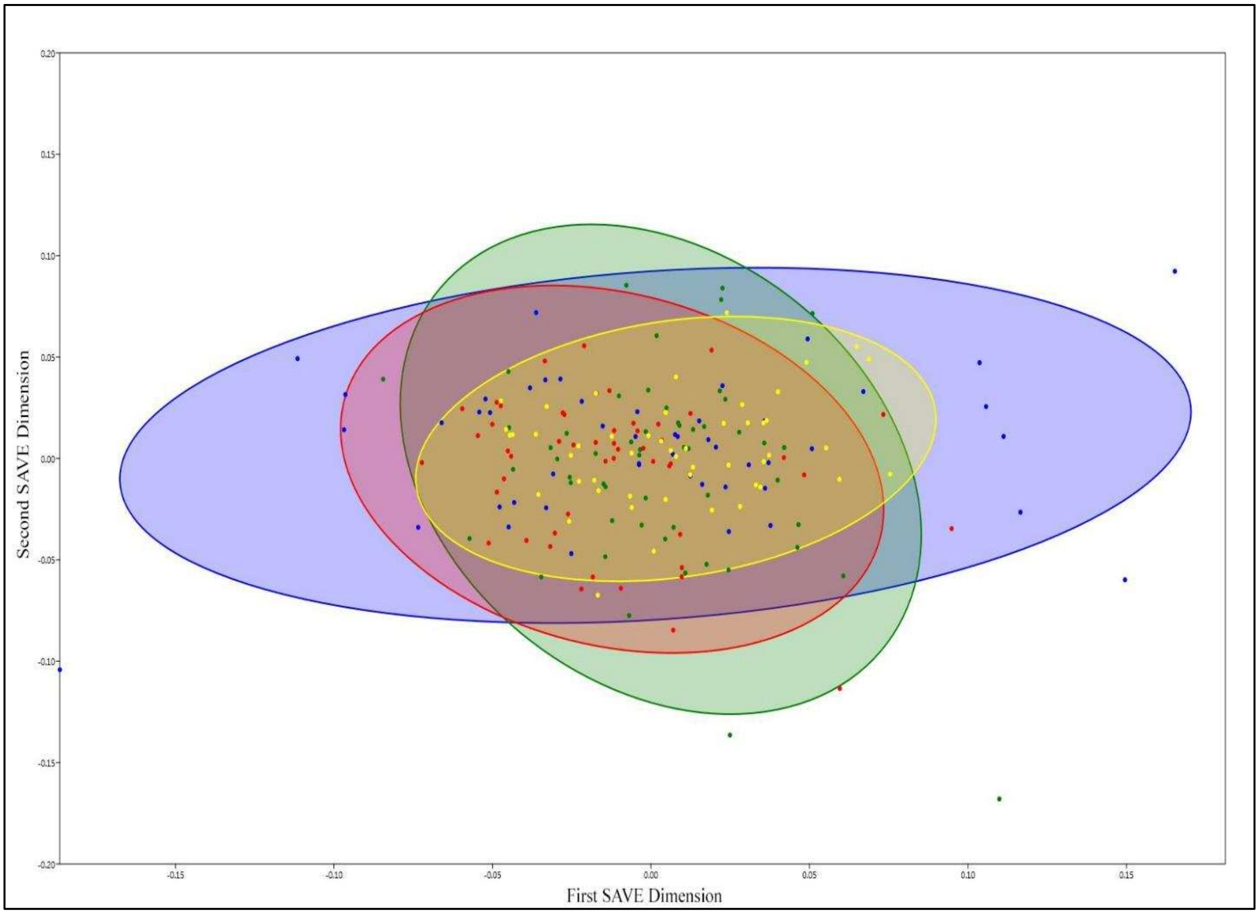

Figure 4.7) Graph showing the distribution of cut mark data points based on the results of a discriminant analysis between cut marks made by tools of different raw material types. Ellipses represent 95% confidence intervals for each cut mark group. Blue dots represent quartzite cut marks, green dots represent basalt cut marks, red dots represent chert cut marks, and yellow dots represent phonolite cut marks.

Specific trends in cut mark classification rates can be identified in the raw material only discriminant model when the confusion matrix is divided back into the original eight cut mark classes separating marks based on both the technological form and raw material type of the tool that made them (Table 4.23). This new confusion matrix reveals that the phonolite flake cut mark group is the most accurately classified group in the model, with 22 of 25 marks identified as having been made by a phonolite tool. Alternatively, the quartzite biface and quartzite flake cut mark groups represent the two most misclassified groups in this model, with both groups having only 15 of 25 cut marks correctly classified.

Table 4.23) Subdivided confusion matrix for the quadratic discriminant analysis between cut marks made by tools of differing raw material type. The original cut mark classes are divided by both tool raw material and technological type to better recognize differences in cut mark classification rates between groups.

	Original Class							
	Quartzite Biface	Quartzite Flake	Basalt Biface	Basalt Flake	Chert Biface	Chert Flake	Phonolite Biface	Phonolite Flake
Quartzite	**15**	**15**	1	3	0	3	1	1
Basalt	2	5	**20**	**19**	1	3	3	1
Chert	3	0	0	4	**20**	**17**	3	1
Phonolite	5	5	6	1	4	3	**18**	**22**

Posterior probabilities for each cut mark analyzed in the raw material only discriminant model were recorded, providing first, second, third, and fourth group probability estimations for each mark. These posterior probability levels provide a classification estimation for each individual cut mark in the four possible raw material groups tested by the model. When considering the 146 cut marks that correctly classified in this model, the average first posterior probability was 81%, with a median probability classification of 86%. When considering the 59 cut marks that incorrectly classified in this model, the average first posterior probability was 61%, with a median probability classification of 57%. Similar to the previous discriminant models, the distribution of the correct and incorrect first posterior probabilities were compared using a *t*-test, recording a *p*-value of <0.001. This significant difference suggests that the raw material only discriminant model tends to have significantly lower first posterior probability percentages when incorrectly classifying cut marks.

Of the 59 cut marks that incorrectly classified at the first posterior probability level in the raw material only discriminant model, 38 classified correctly at the second posterior probability level, 15 classified correctly at the third posterior probability level, and six classified correctly at the fourth posterior probability level. When only the 38 cut marks that classified correctly at the second posterior probability level are analyzed further it is shown that the average second posterior probability of these marks is 28%. Comparatively, the 146 cut marks that correctly classified in this model reported an average second posterior probability of only 14%. When the distribution of the 146 correctly and 39 incorrectly classified second posterior probabilities are compared using a t-test, a p-value of <0.001 is recorded. This p-value suggests that the second posterior probabilities of incorrectly classified cut marks tend to be significantly larger than the second posterior probabilities of correctly classified cut marks.

Similar to the tool technology only model, the classification accuracy of the raw material only discriminant model can be assessed further when the variable of technological from is completely removed from the analysis. A quadratic discriminant model classifying cut marks made by biface tools of different raw material types was capable of discriminating marks by raw material type with 88.24% accuracy (Table 4.24). The cut marks used in this discriminant model were graphed along the first two SAVE dimensions of the model in an effort to visualize and compare the multivariate distribution of cut mark data (Figure 4.8). When considering the first posterior probability of the 90 cut marks that classified correctly in this discriminant model, the average first posterior probability was 94.88%, with a median probability of 99.85%. When considering the first posterior probabilities of the 12 biface cut marks that did not correctly classify in this model, the average first posterior probability was only 70.64%, with a median probability of 67.96%. The significant difference between the first posterior probabilities of correctly and incorrectly classed data suggests that this model will typically record a less confident posterior probability when incorrectly classifying data. Of the 12 biface cut marks that did not correctly classify, ten cut marks correctly classified as the second most probable tool group and two cut marks correctly classified as the third most probable tool group (Table 4.25).

The average probability for these twelve marks at the correct classification level was only 26.39%.

Table 4.24) Confusion matrix for the quadratic discriminant analysis between cut marks made by biface tools of differing raw materials. The classification accuracy of this model is 88.24%. Bolded values indicate the number of correctly classified cut marks for each cut mark grouping.

		Given Group				
		Quartzite Biface	Basalt Biface	Chert Biface	Phonolite Biface	Total
Predicted Groups	Quartzite Biface	**24**	0	1	2	27
	Basalt Biface	1	**23**	0	2	26
	Chert Biface	0	0	**22**	0	22
	Phonolite Biface	0	4	2	**21**	27
	Total	25	27	25	25	102

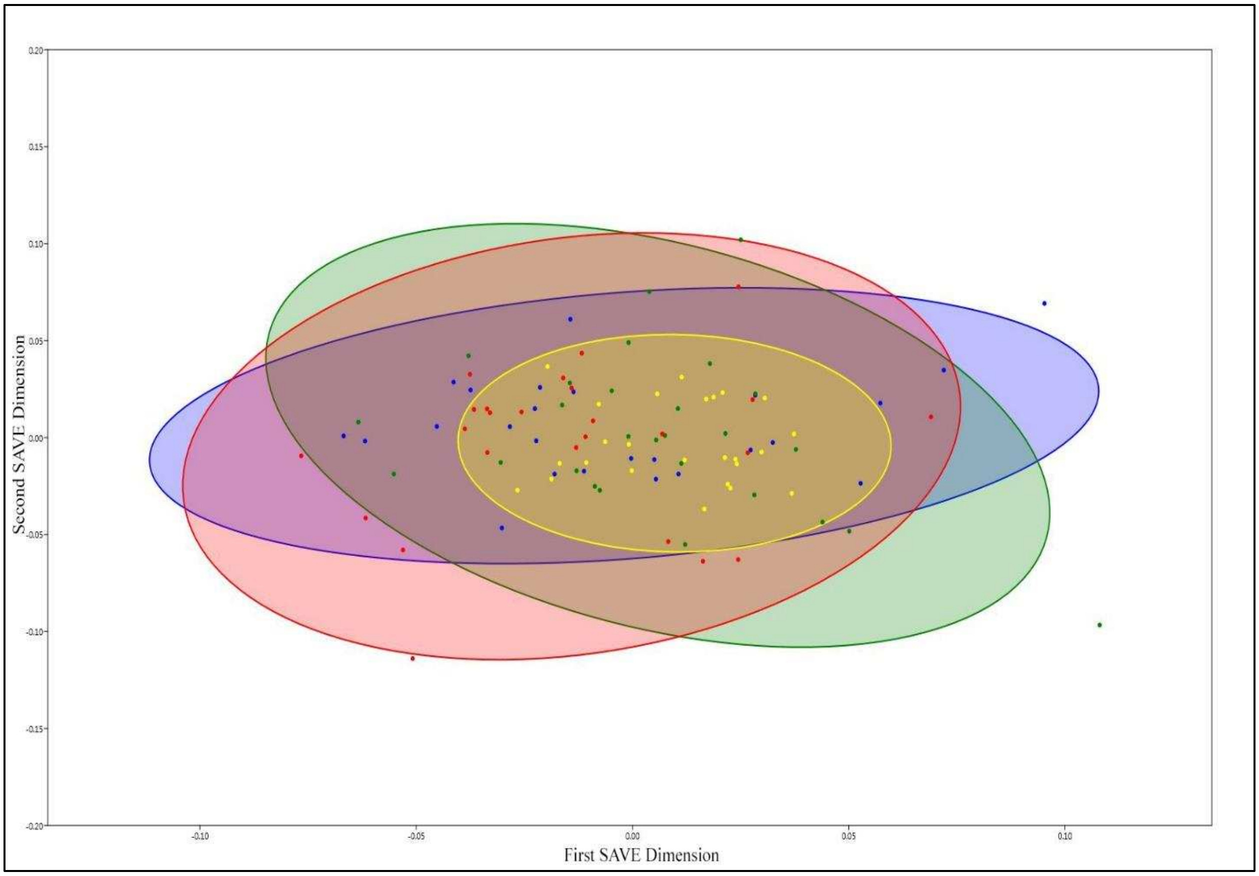

Figure 4.8) Graph showing the distribution of cut mark data points based on the results from a discriminant analysis of cut marks made by biface tools of four different raw material types. Ellipses represent 95% confidence intervals for each cut mark group. Blue dots represent quartzite cut marks, green dots represent basalt cut marks, red dots represent chert cut marks, and yellow dots represent phonolite cut marks.

Table 4.25) Posterior probabilities for the 12 incorrectly classified cut marks in the quadratic discriminant model comparing biface cut marks based on tool raw material type. Correct probability percentages and probability levels are shown only for data that correctly classified below the second posterior probability level. (QBF = Quartzite Biface; BBF = Basalt Biface; CBF = Chert Biface; PBF = Phonolite Biface).

Actual Tool Group	1st Probability Class	1st Probability Percentage	2nd Probability Class	2nd Probability Percentage	Correct Probability Percentage	Correct Probability Level
QBF	BBF	58%	QBF	42%		
BBF	PBF	58%	BBF	42%		
BBF	PBF	75%	BBF	20%		
BBF	PBF	59%	BBF	41%		
BBF	PBF	87%	BBF	13%		
CBF	PBF	92%	BBF	6%	2%	3
CBF	PBF	79%	BBF	20%	0.2%	3
CBF	QBF	59%	CBF	40%		
PBF	BBF	55%	PBF	45%		
PBF	QBF	78%	PBF	22%		
PBF	BBF	87%	PBF	10%		
PBF	QBF	61%	PBF	39%		

A quadratic discriminant model classifying cut marks made by flake tools of different raw material types was able to discriminate between cut marks based on raw material type with 84.47% accuracy (Table 4.26). Similar to the biface discriminant model described above, this model was graphed along the first two SAVE dimensions of the model in order to visualize the multivariate distribution of cut marks (Figure 4.9). The first posterior probabilities of the 87 correctly classified cut marks in this model had an average first posterior probability of 91.69%, with a median probability of 99.38%. Comparatively, the first posterior probabilities of the 16 flake cut marks that did not correctly classify in this model had an average probability of only 62.88%, with a median probability of 66.61%. Of the 16 flake cut marks that did not correctly classify in this discriminant model, 15 marks classified correctly as the second most probable cut mark group and one mark classified correctly as the third most probable cut mark group (Table 4.27). When considering the distribution of incorrectly classified flake cut marks in this model, no clear trends in misclassification rates is observed (Table 4.26). Flake cut marks analyzed in this model tend to misclassify in all four raw material groups at approximately similar rates.

Table 4.26) Confusion matrix for the quadratic discriminant analysis between cut marks made by flake tools of differing raw materials. The classification accuracy of this model is 84.47%. Bolded values indicate the number of correctly classified cut marks for each cut mark grouping.

		Given Group				
		Quartzite Flake	Basalt Flake	Chert Flake	Phonolite Flake	Total
Predicted Group	Quartzite Flake	**20**	2	1	2	25
	Basalt Flake	2	**22**	1	1	26
	Chert Flake	2	2	**23**	0	27
	Phonolite Flake	1	1	1	**22**	25
	Total	25	27	26	25	103

Table 4.27) Posterior probabilities for the 16 incorrectly classified cut marks from the quadratic discriminant model comparing flake cut marks based on tool raw material type. Correct probability percentages and probability levels are shown only for data that correctly classified below the second posterior probability level. (QNR = Quartzite Flake; BNR = Basalt Flake; CNR = Chert Flake; PNR = Phonolite Flake).

Actual Tool Group	**1st Probability Class**	**1st Probability Percentage**	**2nd Probability Class**	**2nd Probability Percentage**	**Correct Probability Percentage**	**Correct Probability Level**
QNR	CNR	75%	QNR	25%		
QNR	BNR	60%	QNR	40%		
QNR	CNR	63%	QNR	19%		
QNR	BNR	75%	QNR	24%		
QNR	PNR	69%	QNR	24%		
BNR	CNR	50%	BNR	29%		
BNR	QNR	63%	BNR	34%		
BNR	PNR	40%	BNR	36%		
BNR	CNR	78%	QNR	8%	7.7%	3
BNR	QNR	86%	BNR	14%		
CNR	BNR	51%	CNR	48%		
CNR	QNR	56%	CNR	42%		
CNR	PNR	53%	CNR	42%		
PNR	BNR	62%	PNR	38%		
PNR	QNR	66%	PNR	34%		
PNR	QNR	58%	PNR	42%		

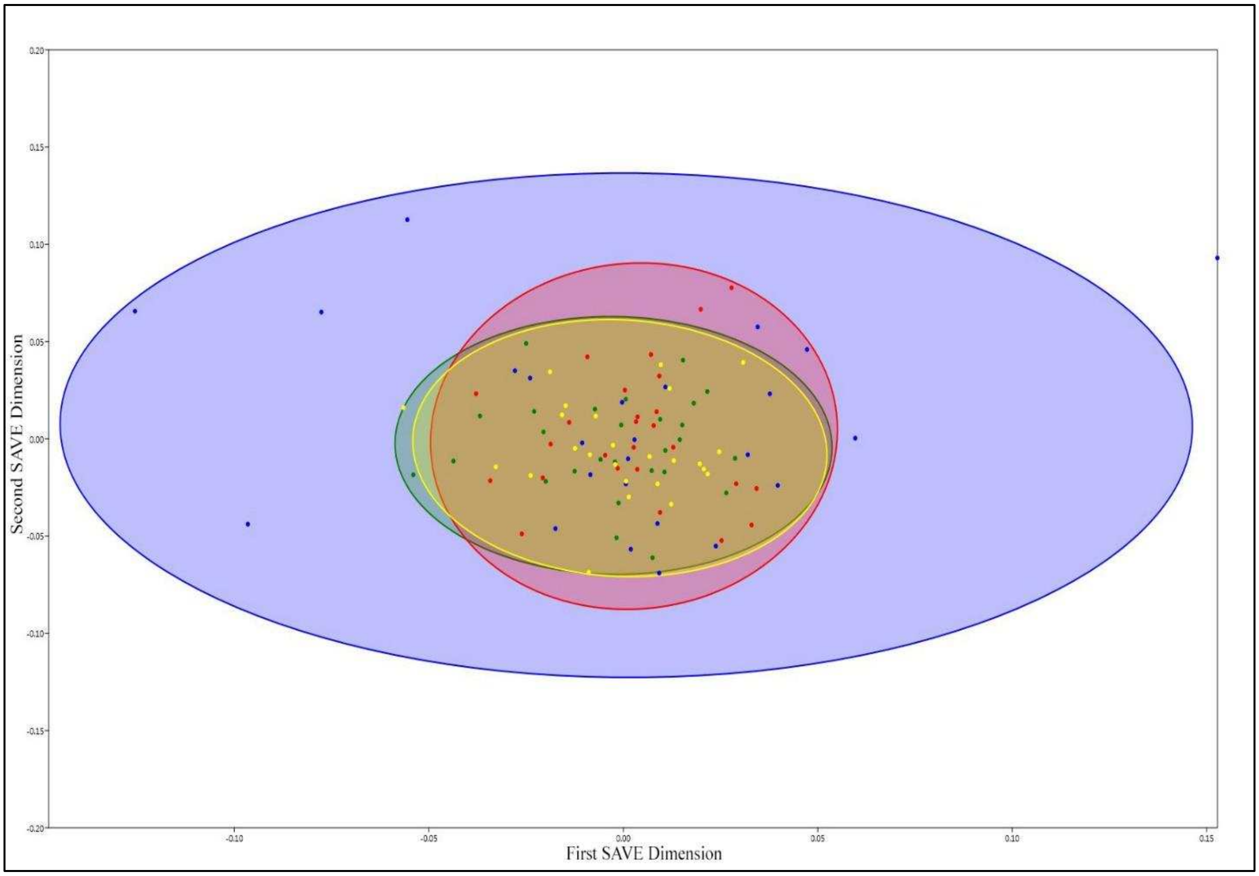

Figure 4.9) Graph showing the distribution of cut mark data points based on the results from a discriminant analysis of cut marks made by flake tools of four different raw material types. Ellipses represent 95% confidence intervals for each cut mark group. Blue dots represent quartzite cut marks, green dots represent basalt cut marks, red dots represent chert cut marks, and yellow dots represent phonolite cut marks.

The overall trend demonstrated by the nine multivariate discriminatory models described in the results of this thesis is that the unique patterns recorded in the micromorphology of a cut mark are primarily associated with the technological form of the tool that made it. This assertion is based primarily on the different classification accuracies recorded by the nine quadratic discriminant models tested by this thesis (Table 4.28-29). The discriminant model classifying cut marks based only on tool technological form was capable of discriminating marks with 78.54% accuracy. This tool technology only discriminant model is almost ten percent more accurate than the 71.22% accuracy of the discriminant model classifying cut marks based only on tool raw material (Table 4.28).

Table 4.28) Summary of all nine quadratic discriminant analyses described in this thesis. Technology groupings differentiate cut marks made by biface and flake tools; Raw material groupings differentiate cut marks made by quartzite, basalt, chert, and phonolite tools.

Cut Mark Groupings	**Number of Cut Mark Groups**	**Discriminant Analysis Accuracy (%)**
Technology and Raw Material	8	80.97
Technology	2	78.54
Raw Material	4	71.22
Quartzite Tools	2	100
Basalt Tools	2	100
Chert Tools	2	92.16
Phonolite Tools	2	96
Bifaces by Raw Material	4	88.24
Flakes by Raw Material	4	84.47

Table 4.29) Summary of tool comparisons between groups of different raw materials not explicitly defined in this thesis. Each raw material grouping is further divided into two tool technology types - biface and flake tools.

Cut Mark Groupings	**Number of Cut Mark Groups**	**Discriminant Analysis Accuracy (%)**
Quartzite and Basalt	4	91.35
Quartzite and Chert	4	90.02
Quartzite and Phonolite	4	91.00
Basalt and Chert	4	93.33
Basalt and Phonolite	4	89.42
Chert and Phonolite	4	90.10
Quartzite, Basalt and Chert	6	87.10
Quartzite, Basalt and Phonolite	6	83.77
Quartzite, Chert and Phonolite	6	85.43
Basalt, Chert and Phonolite	6	86.45

Trends in data misclassification can be identified when each cut mark that did not classify correctly in at least one of the discriminant model is examined individually. Of the 205 cut marks analyzed in this thesis, 98 cut marks misclassified in at least one of the five models each mark was tested in (Appendix D). The five models each cut mark was tested in are the tool technology only model, raw material only model, tool technology and raw material model, a model including cut marks made by tools of only one raw material type, and either a biface only or flake only model. Of the 98 cut marks that did not correctly classify, 56 misclassified in only one of the five models, 12 misclassified in two models, 24 misclassified in three models, and six misclassified in four models. No cut marks misclassified in all five discriminant models they were tested in.

Of the 56 cut mark points that misclassified in only one of the five discriminant models they were tested in: 29 misclassified in the model classifying marks based on tool raw material, 26 misclassified in the model classifying marks based on tool technology, and one mark misclassified in the model classifying marks based on both tool raw material and technology type. The misclassified cut marks in the subdivided biface only model (12 misclassified marks), flake only model (16 misclassified marks), chert only model (4 misclassified marks) and phonolite only model (2 misclassified marks) all misclassified in at least one of the three comprehensive discriminant models that included data from all 205 cut marks. This observation may suggest that these subdivided models share similar discriminatory powers and dimensions as the undivided models that include all 205 cut marks, which would lead to the same cut mark being misclassified in both models. Overall, these results highlight the validity and importance of using multiple discriminant models to understand and classify bone surface modifications of unknown origin.

4.4) Identifying Archaeological Trace Marks of Unknown Origin

Trace marks recovered from archaeological fossils were analyzed and classified using the experimental data recorded in the raw material only (71.22% accuracy), tool technology only (78.54% accuracy), and combined tool and raw material (80.97% accuracy) quadratic discriminant models. One archaeological mark (ID 2784B; Table 4.30) recorded a negative radius measurement relative to the cut mark and was therefore analyzed in the three experimental quadratic discriminant models described above without including experimental radius measurements. Negative radii measurements occur when a trace mark is shallow and broad, leading to a cross-sectional best fit arc that extends in the opposite direction of the cut marks profile. The accuracies of the quadratic discriminant models not including experimental cut mark radii measurements are similar to the models including radii measurements (raw material only model - 72.19% accuracy; tool technology only model - 76.59% accuracy; combined tool and raw material model - 77.07% accuracy). Archaeological cut marks were graphed along the first two SAVE dimensions identified in the tool technology and raw material discriminant model in order to better visualize tool classification trends (Figure 4.10). Overall, the majority of tool technologies and raw material types analyzed by this thesis were determined to have likely created cut marks in this assemblage (Table 4.30). The only experimental cut mark groups that did not classify for a single cut mark in the archaeological assemblage were basalt flakes and chert bifaces.

Table 4.30) Fossil trace mark classifications based on the Tool Technology Only, Raw Material Only, and Tool Technology and Raw Material discriminant models. Bolded ID numbers indicate fossils that had differing tool technology classifications between models. Starred ID numbers indicate fossils that had differing raw material classifications between models.

ID	**Cut Mark Location**	**Taxa, Body Size**	**Raw Material Only**	**Technology Only**	**Raw Material and Technology**
119	Phalanx	Bovid, 3	Quartzite	Biface	Quartzite Biface
928A	Tibia	Indeterminate, 3	Phonolite	Biface	Phonolite Biface
928B	Tibia	Indeterminate, 3	Phonolite	Biface	Phonolite Biface
952A	Atlas	Bovid, 3	Quartzite	Flake	Quartzite Flake
952B	Atlas	Bovid, 3	Quartzite	Biface	Quartzite Flake
1062	Tibia	Indeterminate, 3	Quartzite	Biface	Quartzite Biface
1300	Cervical Vertebra	Bovid, 3	Quartzite	Flake	Quartzite Flake
1418	Mandible	Suid, 3	Quartzite	Flake	Quartzite Flake
1601	Phalanx	Bovid, 3	Quartzite	Flake	Quartzite Flake
1751*	Tibia	Equid, 3	Quartzite	Biface	Phonolite Biface
2135A*	Humerus	Indeterminate, 2	Quartzite	Flake	Chert Flake
2135B*	Humerus	Indeterminate, 2	Chert	Flake	Phonolite Flake
2135C	Humerus	Indeterminate, 2	Basalt	Flake	Basalt Biface
2135D	Humerus	Indeterminate, 2	Basalt	Biface	Basalt Biface
2226A	Mandible	Bovid, 3	Quartzite	Biface	Quartzite Biface
2226B	Mandible	Bovid, 3	Quartzite	Biface	Quartzite Flake
2537	Innominate	Equid, 3	Quartzite	Flake	Quartzite Biface
2784A	Long Bone	Indeterminate, 2	Quartzite	Biface	Quartzite Flake
2784B	Long Bone	Indeterminate, 2	Quartzite	Flake	Quartzite Flake
3025A*	Femur	Hippo, 5	Quartzite	Flake	Basalt Biface
3025B	Femur	Hippo, 5	Quartzite	Flake	Quartzite Flake
3132*	Ulna	Bovid, 3	Quartzite	Biface	Phonolite Biface

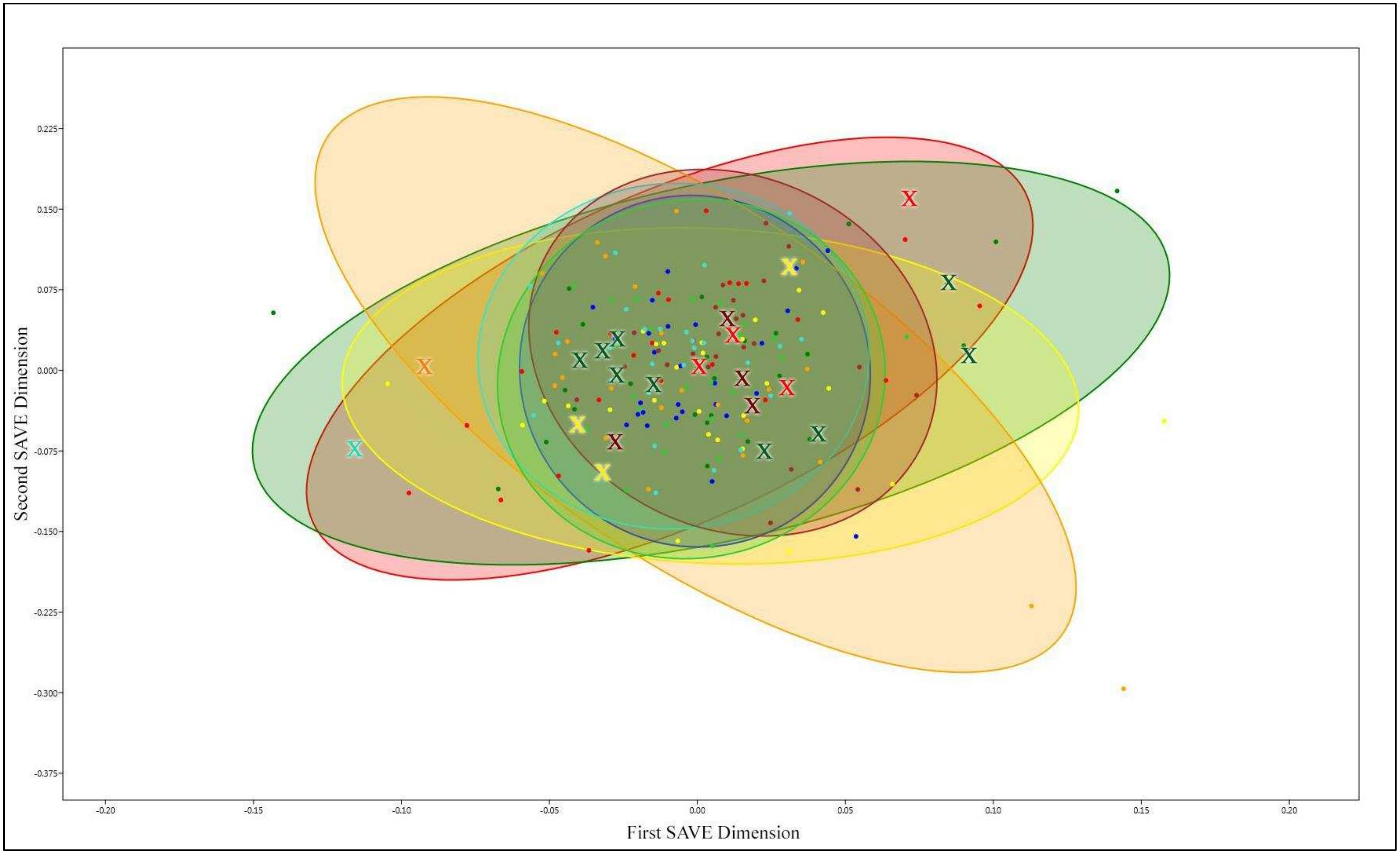

Figure 4.10) Graph showing the distribution of archaeological trace mark based on the results from a discriminant analysis of experimental cut marks made by different tool technologies and raw materials. X's represent archaeological trace marks; see Figure 4.1 for an explanation of dot and X color.

The tool technology classifications of each archaeological cut mark were recorded and compared between the tool technology only discriminant model and the raw material and tool technology combinative discriminant model. Sixteen of the 22 fossil marks analyzed in this thesis had agreeing tool technology classifications in both the technology only and the combinative discriminant models (Table 4.30). Archaeological mark raw material classifications were assessed by comparing the tool classifications in the raw material only model and the combinative discriminant model. Seventeen of the 22 fossil cut marks had agreeing raw material classifications in both the raw material only and combinative discriminant models (Table 4.30). The first and second posterior probabilities of the 11 cut marks that recorded conflicting tool characteristic classifications were recorded in an effort to visualize the classification confidences of each model (Table 4.31; 4.32).

Table 4.31) First posterior probabilities for archaeological cut marks that had disagreeing classifications in the discriminant models identifying tool technology from cut mark micromorphology. Second posterior probabilities are only shown in the raw material and tool technology model when the first posterior probability is less than 95%.

	Technology Model		**Raw Material and Technology Model**		
ID	Classification	1st Posterior Probability	Classification	1st Posterior Probability	2nd Posterior Probability
952B	Biface	81%	Quartzite Flake	100%	
2135C	Flake	65%	Basalt Biface	82%	12% Basalt Flake
2226B	Biface	77%	Quartzite Flake	95%	
2537	Flake	100%	Quartzite Biface	88%	12% Phonolite Flake
2784A	Biface	100%	Quartzite Flake	100%	
3025A	Flake	92%	Basalt Biface	58%	35% Quartzite Flake

Table 4.32) First posterior probabilities for archaeological cut marks that had disagreeing classifications in the discriminant models identifying tool raw material type from cut mark micromorphology. Second and third posterior probabilities are only shown when the first posterior probability is less than 95%.

	Raw Material Model			**Raw Material and Technology Model**		
ID	Classification	1st Posterior Probability	2nd Posterior Probability	Classification	1st Posterior Probability	2nd Posterior Probability
1751	Quartzite	97%	3% Phonolite	Phonolite Biface	100%	
2135A	Quartzite	91%	5% Chert	Chert Flake	60%	40% Quartzite Flake
2135B	Chert	70%	21% Phonolite	Phonolite Flake	46%	41% Chert Biface
3025A	Quartzite	99%		Basalt Biface	58%	35% Quartzite Flake
3132	Quartzite	90%	9% Phonolite	Phonolite Biface	100%	

Instances when archaeological cut marks reported conflicting tool characteristic classifications, between either the tool technology only and the technology and raw material models, or the raw material only and technology and raw material models, were assessed further by investigating the posterior probabilities of each model. When one discriminant model reported a significantly larger first posterior probability than the other discriminant model, the tool characteristic classification with the larger first posterior probability was deemed more accurate. From this analysis, each archaeological cut mark was able to be assigned a final tool effector classification (Table 4.33). However, in one instance, an archaeological cut mark reported disagreeing raw material classifications in the raw material only model and the tool technology and raw material model (ID 2135B; Table 4.33), with similarly low posterior probabilities in each model. Therefore, this archaeological cut mark was classified as being created by a flake tool of unknown raw material type.

Table 4.33) Tool classifications for the 22 archaeological cut marks analyzed. Cut mark classifications are based on the posterior probability data of each cut mark reported in the tool technology only discriminant model, raw material only discriminant model, and tool technology/raw material discriminant model.

ID	Tool Classification
119	Quartzite Biface
928A	Phonolite Biface
928B	Phonolite Biface
952A	Quartzite Flake
952B	Quartzite Flake
1062	Quartzite Biface
1300	Quartzite Flake
1418	Quartzite Flake
1601	Quartzite Flake
1751	Phonolite Biface
2135A	Quartzite Flake
2135B	Indeterminate Flake
2135C	Basalt Biface
2135D	Basalt Biface
2226A	Quartzite Biface
2226B	Quartzite Flake
2537	Quartzite Flake
2784A	Quartzite Flake
2784B	Quartzite Flake
3025A	Quartzite Flake
3025B	Quartzite Flake
3132	Phonolite Biface

CHAPTER 5 DISCUSSION

Interpreting and modeling the dynamic butchery behaviors of past hominins is primarily achieved through the analysis of cut marked fossils and stone tools in the archaeological record. As such, paleoanthropological research is often focused on creating predictable models capable of extracting broader tool use and butchery behavior interpretations of Early Stone Age hominins from these archaeological resources (Binford, 1981; Blumenschine, 1995; Capaldo, 1998; Domínguez-Rodrigo, 1999; Domínguez-Rodrigo and Pickering, 2003; Pante et al., 2012; Selvaggio, 1998; Shipman, 1986). High-resolution 3-D scanning has recently been employed as a quantitative method to reconstruct and model cut mark micromorphology, enhancing the analytical power of bone surface modification studies (Bello and Soligo, 2008; Pante et al., 2017). This thesis seeks to contribute to this body of work by identifying and interpreting the micromorphological patterns of cut marks made by Early Stone Age tools of varying technological form and raw material type.

5.1) Identifying Tool Technology and Raw Material Type from Cut Mark Morphology

5.1.1) Univariate Trends in Cut Mark Micromorphology

Post hoc Dunn's tests identified numerous significant differences between cut marks made by flake and biface tools for all 12 univariate cut mark measurements. Over 65% of the statistically significant pairwise relationships identified by the Dunn's tests were between cut mark groups made by tools of differing technological forms. Previous research, as well as a general examination of the tools used in this study, indicate that bifacially knapped stone tools tend to have broader cutting edges than unmodified flake tools made of the same raw material (McCall, 2005; Merritt, 2015; Walker, 1978). These observations are supported in the univariate results of this study, which note that cut marks made by biface tools tend to have statistically larger cut mark width, opening angle and radius measurements compared to cut marks made by unretouched flake tools. Therefore, it can likely be concluded that stone tools with broader and wider cutting edges, such as biface tools, will tend to leave broader and wider cut marks.

Cut marks made by flakes tools were characterized in this thesis as tending to be longer than marks made by biface tools. This significant difference in cut mark length between flake and biface cut marks can likely be attributed to cutting instances where broader edged biface tools left patches of cut marks of varying lengths. The observation that the more jagged cutting edge of biface tools tend to leave patches of cut marks of varying lengths when it impacts a bone has previously been reported (de Juana et al., 2010; Toth, 1985). However, this trend does not necessarily mean that shorter cut marks are always created by biface tools, as flake tools can similarly create small cut marks and biface tools can create longer cut marks, particularly during actual butchery events (Merritt, 2015). This observation indicates that other morphological aspects of a cut mark must be considered in tandem with length measurements, such as the width, angle and radius of a mark, in order to effectively differentiate biface cut marks from flake cut marks.

Post hoc Dunn's test also show that over 85% of statistically significant pairwise relationships were recorded between cut mark groups of differing raw material type. However, these comparisons also include pairwise relationships between tools of differing technological form. It is therefore difficult to identify whether differences in tool raw material or technological form created the significant morphological difference between cut mark groups in these instances. Of the 91 statistically significant relationships reported between cut mark groups of different raw material type, 34 were between cut mark groups of the same technological form, but different raw material type. It has previously been noted that the cutting edge of Early Stone Age tool forms vary depending on the raw material the tool is made from (Ambrose, 2001; Jones, 1979). However, it also been noted that the cutting edge shape of tools of the same technological form, but different raw material type, do not tend to vary significantly (Gurtov and Eren, 2014; Merritt, 2012; Sharon, 2008; Val et al., 2017). Overall, the presence of statistically significant differences between cut mark groups of the same technological form, but different raw material type indicates that tool raw material does influence cut mark micromorphology at some level.

Pairs of cut mark groups that did not identify at least one statically significant pairwise relationship in all 12 Dunn's tests are between basalt and phonolite flakes, chert bifaces and flakes, and chert and phonolite flakes. The two tool effectors included in each of these three cut mark pairings share either the same technological form or raw material type. This observation is consistent with the conclusion of Gurtov and Eren (2014), who suggest that tools of the same technological form, but different raw material type, often share similar cutting edge shapes. Tools with similar cutting edge features would likely create cut marks that share identical morphological features.

Of the 104 statistically significant pairwise relationships identified by the Dunn's tests, over 50% were between cut mark groups that differed in both tool technological form and raw material type. This observation again supports the hypothesis that when the physical properties of tools differ, they will create cut marks with unique and distinguishable characteristics. This interpretation supports the use of a multivariate statistical approach in the following sections using all 12 measurements in tandem to model the relationship between cut mark micromorphology and the structural properties of a stone tool.

5.1.2) Discriminating Tool Technology from Cut Mark Micromorphology

Discriminant analyses are used throughout the multivariate portion of this thesis to identify and classify the relationship between cut mark micromorphology and stone tool form. One such model is created by grouping cut mark data together based on the technological form of the tool that created each mark. A quadratic discriminant analysis is capable of classifying the technological type of the tool that created each experimental cut mark with 78.54% accuracy.

The cut mark classification accuracy reported by the tool technology discriminant model is comparable to other taphonomic studies using alternative modeling techniques to identify tool form from cut mark morphology. For example, de Juana et al. (2010) use a simple hand lens and 40x magnification microscope to qualitatively differentiate cut marks made by flint and quartzite handaxe tools from chert and quartzite flake tools with 82.3% accuracy (de Juana et al., 2010). However, the results of this hand lens study are not necessarily analogous to this thesis, as a recent reexamination of the replicability and accuracy of using a hand lens to model cut mark morphology notes that the qualitative descriptions used by this method are extremely subjective and tend to disagree between researchers (Domínguez -Rodrigo et al., 2017). Regardless of the slight reduction in model accuracy reported by this thesis compared to this hand lens study, the relatively large classification accuracy of both models indicates that the technological form of a stone tool does influence cut mark morphology.

5.1.3) Discriminating Tool Raw Material from Cut Mark Micromorphology

A quadratic discriminant model classifying cut marks only on the raw material type of the tool that made each mark, ignoring tool technological form, is 71.22% accurate. This classification power is nearly 10% less than the tool technology only discriminant model. The larger misclassification rate noted by the raw material only model may be due to this model having broader and overlapping discriminatory boundaries. However, it has previously been shown that quadratic discriminant analysis is particularly suited for discriminating between data with overlapping boundaries, suggesting that this statistical approach is likely appropriate for this dataset (Dixon and Brereton, 2009). The broader boundaries in this model likely arose from grouping the distinct biface and flake cut mark data together, as biface cut marks tend to be wider, broader, and shorter than flake cut marks. Therefore, the discriminatory boundaries of each group in this model would have both large and small values from the flake and biface data, leading to group boundaries with more variance than models with groups that have discrete and closely related datasets. When other raw material models are created with more discrete datasets, the classification accuracy of the model increases. This can be shown in the results of the biface only and flake only discriminant models, which are each capable of distinguishing cut marks made from tools of only one technological form based on raw material with 88.24% and 84.47% accuracy, respectively. These large classification accuracies suggest that the raw material type of a stone tool does influence the micromorphological characteristics of a cut mark. Overall, the classification accuracy of 71.22% recorded by this discriminant model indicates that the raw material of a tool influences the morphological characteristics of the cut marks it creates.

Similar trends in cut mark classification powers are recorded between this raw material only discriminant model and other studies that identify tool raw material from cut mark morphology. For instance, Maté-Gonzalez et al. (2017) use micro-photogrammetry to model and classify cut marks made by flint and quartzite stone tools with 76.5% accuracy. The accuracy of this micro-photogrammetry study is a similar to the classification accuracy of discriminant models created from the data used in this thesis that compare cut mark data made by tools of only two raw material types. For instance, the classification accuracy of two raw material type models in this thesis range from 82% accuracy between quartzite and phonolite marks to 90.4% between basalt and chert marks. Therefore, when the datasets are compared using similar experimental conditions, it is revealed that the results from this high-resolution scanning approach outperform this micro-photogrammetric study (Maté-Gonzalez et al., 2017). It must also be noted that the micro-photogrammetry methodology is hindered by numerous experimental limitations and biases (see Chapter 2.3), limiting the comparability of the results of any micro-photogrammetry study to this thesis.

The results of the raw material only discriminant model indicate that the raw material of a stone tool does influence the resulting micromorphology of a cut mark; however, the impact of raw material type may not be as significant as other tool characteristics, such as technological form. Models discriminating tool raw material from cut mark morphology may prove more useful in future studies that consider non-lithic tool sources, such as bamboo or metal tools. In particular, such a model may be useful for identifying hominin tool behaviors in Paleolithic faunal assemblages east of the "Movius Line", where later Acheulean bifaces are absent or rare, but cut marked bones are present (Lycett and Bae, 2010).

5.1.4) Identifying Both Tool Technology and Raw Material from Cut Mark Micromorphology

When cut mark data are grouped together based on similarities in both the raw material and technological form of the tool that made each mark, a quadratic discriminant analysis is capable of discriminating marks with 80.97% accuracy. This model is the most accurate of the three discriminant models analyzed in this thesis that incorporate all 205 cut marks.

The confusion matrix created in this multivariate discriminant model notes that approximately 60% of misclassified cut marks incorrectly classified as being a mark made by a tool of the same technological form, but different raw material type. This trend was not observed when considering cut marks that misclassified in a cut mark group of the same raw material type, but different technological form. In fact, only two of the 39 misclassified cut marks in this discriminant model misclassified in a cut mark group of the same raw material type, but different technological form. This observation implies that cut marks made by stone tools of the same technological form are more likely to preserve similar micromorphological features than cut marks made by tools of the same raw material type. This observation is consistent with previous interpretations that suggest that tool technological form influences cut mark morphology more than tool raw material type (Greenfield, 2006).

The 80.97% classification accuracy reported by the tool technology and raw material discriminant model currently exceeds the classification accuracy of other quantitative trace mark modelling studies. For example, Maté-González et al. (2016) utilize micro-photogrammetry to differentiate between cut marks made by three different tool groups, including a metal knife group, with 70% accuracy. The larger classification accuracy reported in this thesis compared to the micro-photogrammetry study further supports the analytical powers of high-resolution 3-D scanning when identifying tool effector characteristic from cut mark micromorphology.

The results of the tool technology and raw material model using high-resolution 3-D scanning has particular relevance for identifying hominin tool use behaviors in archaeological assemblages temporally situated at the Oldowan-Acheulean transition. These lithic assemblages tend to have a variety of tool forms made from multiple different raw material types (de la Torre, 2016; Lepre et al., 2011). However, it is currently unknown whether these tool forms were being used for the same butchery purposes, or whether some tool forms were used for other functions (e.g. Domínguez-Rodrigo et al., 2001; Gamble, 1998; Kohn and Mithen, 1999; Pope et al., 2015). Therefore, establishing a replicable, objective, and accurate methodology to connect tool forms to butchery behaviors is necessary for fully understanding the subsistence behaviors of Early Stone Age hominins.

5.1.5) Discriminating Subgroupings of Tool Effector from Cut Mark Micromorphology

Additional discriminant models were created using a subset of the cut mark data grouped together based on tool effector similarities, which generally increased the classification accuracy of the discriminant models. Constructing discriminant models that includes cut marks made by only some tool technologies or raw materials is potentially useful when analyzing trace marks from a specific archaeological assemblage. Early Stone Age archaeological assemblages typically include a limited number of unique raw material types and tool technology forms. The representative raw material types associated with these early archaeological sites are formed primarily by what lithic materials are locally available and the ranging behaviors of the hominins associated with the assemblage (Goldman-Neuman and Hovers, 2009; Semaw et al., 2003). Therefore, it is practical to create discriminant models that only include experimental cut marks made by the specific lithic tool forms associated with a faunal assemblage in order to classify archaeological cut marks. Quadratic discriminant models classifying cut marks made by biface and flake tools of only one raw material type recorded classification accuracies ranging between 92.16% and 100% (Table 4.28). Quadratic discriminant models classifying biface and flake cut marks made from two different raw material types recorded classification accuracies ranging between 89.42% and 93.33% (Table 4.29).

Dividing cut mark data into smaller groups based on a subset of tool raw material types and technological forms is useful when an archaeological assemblage contains a limited variety of unique stone tools forms. For example, the stone tools recovered from the 3.3 million-year-old Lomekwi 3 lithic assemblage consist primarily of phonolite and basalt chopper tools (Harmand et al., 2015). Therefore, if fossilized cut marks were recovered from this assemblage then a comparative discriminant model consisting of only experimental cut marks made by basalt and phonolite Lomekwi type tools would provide the most informative model for interpreting the carnivorous behaviors of the associated hominins.

Experimental discriminant models created by subdividing cut marks into fewer groups is also a useful practice for evaluating hominin tool use and butchery behaviors in later Early Stone Age archaeological assemblages. However, when analyzing later archaeological assemblages temporally situated near the Oldowan-Acheulean technological transition, comparative cut mark data made from a considerable number of unique tool technologies and raw material types may be required. For instance, the lithic assemblage at the 1.5 million-year-old Acheulean site in Peninj, Tanzania includes a variety of large cutting tools, retouched flakes, and unmodified flake tools made from three different raw material types: basalt, nephelinite and quartz (de la Torre et al., 2008). If a classificatory model were required to connect the cut marks in this assemblage to specific tool forms, then a standardized comparative discriminant model including cut mark made by all tool forms and raw material types present in the entire lithic assemblage would be recommended.

5.2) Inferring Hominin Tool Behaviors from Archaeological Trace Marks

The quadratic discriminant models described in section 5.1 were used to classify archaeological 22 cut marks from a Middle Bed II, Olduvai Gorge site into tool technological from and raw material classes. Archaeological marks were analyzed within the multivariate parameters defined by three different discriminant models: tool technology only model (78.54% accuracy), raw material only model (71.22% accuracy) and technology/raw material model (80.97% accuracy). All experimental tool technologies and raw materials types used throughout the experimental portion of this thesis are typically found within Middle Bed II, Olduvai Gorge and were collected from the modern Olduvai outcrops. Therefore, this experimental stone tool sample and resulting cut marks should be considered near ideal for classifying these archaeological cut marks of unknown origin.

Further investigation of the tool technology classifications for the 22 archaeological marks studied from this fossil assemblage reveals that cut marks made by biface and flake tools are nearly equally represented in the sample (Table 4.33). Thirteen of the 22 archaeological cut marks classified as being created by flake tools, while nine of the 22 archaeological marks classified as being created by biface tools. The relatively high proportion of both Early Stone Age tool forms implies that the hominins associated with this assemblage were using both flake and biface tools when butchering large mammal carcasses. As well, this proportionate relationship may indicate that both tools were being used with equal frequency during the Oldowan-Acheulean transitional period in Olduvai Gorge. However, without an assemblage wide analysis of all cut marks preserved in this site it is difficult to say whether this sample is representative of the broader hominin tool use behaviors of the entire site.

The 22 cut marks analyzed from this archaeological assemblage were primarily categorized as having been created by tools made of quartzite (Table 4.33). Of the 21 archaeological cut marks that recorded noncontroversial raw material classifications, 71% of the marks classified as being made by quartzite tools. The other 29% of cut marks analyzed from this assemblage classified as being made by either basalt or phonolite tools. No cut marks classified as being made by chert tools in this sample. Therefore, the overall trend of this cut mark sample suggests that the hominins associated with this assemblage preferentially selected quartzite tools when butchering large mammal carcasses.

When the tool classifications of the 22 archaeological marks investigated by this thesis are compared to previous descriptions of raw material use in similar Olduvai Gorge sites, informative trends in Early Stone Age hominin tool behaviors can be recognized. In particular, the predominance of cut marks in this sample classified as being made by quartzite tools agrees with the prevalence of quartzite tool forms documented in temporally and geographically similar Middle Bed II, Olduvai Gorge sites (Leakey, 1971). As well, the lack of any cut marks attributed to phonolite or basalt flake tools in this sample is supported by the limited number of these tool forms in similar Middle Bed II, Olduvai Gorge sites (Kimura 1999; 2002; Leakey, 1971). The lack of any cut marks attributed to chert tools in this cut mark sample is also not surprising, as Olduvai Gorge sites contemporaneous with this assemblage tend to lack chert tool forms (Leakey, 1971). The high frequency of cut marks attributed to quartzite tools and the absence of cut marks made by chert tool forms is also consistent with the currently unpublished raw material frequencies of this specific Olduvai Gorge site (de la Torre, personal communication, 2018). Interestingly, the presence of cut marks attributed to phonolite and basalt biface tools is not consistent with the unpublished raw material records of this site, as no biface tools made from volcanic raw materials were reported (de la Torre, personal communication, 2018).

The tool classifications of the 22 archaeological cut marks analyzed by this thesis suggests that the Early Stone Age hominins associated with this site often used the same tool or tool types when processing a single carcass element. This behavioral hypothesis is based on instances where one fossil preserved multiple cut marks classified as being made by tools of the same technological form and raw material type. For instance, two cut marks analyzed from fossil 928 both classified as being created by phonolite biface tools. Similarly, fossils 952, 2784, and 3025 each had two cut marks analyzed from them that classified as being made by quartzite flake tools. Multiple cut marks on the same fossil classifying as being created by the same tool form makes sense when the spatial relationship of each pair of cut marks is considered in tandem with the results of the discriminant analysis. In particular, all four of the pairs of cut marks described above are located adjacent and parallel with each other on their respective fossils. These close spatial relationships may support the interpretation that these cut marks pairs were created during the same cutting or butchery event. Under this assumption, it is reasonable to propose that the butchers associated with these cut marks were using one tool multiple times to process a single carcass element. An alternative scenario that explains why a single fossil might have multiple cut marks all made by identical tool forms could be due to a butcher or multiple butchers using several tools of the same form to process a single carcass element.

Instances where one fossil reported several cut marks identified as being created by multiple unique tool forms were also identified in this archaeological analysis. For example, four cut marks analyzed from fossil 2135 were reported to have been created by two distinct tool forms when analyzed within the three experimental discriminant models. These four cut marks are separated into two spatially distinct groups on the fossil, with cut marks 2135A and 2135B being parallel and grouped together and cut marks 2135C and 2135D being parallel and grouped together. The first group of parallel cut marks had one mark made by a quartzite flake, and another mark made by a flake tool of unknown raw material type. The second group of parallel cut marks on this fossil both classified as being made by basalt biface tools. Similar to the interpretations above, the spatial relationship and identical tool characteristic classification of these two groups of cut marks likely suggests that the same tool made one of these two groups of cut marks during a cutting event, and another tool or two tools made the second set of cut marks during a different cutting event. Similar to the two groups of cut marks analyzed from fossil

2135, two cut marks examined from fossil 2226 classified as being created by two different tool forms, a quartzite biface and a quartzite flake tool.

A single fossil bearing multiple cut marks made by a variety of unique tool forms affords the opportunity to hypothesize on the dynamic butchery behaviors of Early Stone Age hominins. Evidence of diverse tool use when butchering a single skeletal element may suggest that Early Stone Age hominins were capable of switching tools when processing a carcass if they deemed one tool type more or less effective for a specific butchery action, or if one tool became dulled. For instance, when considering the cut marks from fossil 2135, it may be valid to propose that the marks made by the basalt biface and the flake tools were produced during different butchery actions, such as skinning or defleshing. This division of tool use would often lead to fossils in the archaeological record that preserve cut marks made by multiple different tool forms. The interpretation of one fossil containing cut marks produced by multiple unique tool forms could also indicate that several hominin butchers, each using different stone tool types processed the element together. This butchery behavior would also tend to leave multiple cut marks created by numerous different tools of varying technological form and raw material type. Overall, the tool classifications of these 22 archaeological cut marks supports the inference that Early Stone Age hominins were capable of creating and utilizing a diverse Oldowan and Acheulean toolkit for butchery related behaviors.

5.3) Methodological Considerations and Future Directions

This thesis highlights the application of using high-resolution 3-D scanning to quantitatively model and interpret the micromorphological patterns of cut marks created by different Early Stone Age tool forms. The results of this thesis provide a foundation for expanding previous paradigms that model fossilized bone surface modification by offering a way to recognize and interpret hominin tool use behaviors in the archaeological record. From this experimental framework, controversies regarding the validity of contentiously identified Early Stone Age bone surface modifications can be assessed and reinterpreted (e.g. Domínguez-Rodrigo et al., 2010; 2011; Sahle et al., 2017).

The high-resolution 3-D scanning methodology used in this thesis provides numerous technological benefits in comparison to other experimental techniques currently employed to model cut mark morphology. It is known that this scanning technique is considerably cheaper, easier to access and maintain, and more accurate than SEM analysis (Schroettner et al., 2006). As well, high-resolution cut mark scanning is able to provide quantitative measurements of trace mark micromorphology, whereas SEM analysis is primarily limited to qualitative descriptions of cut mark morphology (e.g. Greenfield 1999; 2006). Confocal scanning is considerably more expensive and less mobile compared to the alternative quantitative trace mark modeling methodology using micro-photogrammetry (Maté -González et al., 2015). However, unlike cut mark micro-photogrammetry studies, the scanning methodology described in this thesis has been compared using an inter-observer error approach, which shows that with minimal training this method is capable of providing precise and accurate results (Pante et al., 2017). As well, analyzing cut marks with a high-resolution 3-D confocal laser scanner creates models with significantly better model precision than micro-photogrammetry (Pante et al. 2017). Therefore, the increased model accuracy and ease of using a confocal profilometer greatly outweigh the necessary costs associated with the technology.

As with most middle-range research projects, the experimental variables that may influence the applicability and results of this novel scanning methodology must be carefully considered. The methodology of this experiment was designed with an emphasis on minimizing the influence of extrinsic variables and, therefore, lacks the realism of an actual butchery event. Bones cut during this experiment were restricted to coming from animals of the same size class, skeletal element, taxa, and bone section. Instances of bone cut marking were also kept constant throughout this study by designing a machine capable of maintaining tool force and angle of impact. Cut marks created using this methodology contrast cut marks created during actualistic butchery events, where tools can be applied to bone surfaces at different forces and impact angles. However, this experimental methodology was chosen to minimize artificial differences in cut mark features, such as length, width, and depth, and isolate only how the different characteristics of a stone tools cutting edge can influence resulting cut mark micromorphology. This standardized approach prevents arbitrary differences in how an actual butcher might randomly use different tool forms from being attributed as a defining morphological feature of that tools cut marks.

Due to the controlled nature of the data in this thesis, the applicability of comparing experimentally created cut marks to archaeological marks created during actual butchery events must be assessed. This is particularly important to acknowledge, as all experimental biface cut marks in this thesis were created using only one tool, and all flake cut marks were created using only five flake tools for each raw material type. Therefore, it is possible that the marks created for this thesis will not be representative of all tools of that technological form or raw material type. However, regardless of this limitation, the morphological similarities between the experimental tools used in thesis and the archaeological stone tools found in Middle Bed II, Olduvai Gorge sites demonstrates the applicability of using the experimental cut marks created in this thesis to analyze archaeological cut marks.

Some archaeological cut marks analyzed in this thesis did not record consistent tool characteristic classifications in the three discriminant models each mark was tested in. These contradictory tool classifications may have occurred due to different morphological characteristics and post-depositional conditions between the experimental bones and archaeological fossils. In particular, the experimental cut marks used in this study were always created on size four bovid long bone midshafts, while the archaeological marks occurred on a variety of skeletal elements, taxa, and size classes (see Table 3.2). Bones of different skeletal elements and animal taxon tend to have unique mechanical properties that can influence resulting bone surface modification morphology (Braun et al., 2016; Ioannidou, 2003; Lam and Pearson, 2004). As well, archaeological fossils are often subjected to fluvial and sediment abrasion during their depositional process, which can also alter a trace marks micromorphology (Fernández-Jalvo and Andrews, 2003; Shipman and Rose, 1983). Furthermore, not all raw material types found in Middle Bed II Olduvai Gorge sites, such as fine-grained quartz, gneiss, feldspar, and nephelinite, were used to create cut marks in the experimental portion of this thesis (Leakey, 1971). However, as noted above, the primary raw material types recovered from this specific Middle Bed II, Olduvai Gorge site are quartzite and some lavas (de la Torre, personal communication, 2018). Therefore, not including raw material types found only in other Middle Bed II, Olduvai Gorge sites likely did not influence archaeological cut mark classification. These depositional, archaeological, and experimental factors may explain instances of contradictory tool classifications between the discriminant models and should be considered in future high-resolution scanning studies.

Another experimental factor that may have influenced the accurate identification of tool effector from trace mark morphology may have arisen from comparing molded archaeological cut marks to unmolded experimental marks. Archaeological cut marks needed to be molded using an STD firmer due to the immobile nature of both the scanner used for this project and fossils in Olduvai Gorge. Replicating the micromorphology of cut marks using molding materials has previously shown to provide an accurate representation of the original mark (Bello, 2011; Rose, 1983). Furthermore, Muttart (2017) recently used the quantitative scanning methodology outlined by Pante et al. (2017) to compare the morphology of an original bone surface modification to its molded counterpart and found no statistical differences. As such, it is likely that molded archaeological cut marks provide an accurate representation of the marks they represent and did not influence tool classification in this thesis.

High-resolution 3-D scanning has the ability to revolutionize the way archaeologists interpret hominin butchery and tool related behaviors in the archaeological record. However, for this methodology to have any comparative ability, future research must continue to expand the trace mark database described in this study. Research projects using this high-resolution scanning methodology are currently invested in identifying the micromorphological characteristics associated with multiple other bone surface modifications, such as carnivore tooth marks (Muttart and Pante, 2016), bovid trampling marks (Orlikoff et al., 2017) and fluvial abrasion (Gumrukcu et al., 2017). Future studies modeling the micromorphological features of cut mark created during actualistic butchery trials are also of particular interest for furthering the research and database described by this thesis. Additionally, archaeological cut marks recovered from faunal assemblages situated at various time periods and geographic locations should continue to be analyzed and compared to this growing cut mark database in an effort to continue expanding behavioral interpretations of Early Stone Age hominin carnivory and tool use.

CHAPTER 6 CONCLUSION

This thesis describes the first methodologically and theoretically grounded study to use high-resolution 3-D scanning to characterize the micromorphological features of cut marks created by different Early Stone Age tool forms. This methodology expands upon previously described qualitative and quantitative bone surface modification morphology models and provides a foundation upon which future research may expand. The results from this study provide new and detailed information regarding stone tool use in Early Stone Age archaeological assemblages, which can be incorporated into predictive models that focus on reconstructing the butchery behaviors and paleoecological interactions of early hominins.

This thesis highlights the applicability of using high-resolution scanning to accurately model and interpret the variable micromorphological features associated with cut marks created by different tool forms. The methodology outlined in this thesis is designed to be replicable and comparative with other high-resolution scanning studies that model the micromorphological characteristics of bone surface modifications. As well, this foundational study provides the framework to which future projects may contribute data, allowing for an expanded understanding of how the physical and structural properties of stone tools influence the micromorphological characteristics of cut marks. Currently, research using this high-resolution laser scanning methodology is expanding this cut mark database by analyzing and describing the morphological characteristics of cut marks created during actualistic butchery events. This methodology is also being employed to investigate the morphological features of other bone surface modification types, including abrasive trampling, percussion, and carnivore tooth markings.

The goal of this thesis was to provide new interpretations regarding early hominin tool and butchery behaviors in the archaeological record by demonstrating the potential effectiveness of using high-resolution 3-D scanning to model the relationship between the structural properties of a tool effector and the cut marks it creates. Recognizing the distinct relationship between cut mark micromorphology and stone tool properties affords new insight into how Early Stone Age hominins were utilizing different tool forms when butchering and processing large mammal carcasses. Understanding this relationship is of particular interest for interpreting the butchery behaviors of hominins during the Oldowan-Acheulean transition. This time period is relevant to the results of this thesis, as lithic assemblages during the Oldowan-Acheulean transition often contain multiple different tool forms and raw material types that have never been successfully attributed to a specific butchery function. Furthermore, the results and methodological achievements documented in this thesis are also broadly applicable for understanding hominin tool use behaviors in most Early Stone Age archaeological assemblages outside the Oldowan-Acheulean transition that preserve tools of differing technological form and raw material type. Establishing objective and replicable methods for connecting specific stone tool forms to cut marks in the archaeological record can provide new insight into the tool technology and raw material preferences of Early Stone Age hominins when butchering. When this relationship between cut mark micromorphology and tool form is fully understood, new interpretations of Early Stone Age hominin subsistence behaviors can be made.

REFERENCES

Aiello, L.C., Wheeler, P. 1995. The expensive-tissue hypothesis: The brain and the digestive system in human and primate evolution. *Current Anthropology* 36: 199-221.

Ambrose, S.H. 2001. Paleolithic technology and human evolution. *Science* 291:1748-1753.

Antón, S.C. 2003. Natural history of *Homo erectus*. *American Journal of Physical Anthropology* 122: 126-170.

Antón, S.C., Potts, R.C., Aiello, L.C. 2014. Evolution of early *Homo*: An integrated biological perspective. *Science* 345: 1236828.

Antón, S.C., Snodgrass, J.J. 2012. Origins and the evolution of the genus *Homo* new perspectives. *Current Anthropology* 53: 2479-S496.

Aramendi, J., Maté-González, M.A., Yravedra, J., Ortega, M.C., Arriaza, M.C., González-Aguilera, D., Baquedano, E., Domínguez-Rodrigo, M. 2017. Discerning carnivore agency through the three-dimensional study of tooth pits: Revisiting crocodile feeding behaviour at FLK-Zinj and FLK NN3 (Olduvai Gorge, Tanzania). *Palaeogeography, Palaeoclimatology, Palaeoecology* 488: 93-102.

Arriaza, M.C., Yravedra, J., Domínguez-Rodrigo, M., Mate-González, M.Á., Vargas, E.G., Palomeque-González, J.F., Aramendi, J., González-Aguilera, D., Baquedano, E. 2017. On applications of micro-photogrammetry and geometric morphometrics to studies of tooth mark morphology: The modern Olduvai Carnivore Site (Tanzania). *Palaeogeography, Palaeoclimatology, Palaeoecology* 488: 103-112.

Asfaw, B., Beyene, Y., Suwa, G., Walter, R.C., White, T.D., Wolde Gabriel, G., Yemane, T. 1992. The earliest Acheulean from Konso-Gardula. *Nature* 360: 732-735.

Ashton, N., McNabb, J., Irving, B., Lewis, S., Parfitt, S. 1994. Contemporaneity of Clactonian and Acheulean flint industries at Barnham, Suffolk. *Antiquity* 68: 585-589.

Bar-Yosef, O. 1994. The lower Paleolithic of the Near East. *Journal of World Prehistory* 8: 211-265.

Barsky, D., Chapon-Sao, C., Bahain, J., Beyene, Y., Cauche, D., Celiberti, V., Desclaux, E., de Lumley, H., de Lumley, M., Marchal, F., Moullé, P., Pleurdeau, D. 2011. The early Oldowan stone-tool assemblage from Fejej FJ-1A, Ethiopia. *Journal of African Archaeology* 9: 207-224.

Bartelink, E.J., Wiersema, J.M., Demaree, R. 2001. Quantitative analysis of sharp-force trauma: An application of scanning electron microscopy in forensic anthropology. *Journal of Forensic Sciences* 46: 1288-1293.

Bello, S.M. 2011. New results from the examination of cut-marks using three-dimensional imaging. *Developments in Quaternary Science* 14: 249-262.

Bello, S.M., Groote, I.D., Delbarre, G. 2013. Application of 3-dimensional microscopy and micro-CT scanning to the analysis of Magdalenian portable art on bone and antler. *Journal of Archaeological Science* 40: 2464-2476.

Bello, S.M., Parfitt, S.A., Stringer, C. 2009. Quantitative micromorphological analyses of cut marks produced by ancient and modern hand axes. *Journal of Archaeological Science* 36: 1869-1880.

Bello, S.M., Soligo, C. 2008. A new method for the quantitative analysis of cutmark micromorphology. *Journal of Archaeological Science* 35: 1542-1552.

Berthelet, A., Chavaillon, J. 2001. The early Paleolithic butchery site of Barogali (Republic of Djibouti). In: Cavarretta, G., Gioia, P., Mussi, M., and Palomno, M.R. (Eds.), Proceedings of the first International Congress: The World of Elephants. Consiglio Nazionale delle Ricerche: Rome, pp. 176-179.

Beyene, Y., Katoh, S., WoldeGabriel, G., Hart, W.K., Uto, K., Sudo, M., Kondo, M., Hyodo, M., Renne, P.R., Suwa, G., Asfaw, B. 2013. The characteristics and chronology of the earliest Acheulean at Konso, Ethiopia. *Proceedings of the National Academy of Sciences* 110: 1584-1591.

Binford, L. 1981. Bones: Ancient Men and Modern Myths. Academic Press Inc.: San Diego.

Binneman, J., Beaumont, P. 1992. Use-wear analysis of two Acheulean handaxes from Wonderwerk Cave, Northern Cape. *Southern African Field Archaeology* 1: 92-97.

Bishop, L.C., Plummer, T.W., Ferraro, J.V., Braun, D., Ditchfield, P.W., Hertel, F., Kingston, J.D., Hicks, J., Potts, R. 2006. Recent research into Oldowan hominin activities at Kanjera South, Western Kenya. *The African Archaeological Review* 23: 31-40.

Blumenschine, R.J. 1986. Carcass consumption sequences and the archaeological distinction of scavenging and hunting. *Journal of Human Evolution* 15: 639-659.

Blumenschine, R.J. 1989. A landscape taphonomic model of the scale of prehistoric scavenging opportunities. *Journal of Human Evolution* 18: 345-371.

Blumenschine, R.J. 1995. Percussion marks, tooth marks, and experimental determinations of the timing of hominid and carnivore access to long bones at FLK *Zinjanthropus*, Olduvai Gorge, Tanzania. *Journal of Human Evolution* 29: 21-51.

Blumenschine, R.J., Bunn, H.T., Geist, V., Ikawa-Smith, F., Marean, C.W., Payne, A.G., Tooby, J., van der Merwe, N.J. 1987. Characteristics of an early hominid scavenging niche [and comments and reply]. *Current Anthropology* 28: 383-407.

Blumenschine, R.J., Marean, C.W., Capaldo, S.D. 1996. Blind tests of inter-analyst correspondence and accuracy in the identification of cut marks, percussion marks, and carnivore tooth marks on bone surfaces. *Journal of Archaeological Science* 23: 493-507.

Blumenschine, R.J., Peters, C.R., Masao, F.T., Clarke, R.J., Deino, A.L., Hay, R.L., Swisher, C.C., Stanistreet, I.G., Ashley, G.M., McHenry, L.J., Sikes, N.E. 2003. Late Pliocene *Homo* and hominid land use from western Olduvai Gorge, Tanzania. *Science* 299: 1217-1221.

Blumenschine, R.J., Pobiner, B.L. 2007. Zooarchaeology and the ecology of Oldowan hominin carnivory. In: Ungar, P.S. (Ed.), Evolution of the human diet: The known, the unknown, and the unknowable. Oxford University Press: Oxford, pp. 167-190.

Blumenschine, R.J., Selvaggio, M.M. 1988. Percussion marks on bone surfaces as a new diagnostic of hominid behaviour. *Nature* 333: 763-765.

Bobe, R., Behrensmeyer, A.K. 2004. The expansion of grassland ecosystems in Africa in relation to mammalian evolution and the origin of the genus *Homo*. *Palaeogeography, Palaeoclimatology, Palaeoecology* 207: 399-420.

Boschin, F., Crezzini, J. 2012. Morphometrical analysis on cut marks using a 3D digital microscope. *International Journal of Osteoarchaeology* 22: 549-562.

Braun, D.R., Harris, J.W.K., Levin, N.E., McCoy, J.T., Herries, A.I.R., Bamford, M.K., Bishop, L.C., Richmond, B.G., Kibunjia, M. 2010. Early hominin diet included diverse terrestrial and aquatic animals 1.95 Ma in East Turkana, Kenya. *Proceedings of the National Academy of Sciences* 107: 10002-10007.

Braun, D., Pante, M.C., Archer, W. 2016. Cut marks on bone surfaces: Influences on variation in the form of traces of ancient behavior. *Interface Focus* 6: 20160006.

Braun, D.R., Plummer, T., Ditchfield, P., Ferraro, J.V., Maina, D., Bishop, L.C., Potts, R. 2008. Oldowan behavior and raw material transport: Perspectives from the Kanjera Formation. *Journal of Archaeological Science* 35: 2329-2345.

Bunn, H.T. 1981. Archaeological evidence for meat-eating by Plio-Pleistocene hominids from Koobi Fora and Olduvai Gorge. *Nature* 291: 574-577.

Bunn, H.T. 1982. Meat-eating and human evolution: Studies on the diet and subsistence practices of Plio-Pleistocene hominids in East Africa. PhD Dissertation, University of California, Berkley.

Bunn, H.T., Kroll, E.M. 1986. Systematic butchery by Plio/Pleistocene hominids at Olduvai Gorge, Tanzania. *Current Anthropology* 27: 431-452.

Capaldo, S.D. 1998. Simulating the formation of dual-patterned archaeofaunal assemblages with experimental control samples. *Journal of Archaeological Science* 25: 311-330.

Cavallo, J.A., Blumenschine, R.J. 1989. Tree-stored leopard kills: Expanding the hominid scavenging niche. *Journal of Human Evolution* 18: 393-399.

Cerling, T.E., Bowman, J.R., O'Neil, J.R. 1988. An isotopic study of a fluvial-lacustrine sequence: The Plio-Pleistocene Koobi Fora sequence, East Africa. *Palaeogeography, Palaeoclimatology, Palaeoecology* 63: 335-356.

Cerling, T.E., Wynn, J.G., Andanje, S.A., Bird, M.I., Korir, D.K., Levin, N.E., Mace, W., Macharia, A.N., Quade, J., Remien, C.H. 2011. Woody cover and hominin environments in the past 6 million years. *Nature* 476: 51-56.

Clarke, W.R., Lachenbruch, P.A., Broffitt, B. 1979. How non-normality affects the quadratic discriminant function. *Communications in Statistics-Theory and Methods* 8: 1285-1301.

Cook, R.D, Yin, X. 2001. Theory and methods: Special invited paper: Dimension reduction and visualization in discriminant analysis (with discussion). *Australian & New Zealand Journal of Statistics* 43:147-99.

da Silva, A.R. 2017. Biotools: Tools for Biometry and Applied Statistics in Agricultural Science. R package version 3.1.

de Heinzelin, J., Clark, J.D., White, T., Hart, W., Renne, P., Woldegabriel, G., Beyne, Y., Vrba, E. 1999. Environment and behavior of 2.5-million-year-old Bouri hominids. *Science* 284: 625-629.

de Juana, S., Galán, A.B., Domínguez-Rodrigo, M. 2010. Taphonomic identification of cut marks made with lithic handaxes: An experimental study. *Journal of Archaeological Science* 37: 1841-1850.

de la Torre, I. 2011. The Early Stone Age lithic assemblages of Gadeb (Ethiopia) and the Developed Oldowan/early Acheulean in East Africa. *Journal of Human Evolution* 60: 768-812.

de la Torre, I. 2016. The origins of the Acheulean: Past and present perspectives on a major transition in human evolution. *Philosophical Transactions of the Royal Society B* 371: 20150245.

de la Torre, I., Mora, R. 2014. The transition to the Acheulean in East Africa: An assessment of paradigms and evidence from Olduvai Gorge (Tanzania). *Journal of Archaeological Method and Theory* 21: 781-823.

de la Torre, I., Mora, R., Martinez-Moreno, J. 2008. The early Acheulean in Peninj (Lake Natron, Tanzania). *Journal of Anthropology Archaeology* 27: 244-264.

Debénath, A., Dibble, H.L. 1994. Handbook of Paleolithic Typology Volume 1: Lower and middle Paleolithic of Europe. University of Pennsylvania Museum of Archaeology, University of Pennsylvania Press, Philadelphia.

Delagnes, A., Roche, H. 2005. Late Pliocene hominid knapping skills: The case of Lokalalei 2C, West Turkana, Kenya. *Journal of Human Evolution* 48: 435-472.

Diez-Martín, F., Yustos, P.S., Domínguez-Rodrigo, M., Prendergast, M.E. 2011. An experimental study of bipolar and freehand knapping of Naibor Soit quartz from Olduvai Gorge (Tanzania). *American Antiquity* 76: 690-708.

Diez-Martín, F., Yustos, P.S., Uribelarrea, D., Baquedano, E., Mark, D.F., Mabulla, A., Fraile, C., Duque, J., Díaz, I., Pérez-González, A., Yravedra, J. 2015. The origin of the Acheulean: The 1.7 million-year-old site of FLK West, Olduvai Gorge (Tanzania). *Scientific Reports* 5: 1-9.

Dinno, A. 2017. dunn.test: Dunn's Test of Multiple Comparisons using Rank Sums. R package version 1.3.4.

Dixon, S.J., Brereton, R.G. 2009. Comparison of performance of five common classifiers represented as boundary methods: Euclidean distance to centroids, linear discriminant analysis, quadratic discriminant analysis, learning vector quantization and support vector machines, as dependent on data structure. *Chemometrics and Intelligent Laboratory Systems* 95: 1-17.

Domínguez-Rodrigo, M. 1997. A reassessment of the study of cut mark patterns to infer hominid manipulation of fleshed carcasses at the FLK Zinj 22 Site, Olduvai Gorge, Tanzania. *Trabajos de Prehistoria* 54: 29-42.

Domínguez-Rodrigo, M. 1999. Flesh availability and bone modifications in carcasses consumed by lions: Palaeoecological relevance in hominid foraging patterns. *Paleogeographic, Paleoclimatology, Palaeoecology* 149: 373-388.

Domínguez-Rodrigo, M., Alcalá, L. 2016. 3.3-million-year-old stone tools and butchery traces? More evidence needed. *PaleoAnthropology* 2016: 46-53.

Domínguez-Rodrigo, M., Barba, R. 2006. New estimates of tooth mark and percussion mark frequencies at the FLK Zinj site: The carnivore-hominid-carnivore hypothesis falsified. *Journal of Human Evolution* 50: 170-194.

Domínguez-Rodrigo, M., Barba, R. 2007. Five more arguments to invalidate the passive scavenging version of the carnivore-hominid-carnivore model: A reply to Blumenschine et al. (2007a). *Journal of Human Evolution* 53: 427-433.

Domínguez-Rodrigo, M., Bunn, H.T., Yravedra, J. 2014. A critical re-evaluation of bone surface modification models for inferring fossil hominin and carnivore interactions through a multivariate approach: Application to the FLK *Zinj* archaeofaunal assemblage (Olduvai Gorge, Tanzania). *Quaternary International* 322: 32-43.

Domínguez-Rodrigo, M., de Juana, S., Galan, A.B., Rodríguez, M. 2009. A new protocol to differentiate trampling marks from butchery cut marks. *Journal of Archaeological Science* 36: 2643-2654.

Domínguez-Rodrigo, M., Pickering, T.R. 2003. Early hominid hunting and scavenging: A zooarchaeological review. *Evolutionary Anthropology* 12: 275-282.

Domínguez-Rodrigo, M., Pickering, T.R., Bunn, H.T. 2010. Configurational approach to identifying the earliest hominin butchers. *Proceedings of the National Academy of Sciences* 107: 20929-20934.

Domínguez-Rodrigo, M., Pickering, T.R., Bunn, H.T. 2011. Reply to McPherron et al.: Doubting Dikika is about data, not paradigms. *Proceedings of the National Academy of Sciences* 108: E117-E117.

Domínguez-Rodrigo, M., Pickering, T.R., Bunn, H.T. 2012. Experimental study of cut marks made with rocks unmodified by human flake and its bearing on claims of ~3.4-million-year-old butchery evidence from Dikika, Ethiopia. *Journal of Archaeological Science* 39: 205-214.

Domínguez-Rodrigo, M., Pickering, T.R., Semaw, S., Rogers, M.J. 2005. Cutmarked bones from Pliocene archaeological sites at Gona, Afar, Ethiopia: Implications for the function of the world's oldest stone tools. *Journal of Human Evolution* 48: 109-121.

Domínguez-Rodrigo, M., Saladié, P., Cáceres, I., Huguet, R., Yravedra, J., Rodríguez-Hidalgo, A., Martín, P., Pineda, A., Marín, J., Gené, C., Aramendi, J. 2017. Use and abuse of cut mark analyses: The Rorschach effect. *Journal of Archaeological Science* 86: 14-23.

Domínguez-Rodrigo, M., Serrallonga, J., Juan-Tresserras, J., Alcala, L., Luque, L. 2001. Woodworking activities by early humans: A plant residue analysis on Acheulian stone tools from Peninj (Tanzania). *Journal of Human Evolution* 40: 289-299.

Eren, M.I., Roos, C.I., Story, B.A., von Cramon-Taubadel, N., Lycett, S.J. 2014. The role of raw material differences in stone tool shape variation: An experimental assessment. *Journal of Archaeological Science* 49: 472-487.

Fernández-Jalvo, Y., Andrews, P. 2003. Experimental effects of water abrasion on bone fragments. *Journal of Taphonomy* 1: 147-163.

Ferraro, J,V., Plummer, T.W., Pobiner, B.L., Oliver, J.S., Bishop, L.C., Braun, D.R., Ditchfield, P.W., Seaman III., J.W., Binetti, K.M., Seaman Jr, J.W., Hertel, F. 2013. Earliest archaeological evidence of persistent hominin carnivory. *PloS one* 8: e62174.

Fisher, J.W. 1995. Bone surface modifications in zooarchaeology. *Journal of Archaeological Method and Theory* 2: 7-68.

Foley, R.A., Lee, P.C. 1991. Ecology and energetics of encephalization in hominid evolution. *Philosophical Transactions of the Royal Society B* 334: 223-232.

Galán, A.B., Domínguez-Rodrigo, M. 2014. Testing the efficiency of simple flakes, retouched flakes and small handaxes during butchery. *Archaeometry* 56: 1054-1074.

Gamble, C. 1998. Handaxes and Paleolithic Individuals. In: Ashton, N., Healey, F., and Pettit, P. (Eds.), Stone Age Archaeology: Essays in Honour of John Wymer. Oxbow Books: Oxford, pp. 105-109.

Gibbon, R.J., Granger, D.E., Kuman, K., Partridge, T.C. 2009. Early Acheulean technology in the Rietputs Formation, South Africa, dated with cosmogenic nuclides. *Journal of Human Evolution* 56: 152-160.

Gifford, D.P. 1981. Taphonomy and paleoecology: A critical review of archaeology's sister disciplines. *Advances in Archaeological Method and Theory* 4: 365-438.

Gifford-Gonzalez, D. 1991. Bones are not enough: Analogues, knowledge, and interpretive strategies in zooarchaeology. *Journal of Anthropological Archaeology* 10: 215-254.

Gilbert, W.H., Richards, G.D. 2000. Digital imaging of bone and tooth modification. *The Anatomical Record* 261: 237-246.

Goldman-Neuman, T., Hovers, E. 2009. Methodological considerations in the study of Oldowan raw material selectivity: Insights from AL 894 (Hadar, Ethiopia). In: Hovers, E., and Braun, D.R. (Eds.), Interdisciplinary Approaches to the Oldowan. Springer: Dordrecht, The Netherlands, pp.71-84.

Goldman-Neuman, T., Hovers, E. 2011. Raw material selectivity in Late Pliocene Oldowan sites in the Makaamitalu Basin, Hadar, Ethiopia. *Journal of Human Evolution* 62: 353-366.

Gould, S.J. 1965. Is uniformitarianism necessary? *American Journal of Science* 263: 223-228.

Greenfield, H.J. 1999. The origins of metallurgy: Distinguishing stone from metal cut-marks on bones from archaeological sites. *Journal of Archaeological Science* 26: 797-808.

Greenfield, H.J. 2006. Slicing cut marks on animal bones: Diagnostics for identifying stone tool type and raw material. *Journal of Field Archaeology* 31: 147-163.

Gumrukcu, M., Muttart, M.V., Pante, M.C. 2017. Assessing the effects of fluvial abrasion on bone surface modifications using high-resolution 3-D scanning. Abstracts of the Paleoanthropology Society 2017 Meeting. *PaleoAnthropology*: A1-A41.

Gurtov, A.N., Eren, M.I. 2014. Lower Paleolithic bipolar reduction and hominin selection of quartz at Olduvai Gorge, Tanzania: What's the connection?. *Quaternary International* 322: 285-291.

Hammer, Ø., Harper, D.A.T., Ryan, P.D. 2001. PAST: Paleontological Statistics Software Package for education and data analysis. *Palaeontologia Electronica* 4: 1-9.

Harmand, S., Lewis, J.E., Feibel, C.S., Lepre, C.J., Prat, S., Lenoble, A., Boës, X., Quinn, R.L., Brenet, M., Arroyo, A., Taylor, N., Clément, S., Daver, G., Brugal, J., Leakey, L., Mortlock, R.A., Wright, J.D., Lokorodi, S., Kirwa, C., Kent, D.V., Roche, H. 2015. 3.3-million-year-old stone tools from Lomekwi 3, West Turkana, Kenya. *Nature* 521: 310-315.

Hutton, J. 1795. Theory of the Earth (2 vols.). Cadell, Junior and Davies, London; William Creech, Edinburgh.

Isaac, G.L. 1997. Koobi Fora Research Project Volume 5: Plio-Pleistocene Archaeology. Oxford: Oxford University Press.

Isaacs, G.L., Curtis, G.H. 1974. Age of early Acheulian industries from the Peninj Group, Tanzania. *Nature* 249: 624-627.

Ioannidou, E. 2003. Taphonomy of animal bones: Species, sex, age and breed variability of sheep, cattle and pig bone density. *Journal of Archaeological Science* 30: 355-365.

Isler, K., van Schaik, C.P. 2009. The expensive brain: A framework for explaining evolutionary changes in brain size. *Journal of Human Evolution* 57: 392-400.

Jones, P.R. 1979. Effects of raw materials on biface manufacture. *Science* 204: 835-836.

Jones, P.R. 1980. Experimental butchery with modern stone tools and its relevance for Palaeolithic archaeology. *World Archaeology* 12: 153-165.

Kaiser, T.M., Katterwe, H. 2001. The application of 3D-microprofilometry as a tool in the surface diagnosis of fossil and sub-fossil vertebrate hard tissue. An example from the Pliocene upper Laetoli beds, Tanzania. *International Journal of Osteoarchaeology* 11: 350-356.

Keeley, L.H., Toth, N. 1981. Microwear polishes on early stone tools from Koobi Fora, Kenya. *Nature* 293: 464-465.

Key, A.J.M., Lycett, S.J. 2011. Technology based evolution? A biometric test of the effects of handsize versus tool form on efficiency in an experimental cutting task. *Journal of Archaeological Science* 38: 1663-1670.

Key, A.J.M., Lycett, S.J. 2017. Reassessing the production of handaxes versus flakes from a functional perspective. *Archaeological and Anthropological Sciences* 9: 737-753.

Kimbel, W.H., Walter, R.C., Johanson, D.C., Reed, K.E., Aronson, J.L., Assefa, Z., Marean, C.W., Eck, G.G., Bobe, R., Hovers, E., Rak, Y., Vondra, C., Yemane, T., York, D., Chen, Y., Evensen, N.M., Smith, P.E. 1996. Late Pliocene *Homo* and Oldowan tools from the Hadar Formation (Kada Hadar Member), Ethiopia. *Journal of Human Evolution* 31: 549-561.

Kimura, Y. 1999. Tool-using strategies by early hominids at Bed II, Olduvai Gorge, Tanzania. *Journal of Human Evolution* 37: 807-831.

Kimura, Y. 2002. Examining time trends in the Oldowan technology at Beds I and II, Olduvai Gorge. *Journal of Human Evolution* 43: 291-321.

Kleindienst, M.R. 1961. Variability within the Late Acheulian assemblage in Eastern Africa. *The South African Archaeological Bulletin* 16: 35-52.

Kohn, M., Mithen, S. 1999. Handaxes: Products of sexual selection? *Antiquity* 73: 518-526.

Korkmaz, S., Goksuluk, D., Zararsiz, G. 2016. MVN: Multivariate Normality Tests. R package version 4.0.2.

Kuman, K. 1994. The archaeology of Sterkfontein - past and present. *Journal of Human Evolution* 27: 471-495.

Kuman, K., Clarke, R.J. 2000. Stratigraphy, artefact industries and hominid associations for Sterkfontein, Member 5. *Journal of Human Evolution* 38: 827-847.

Kuzminsky, S.C., Gardiner, M.S. 2012. Three-dimensional laser scanning: Potential uses for museum conservation and scientific research. *Journal of Archaeological Sciences* 39: 2744-2751.

Lam, Y.M., Pearson, O.M. 2004. The fallibility of bone density values and their use in archaeological analyses. *Journal of Taphonomy* 2: 99-115.

Lam, Y.M., Pearson, O.M. 2005. Bone density studies and the interpretation of the faunal record. *Evolutionary Anthropology* 14: 99-108.

Leakey, M.D. 1966. A review of the Oldowan culture from Olduvai Gorge, Tanzania. *Nature* 210: 462-466.

Leakey, M.D. 1971. Olduvai Gorge, Volume 3. Excavations in Beds I and II, 1960-1963. Cambridge University Press: Cambridge.

Lemorini, C., Plummer, T.W., Braun, D.R., Crittenden, A.N., Ditchfield, P.W., Bishop, L.C., Hertel, F., Oliver, J.S., Marlowe, F.W., Schoeninger, M.J., Potts, R. 2014. Old stones' song: Use-wear experiments and analysis of the Oldowan quartz and quartzite assemblage from Kanjera South (Kenya). *Journal of Human Evolution* 72: 10-25.

Leonard, W.R., Snodgrass, J.J., Robertson, M.L. 2007. Effects of brain evolution on human nutrition and metabolism. *Annual Review of Nutrition* 27: 311-327.

Lepre, C.J., Roche, H., Kent, D.V., Harmand, S., Quinn, R.L., Brugal, J.P., Texier, P.J., Lenoble, A., Feibel, C.S. 2011. An earlier origin for the Acheulian. *Nature* 477: 82-85.

Lewis, J.E., Harmand, S. 2016. An earlier origin for stone tool making: Implications for cognitive evolution and the transition to *Homo*. *Philosophical Transactions of the Royal Society B* 371: 20150233.

Lupo, K.D., O'Connell, J.F. 2002. Cut and tooth mark distributions on large animal bones: Ethnoarchaeological data from the Hadza and their implications for current ideas about early human carnivory. *Journal of Archaeological Science* 29: 85-109.

Lycett, S.J. 2008. Acheulean variation and selection: Does handaxe symmetry fit neutral expectations? *Journal of Archaeological Science* 35: 2640-2648.

Lycett, S.J., Bae, C.J. 2010. The Movius Line controversy: The state of the debate. *World Archaeology* 42: 521-544.

Magill, C.R., Ashley, G.M., Freeman, K.H. 2013. Ecosystem variability and early human habitats in Eastern Africa. *Proceedings of the National Academy of Sciences* 110: 1167-1174.

Maté-González, M.Á., Palomeque-González, J.F., Yravedra, J., González-Aguilera, D., Domínguez-Rodrigo, M. 2016. Micro-photogrammetric and morphometric differentiation of cut marks on bones using metal knives, quartzite, and flint flakes. *Archaeological and Anthropological Sciences*: 1-12.

Maté-González, M.Á., Yravedra, J., González-Aguilera, D., Palomeque-González, J.F., Domínguez-Rodrigo, M. 2015. Micro-photogrammetric characterization of cut marks on bones. *Journal of Archaeological Science* 62: 128-142.

Maté-González, M.Á., Yravedra, J., Martín-Perea, D.M., Palomeque-González, J.F., San-Juan-Blazquez, V., Estaca-G Gómez, V., Uribelarrea, D., Álvarez-Alonso, D., Cuartero, F., González-Aguilera, D., Domínguez-Rodrigo, M. 2017. Flint and quartzite: Distinguishing raw material through bone cut marks. *Archaeometry* doi: 10.1111/arcm.12327.

McCall, G.S. 2005. An experimental examination of the potential function of Early Stone Age tool technology and implications for subsistence behavior. *Lithic Technology* 30: 29-43.

McLachlan, G.J. Discriminant Analysis and Statistical Pattern Recognition. John Wiley & Sons, Inc.: Hoboken, New Jersey.

McPherron, S.P., Alemseged, Z., Marean, C.W., Wynn, J.G., Reed, D., Geraads, D., Bobe, R., Béarat, H.A. 2010. Evidence for stone-tool-assisted consumption of animal tissues before 3.39 million years ago at Dikika, Ethiopia. *Nature* 466: 857-860.

Merritt, S.R. 2012. Factors affecting Early Stone Age cut mark cross-sectional size: Implications from actualistic butchery trials. *Journal of Archaeological Science* 39: 2984-2994.

Merritt, S.R. 2015. Cut mark cluster geometry and equifinality in replicated in Early Stone Age butchery. *International Journal of Osteoarchaeology* 26: 585-598.

Mgeladze, A., Lordkipanidze, D., Moncel, M.H., Despriee, J., Chagelishvili, R., Nioradze, M., Nioradze, G. 2011. Hominin occupations at the Dmanisi site, Georgia, Southern Caucasus: Raw materials and technical behaviours of Europe's first hominins. *Journal of Human Evolution* 60: 571-596.

Mitchell, J.C. 1995. Studying biface butchery at Boxgrove: Roe deer butchery with replica handaxes. *Lithics* 16: 64-69.

Mosquera, M., Ollé, A., Saladié, P., Cáceres, I., Huguet, R., Rosas, A., Villalaín, J., Carrancho, A., Bourles, D., Braucher, R., Pineda, A. 2016. The Early Acheulean technology of Barranc de la Boella (Catalonia, Spain). *Quaternary International* 393: 95-111.

Muttart, M.V. 2017. Taxonomic distinctions in the 3D micromorphology of tooth marks with applications to feeding traces from Middle Bed II, Olduvai Gorge, Tanzania. Master's Thesis, Colorado State University.

Muttart, M.V., Pante, M.C. 2016. Quantifying taxonomic distinctions in tooth mark morphology with high-resolution 3-D scanning. Abstracts of the Paleoanthropology Society 2016 Meeting. *PaleoAnthropology*: A1-A34.

Njau, J.K., Blumenschine, R.J., 2006. A diagnosis of crocodile feeding traces on larger mammal bone, with fossil examples from the Plio-Pleistocene Olduvai Basin, Tanzania. *Journal of Human Evolution* 50: 142-162.

O'Brien, E.M. 1981. The projectile capabilities of an Acheulian handaxe from Olorgesailie. *Current Anthropology* 22: 76–79.

Oliver, J.S. 1994. Estimates of hominid and carnivore involvement in the FLK Zinjanthropus fossil assemblage: Some socioecological implications. *Journal of Human Evolution* 27: 267-294.

Olsen, S.L., Shipman, P. 1988. Surface modification on bone: Trampling versus butchery. *Journal of Archaeological Science* 15: 535-553.

Orlikoff, E.R., Keevil, T.L., Pante, M.C. 2017. A quantitative assessment of trampling-induced modification to bone surfaces. Abstracts of the Paleoanthropology Society 2017 Meeting. *PaleoAnthropology*: A1-A41.

Pante, M.C. 2013. The larger mammal fossil assemblage from JK2, Bed III, Olduvai Gorge, Tanzania: Implications for the feeding behavior of Homo erectus. *Journal of Human Evolution* 64: 68-82.

Pante, M.C., Blumenschine, R.J., Capaldo, S.D., Scott, R.S. 2012. Validation of bone surface modification models for inferring fossil hominin and carnivore feeding interactions, with reapplication to FLK 22, Olduvai Gorge, Tanzania. *Journal of Human Evolution* 63: 395-407.

Pante, M.C., Blumenschine, R.J., Capaldo, S.D., Scott, R.S. 2015. Revalidation of bone surface modification models for inferring fossil hominin and carnivore feeding interactions. *Quaternary International* 355: 164-168.

Pante, M.C., Muttart, M.V., Keevil, T.L., Blumenschine, R.J., Njau, J.K., Merritt, S.R. 2017. A new high-resolution 3-D quantitative method for identifying bone surface modifications with implications for the Early Stone Age archaeological record. *Journal of Human Evolution* 102: 1-11.

Pappu, S., Gunnell, Y., Akhilesh, K., Braucher, R., Taieb, M., Demory, F., Thouveny, N. 2011. Early Pleistocene presence of Acheulian hominins in south India. *Science* 331: 1596-1599.

Pardoe, I., Yin, X., Cook, R.D. 2007. Graphical tools for quadratic discriminant analysis. *Technometrics* 49:172-83.

Pickering, T.R., Domínguez-Rodrigo, M., Egeland, C., Brain, C.K. 2004. New data and ideas on the foraging behaviour of Early Stone Age hominins at Swartkrans Cave, South Africa. *South African Journal of Science* 100: 215-219.

Piperno, M., Collina, C., Gallotti, R., Raynal, J.P., Kieffer, G., Le Bourdonnec, F.X., Poupeau, G., Geraads, D. 2009. Obsidian exploitation and utilization during the Oldowan at Melka Kunture (Ethiopia). In: Hovers, E., and Braun, D.R. (Eds.), Interdisciplinary Approaches to the Oldowan. Springer: Dordrecht, The Netherlands, pp. 111-128.

Plummer, T. 2004. Flaked stones and old bones: Biological and cultural evolution at the dawn of technology. *Yearbook of Physical Anthropology* 47: 118-164.

Plummer, T., Bishop, L.C., Ditchfield, P., Hicks, J. 1999. Research on Late Pliocene Oldowan sites at Kanjera South, Kenya. *Journal of Human Evolution* 36: 151-170.

Pobiner, B.L., Roger, M.J., Monahan, C.M., Harris, J.W.K. 2008. New evidence for hominin carcass processing strategies at 1.5 Ma, Koobi Fora, Kenya. *Journal of Human Evolution* 55: 103-130.

Pope, M., Russel, K., Watson, K. 2015. Biface form and structured behaviour in the Acheulean. *Lithics: The Journal of Lithic Studies Society* 27: 44-57.

Potts, R., Shipman, P. 1981. Cutmarks made by stone tools on bones from Olduvai Gorge, Tanzania. *Nature* 291: 577-580.

R Core Team. 2017. R: A language and environment for statistical computing. R Foundation for Statistical Computing, Vienna, Austria. URL: https://www.R-project.org/.

Raab, L. M., Goodyear, A.C. 1984. Middle-range theory in archaeology: A critical review of origins and applications. *American Antiquity* 49: 255-268.

Rabinovich, R., Gaudzinski-Windheuser, S., Goren-Inbar, N. 2008. Systematic butchering of fallow deer (Dama) at the early middle Pleistocene Acheulian site of Gesher Benot Ya 'aqov (Israel). *Journal of Human Evolution* 54: 134-149.

Ripley, B., Venables, B., Bates, D.M., Hornik, K., Cebhardt, A., Firth, D. 2017. MASS: Support Function and Datasets for Venables and Ripley's MASS. R package version 7.3-47.

Roche, H., Delagnes, A., Brugal, J.P., Feibel, C. 1999. Early hominid stone tool production and technical skill 2.34 Myr ago in West Turkana, Kenya. *Nature* 399: 57-60.

Rose, J.J. 1983. A replication technique for scanning electron microscopy: Applications for anthropologists. *American Journal of Physical Anthropology* 62: 255-261.

Rothman, K.J. 1990. No adjustments are needed for multiple comparisons. *Epidemiology* 1: 43-46.

Sahle, Y., El Zaatari, S., White, T.D. 2017. Hominid butchers and biting crocodiles in the African Plio–Pleistocene. *Proceedings of the National Academy of Sciences* 114: 13164-13169.

Sahnouni, M., de Heinzelin, J. 1998. The site of Ain Hanech revisited: New investigations at this Lower Pleistocene site in Northern Algeria. *Journal of Archaeological Science* 25: 1083-1101.

Schick, K.D., Toth, N.P., 1993. Making silent stones speak: Human evolution and the dawn of technology. Simon and Schuster: New York.

Schroettner, H., Schmied, M., Scherer, S. 2006. Comparison of 3D surface reconstruction data from certified depth standards obtained by SEM and an infinite focus measurement machine (IFM). *Microchimica Acta* 155: 279-284.

Selvaggio, M.M. 1998. Evidence for a three-stage sequence of hominid and carnivore involvement with long bones at FLK *Zinjanthropus*, Olduvai Gorge, Tanzania. *Journal of Archaeological Science* 25: 191-202.

Semaw, S., Renne P., Harris, J.W.K., Feibel, C.S., Bernor, R.L., Fesseha, N., Mowbray, K. 1997. 2.5-million-year-old stone tools from Gona, Ethiopia. *Nature* 385: 333-336.

Semaw, S., Rogers, M., Stout, D. 2009. The Oldowan-Acheulian transition: Is there a “Developed Oldowan” artifact tradition? In: Camps, M., and Chauhan, P. (Eds.), Sourcebook of Paleolithic Transitions. Springer: New York, pp. 173-192.

Semaw, S., Rogers, M.J., Quade, J., Renne, P.R., Butler, R.F., Domínguez-Rodrigo, M., Stout, D., Hart, W.S., Pickering, T., Simpson, S.W. 2003. 2.6-million-year-old stone tools and associated bones from OGS-6 and OGS-7, Gona, Afar, Ethiopia. *Journal of Human Evolution* 45: 169-177.

Sharon, G. 2008. The impact of raw material on Acheulian large flake production. *Journal of Archaeological Science* 35: 1329-1344.

Shea, J.J. 2007. Lithic archaeology, or, what stone tools can (and can’t) tell us about early hominin diets. In: Ungar, P.S. (Ed.), Evolution of the human diet: The known, the unknown, and the unknowable. Oxford University Press: Oxford.

Shipman, P. 1986. Scavenging or hunting in early hominids: Theoretical framework and tests. *American Anthropologist* 88: 27-43.

Shipman, P., Rose, J., 1983. Early hominid hunting, butchering, and carcass-processing behaviors: Approaches to the fossil record. *Journal of anthropological Archaeology* 2: 57-98.

Solodenko, N., Zupancich, A., Cesaro, S.N., Marder, O., Lemorini, C., Barkai, R. 2015. Fat residue and use-wear found on Acheulian biface and scraper associated with butchered elephant remains at the site of Revadim, Israel. *PloS one* 10: 0118572.

Stout, D., Quade, J., Semaw, S., Rogers, M.J., Levin, N.E. 2005. Raw material selectivity of the earliest stone toolmakers at Gona, Afar, Ethiopia. *Journal of Human Evolution* 48: 365-380.

Susman, R.L. 1991. Who made the Oldowan tools? Fossil evidence for tool behavior in Plio-Pleistocene hominids. *Journal of Anthropological Research* 47: 129-151.

Thali, M.J., Taubenreuther, U., Karolczak, M., Braun, M., Brueschweiler, W., Kalender, W.A., Dirnhofer, R. 2003. Forensic microradiology: Micro-computed tomography (Micro-CT) and analysis of patterned injuries inside of bone. *Journal of Forensic Sciences* 48: 1336-1342.

Thompson, J.C., McPherron, S.P., Bobe, R., Reed, D., Barr, W.A., Wynn, J.G., Marean, C.W., Geraads, D., Alemseged, Z. 2015. Taphonomy of fossils from the hominin-bearing deposits at Dikika, Ethiopia. *Journal of Human Evolution* 86: 112-135.

Toth, N. 1985. The Oldowan reassessed: A closer look at early stone artifacts. *Journal of Archaeological Science* 12: 101-120.

Val, A., Costamagno, S., Discamps, E., Chong, S., Claud, E., Deschamps, M., Mourre, V., Soulier, M.C., Thiébaut, C. 2017. Testing the influence of stone tool type on microscopic morphology of cut-marks: Experimental approach and application to the archaeological record with a case study from the Middle Palaeolithic site of Noisetier Cave (Fréchet-Aure, Hautes-Pyrénées, France). *Journal of Archaeological Science: Reports* 11:17-28.

Vallverdú, J., Saladié, P., Rosas, A., Huguet, R., Cáceres, I., Mosquera, M., Garcia-Tabernero, A., Estalrrich, A., Lozano-Fernández, I., Pineda-Alcalá, A., Carrancho, Á. 2014. Age and date for early arrival of the Acheulian in Europe (Barranc de la Boella, la Canonja, Spain). *PLoS One* 9: e103634.

Walker, P.L. 1978. Butchering and stone tool function. *American Antiquity* 43: 710-715.

Weisberg, S. 2015. dr: Methods for dimension reduction for regression. R package version 7.3-47.

Yravedra, J., Diez-Martín, F., Egeland, C.P., Maté-González, M.Á., Palomeque-González, J.F., Arriaza, M.C., Aramendi, J., García Vargas, E., Estaca-Gómez, V., Sánchez, P., Fraile, C., Duque, J., Rodríguez, S.F., González-Aguilera, D., Uribelarraea, D., Mabulla, A., Baquedano, E., Domínguez-Rodrigo, M. 2017a. FLK West (Lower Bed II, Olduvai Gorge, Tanzania): A new early Acheulean site with evidence for human exploitation of fauna. *Boreas* 46: 816-830.

Yravedra, J., Domínguez-Rodrigo, M., Santonja, M., Pérez-González, A., Panera, J., Rubio-Jara, S., Baquedano, E. 2010. Cut marks on the Middle Pleistocene elephant carcass of Áridos 2 (Madrid, Spain). *Journal of Archaeological Science* 37: 2469-2476.

Yravedra, J., Maté-González, M.Á., Palomeque-González, J.F., Aramendi, J., Estaca-Gómez, V., San Juan Blazquez, M., García Vargas, E., Organista, E., González-Aguilera, D., Arriaza, M.C., Cobo-Sánchez, L. 2017b. A new approach to raw material use in the exploitation of animal carcasses at BK (Upper Bed II, Olduvai Gorge, Tanzania): A micro-photogrammetric and geometric morphometric analysis of fossil cut marks. *Boreas 46:* 860-873.

APPENDIX A – BOX PLOT DISTRIBUTIONS OF UNIVARIATE CUT MARK DATA

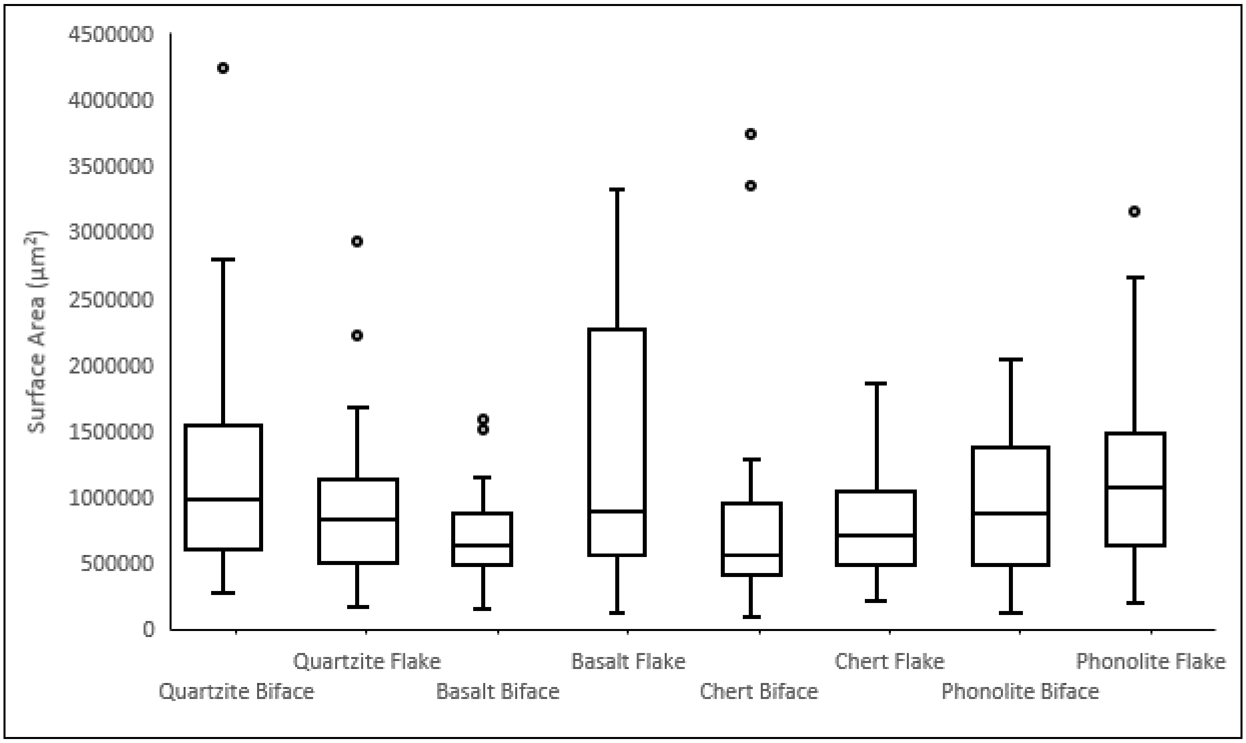

Figure C.1) Box plots of cut mark surface area (3-D) measurements for different tool technologies and raw materials.

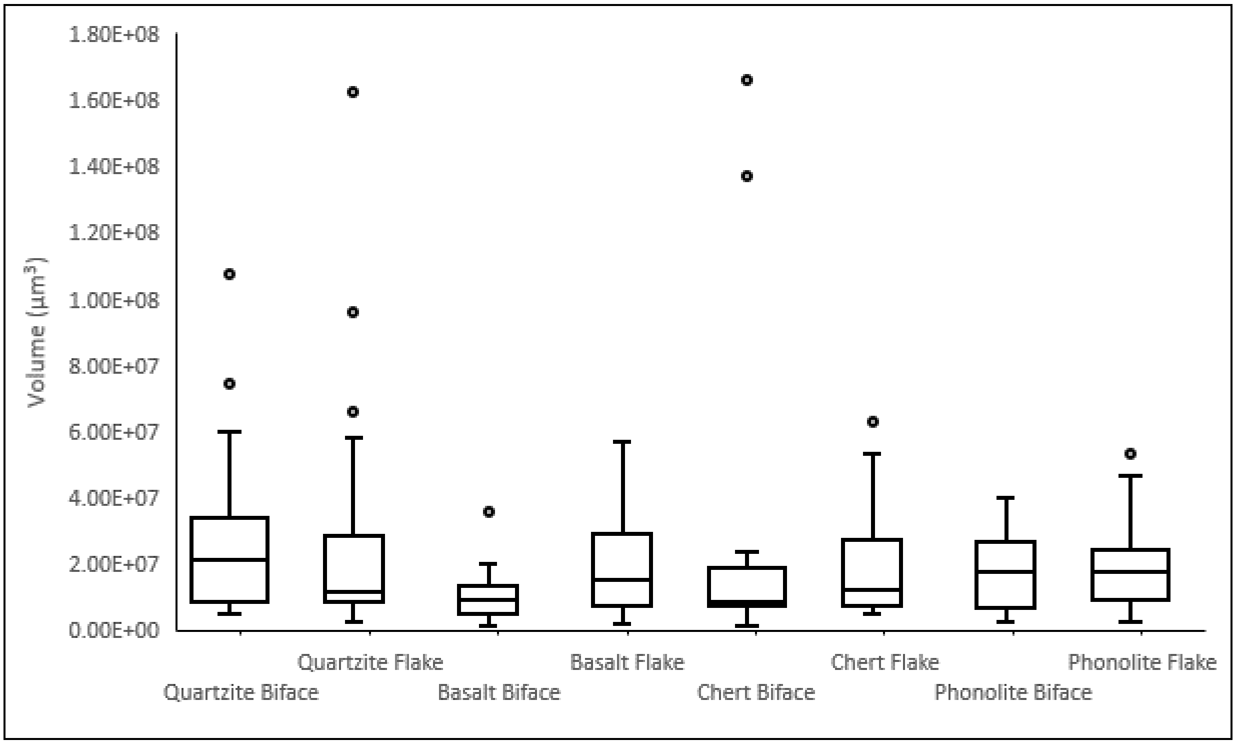

Figure C.2) Box plots of cut mark volume (3-D) measurements for different tool technologies and raw materials.

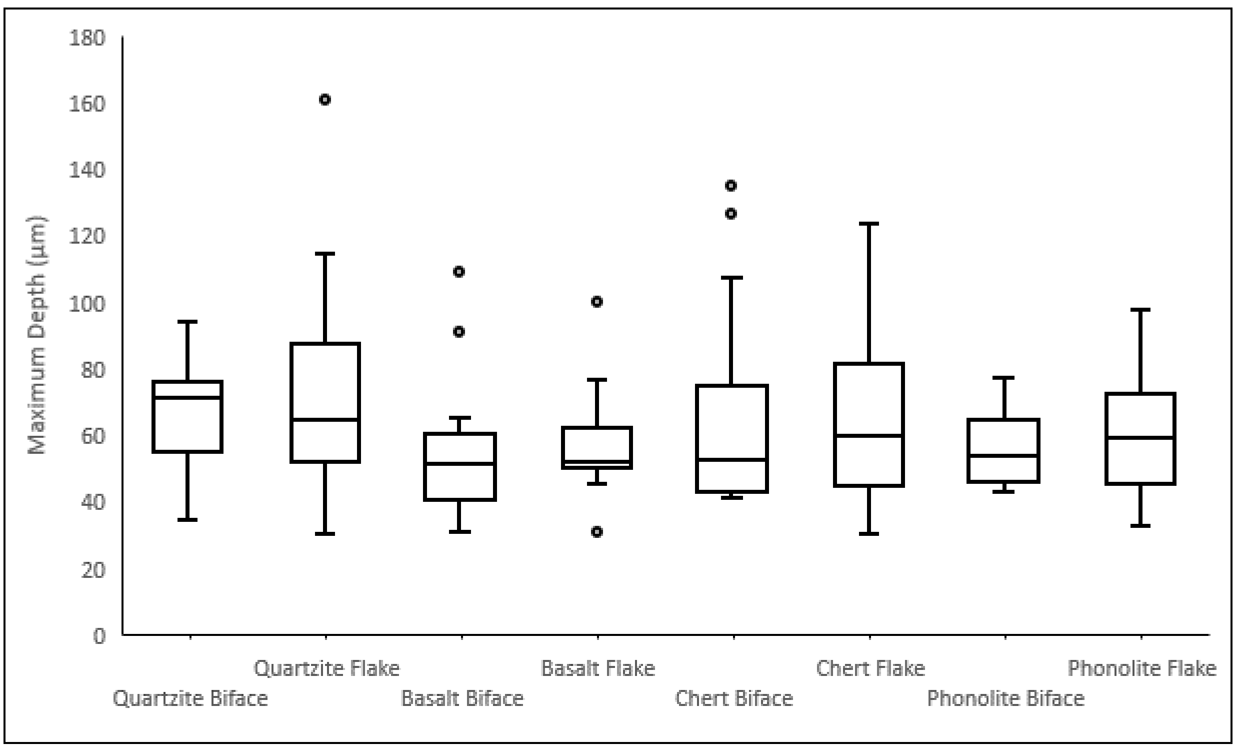

Figure C.3) Box plots of cut mark maximum depth (3-D) measurements for different tool technologies and raw materials.

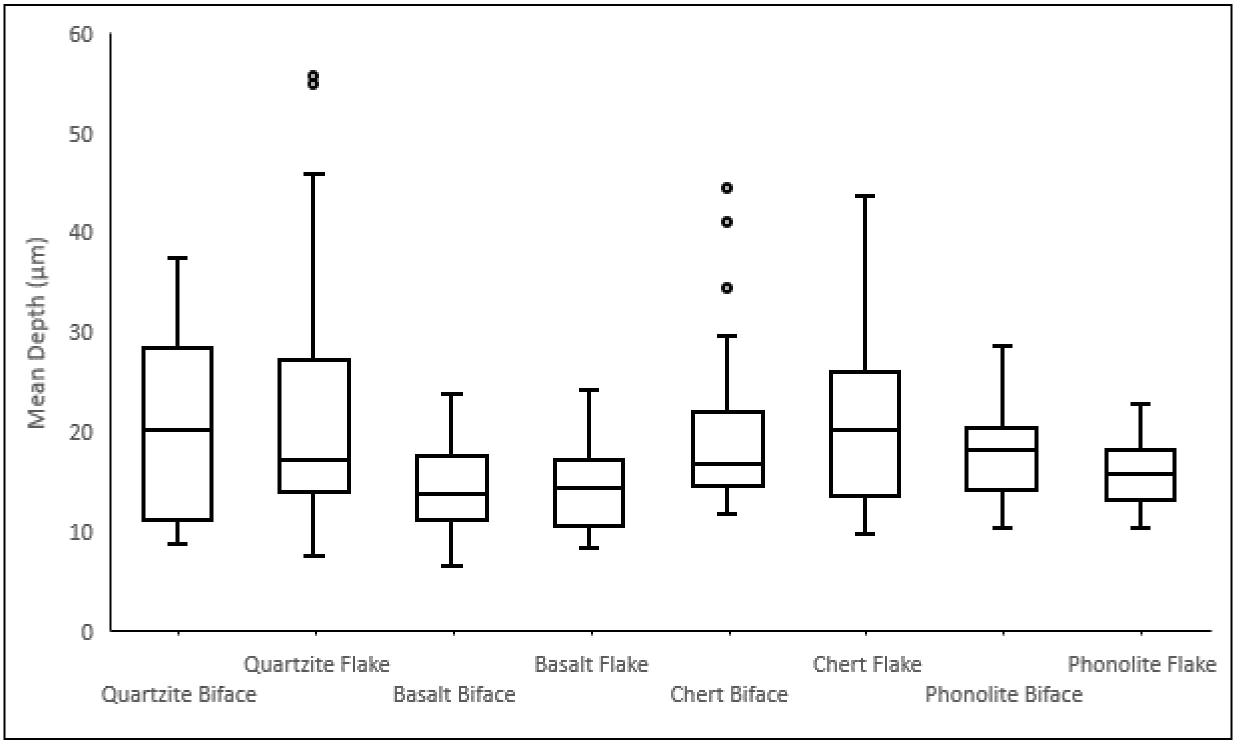

Figure C.4) Box plots of cut mark mean depth (3-D) measurements for different tool technologies and raw materials.

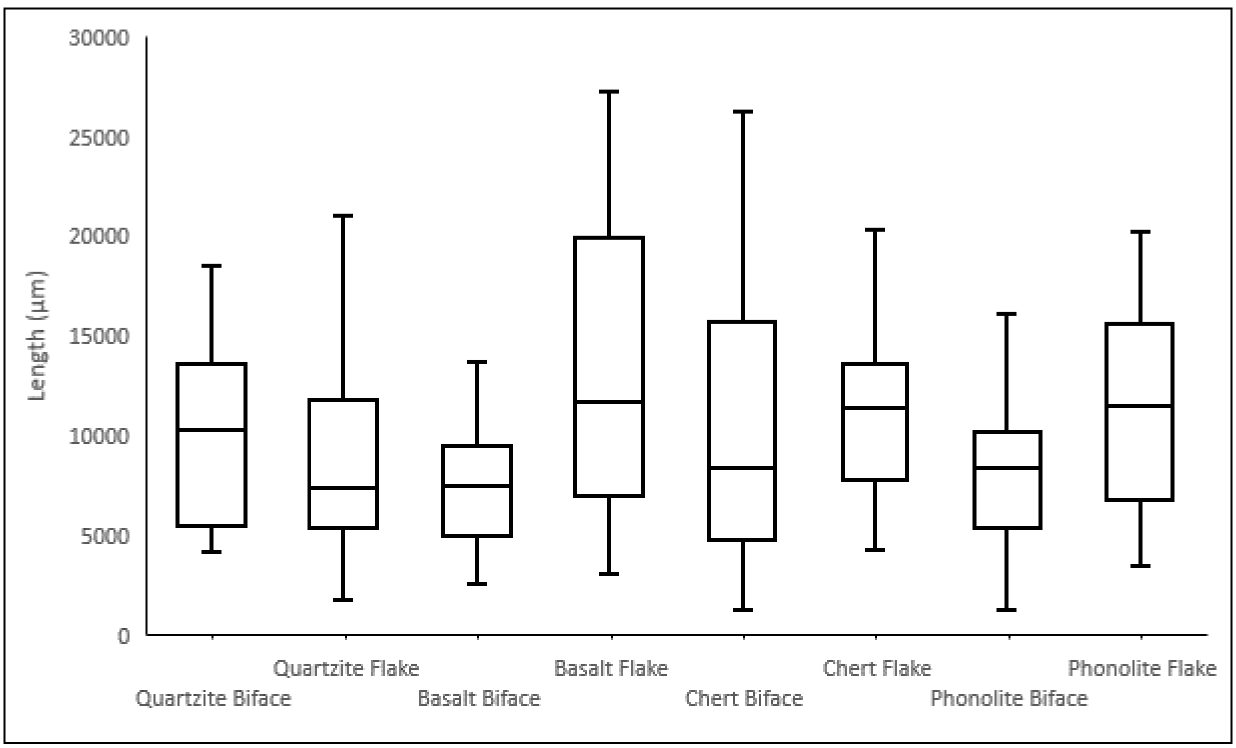

Figure C.5) Box plots of cut mark maximum length (3-D) measurements for different tool technologies and raw materials.

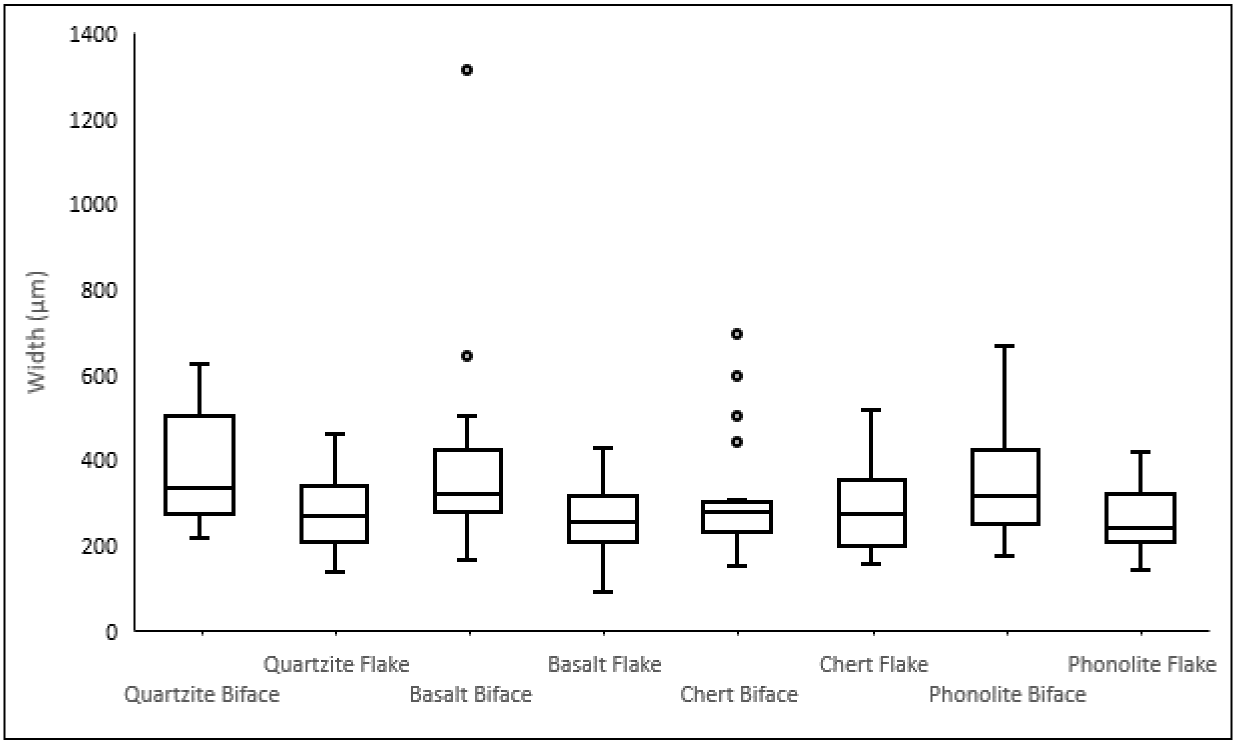

Figure C.6) Box plots of cut mark maximum width (3-D) measurements for different tool technologies and raw materials.

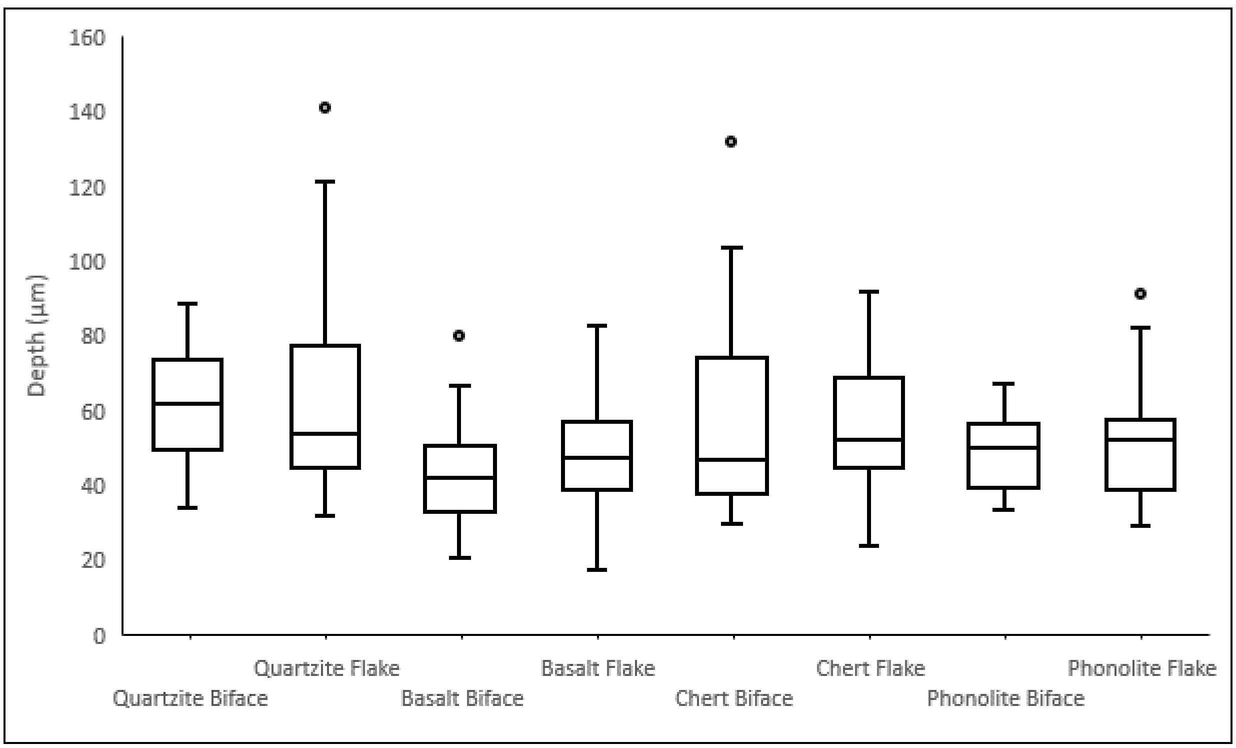

Figure C.7) Box plots of cross-sectional cut mark maximum depth measurements for different tool technologies and raw materials.

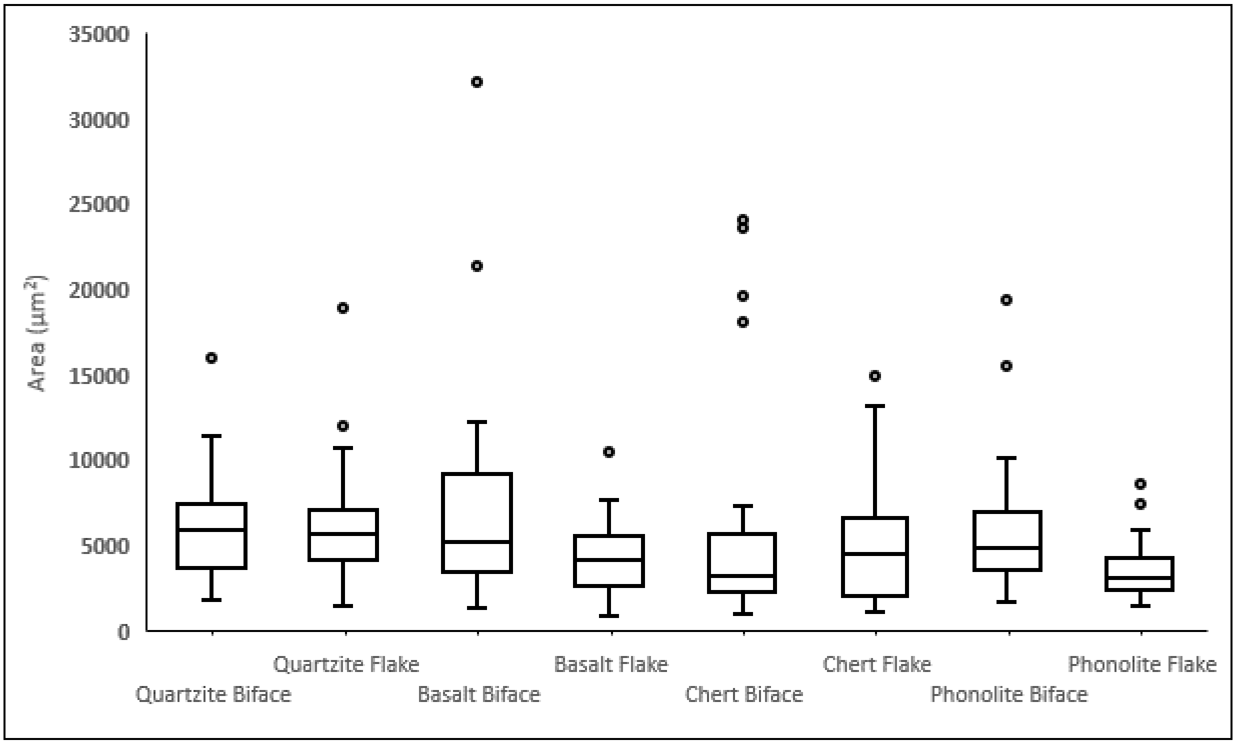

Figure C.8) Box plots of cross-sectional cut mark area measurements for different tool technologies and raw materials.

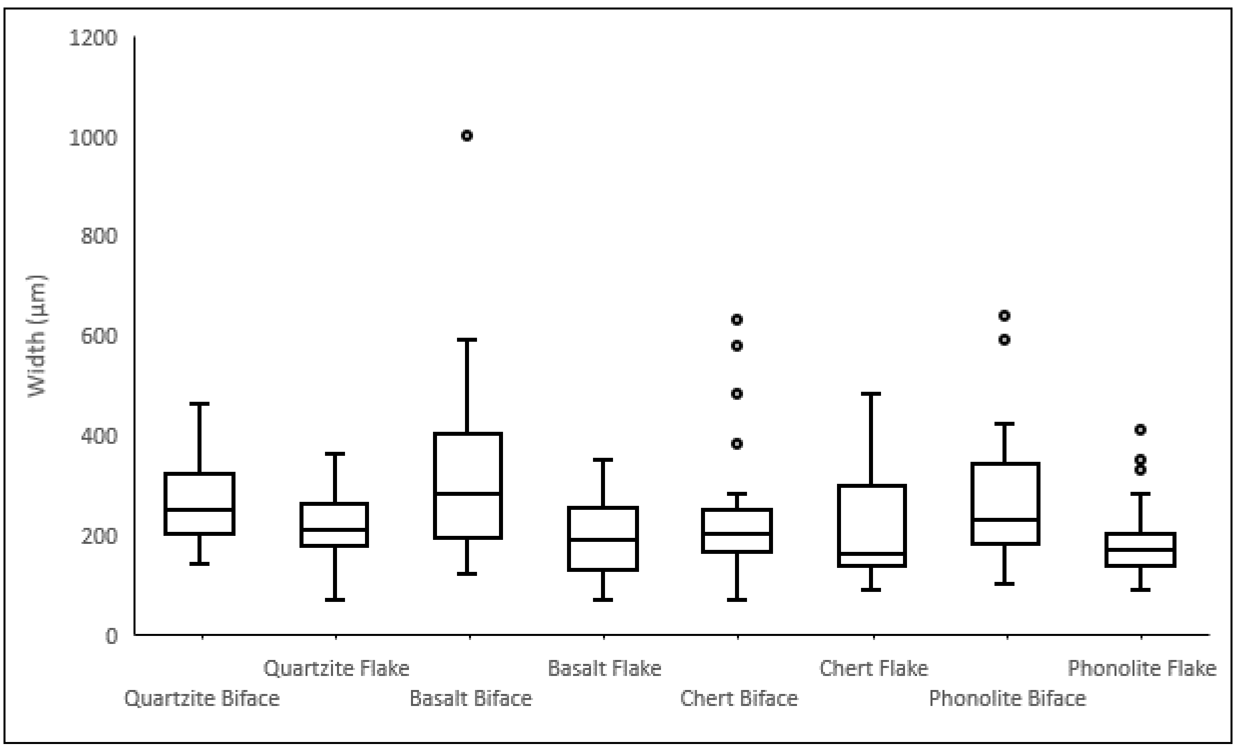

Figure C.9) Box plots of cross-sectional cut mark width measurements for different tool technologies and raw materials.

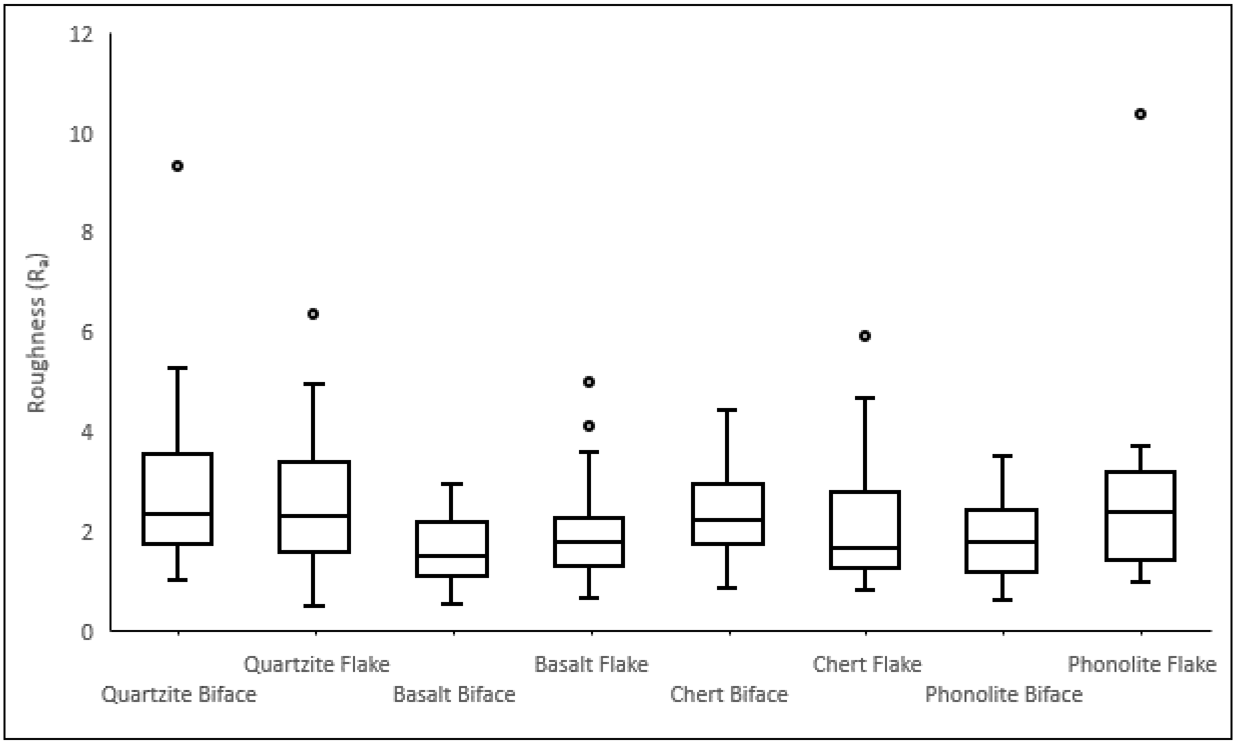

Figure C.10) Box plots of cross-sectional cut mark roughness measurements for different tool technologies and raw materials.

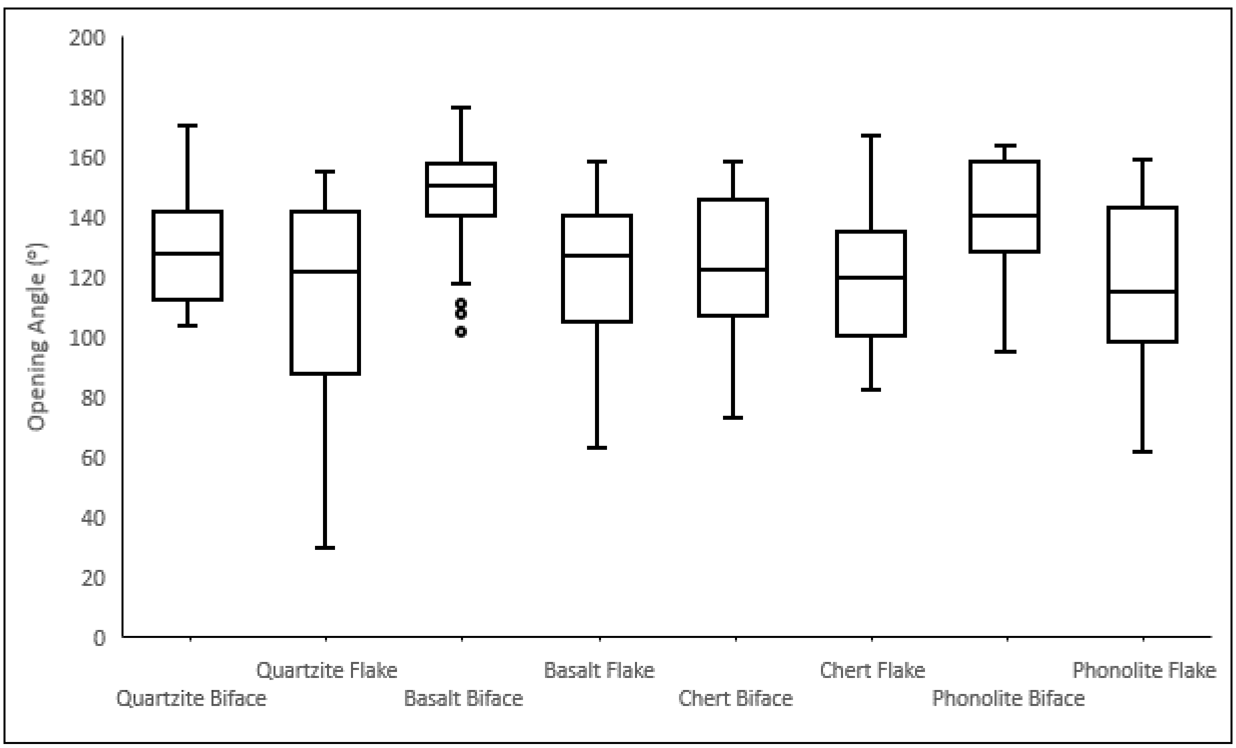

Figure C.11) Box plots of cross-sectional cut mark opening angle measurements for different tool technologies and raw materials.

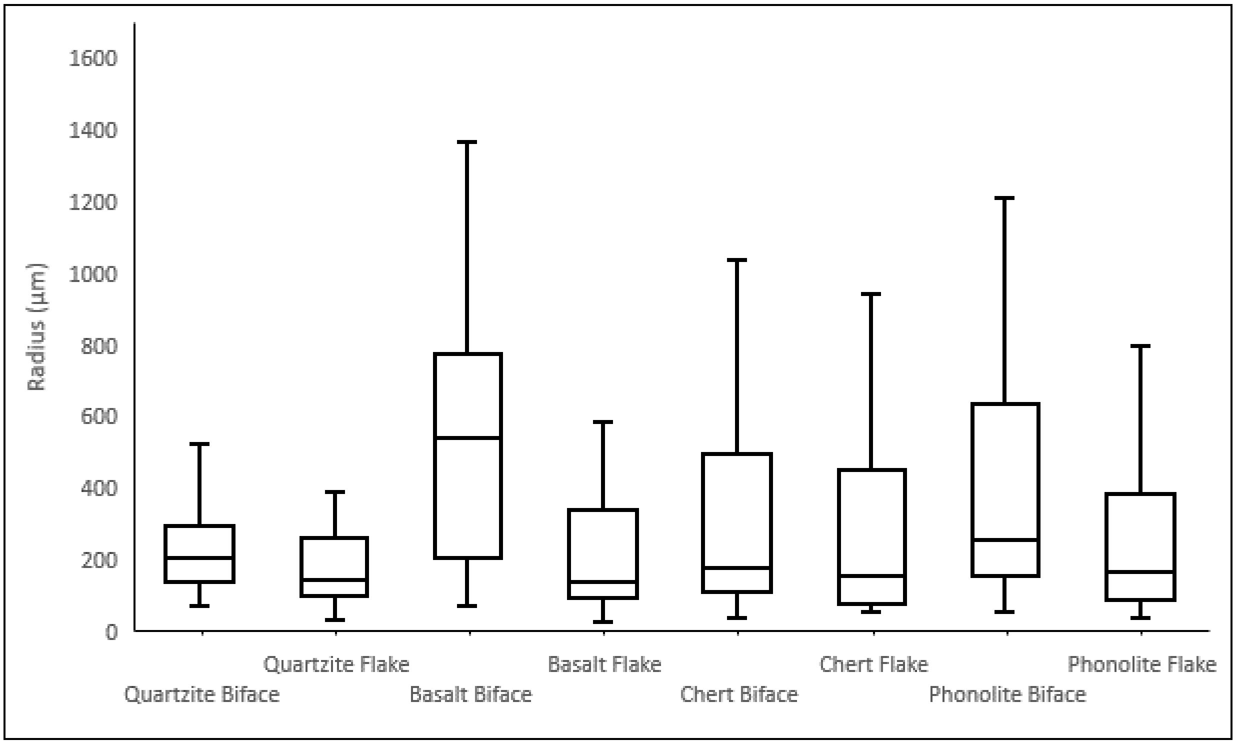

Figure C.12) Box plots of cross-sectional cut mark radius measurements for different tool technologies and raw materials.

APPENDIX B - RAW MEASUREMENTS FROM EXPERIMENTAL CUT MARKS

Tool Type	ID	Surface Area (3-D)	Volume (3-D)	Maximum Depth (3-D)	Mean Depth (3-D)	Maximum Length (3-D)	Maximum Width (3-D)	Maximum Depth (Profile)	Area (Profile)	Width (Profile)	Roughness (Profile)	Angle (Profile)	Radius (Profile)
Quartzite Biface	QBF1_A	4222774.8	1.07E+08	70.7	25.4	10816.8	594.1	61.6	8076.2	260.0	1.9	114.8	179.2
Quartzite Biface	QBF1_B_1	921325.0	2.52E+07	59.3	27.3	6084.1	253.5	64.1	6265.8	220.0	1.7	110.1	126.7
Quartzite Biface	QBF1_B_2	2379674.9	3.53E+07	76.9	14.8	8391.5	499.4	73.7	6196.7	330.0	3.6	144.7	389.8
Quartzite Biface	QBF1_B_3	1199874.9	1.48E+07	48.1	12.4	6022.1	408.7	40.3	6278.0	360.0	1.0	157.0	520.5
Quartzite Biface	QBF1_C	670050.0	7.50E+06	78.1	11.2	13621.2	217.6	79.2	3775.3	205.0	5.3	115.9	147.5
Quartzite Biface	QBF1_D_1	1581574.9	2.12E+07	57.3	13.4	18489.4	434.8	57.2	4564.7	250.0	3.5	139.0	200.0
Quartzite Biface	QBF1_D_2	2777099.8	5.58E+07	73.1	20.1	9044.8	551.4	72.9	10989.7	400.0	2.0	138.0	553.9
Quartzite Biface	QBF1_E	1472299.9	2.90E+07	70.9	19.7	18142.0	501.8	60.4	8599.9	460.0	1.7	157.8	729.4
Quartzite Biface	QBF1_F_1	493800.0	5.25E+06	51.9	10.6	12577.4	223.3	47.8	1728.6	140.0	3.5	116.2	94.7
Quartzite Biface	QBF2_A_1	488900.0	4.38E+06	44.5	9.0	17103.2	283.9	47.2	3675.5	200.0	2.2	110.1	265.9
Quartzite Biface	QBF2_A_2	261075.0	8.64E+06	74.4	33.1	4368.5	324.4	65.6	6525.6	310.0	2.8	137.5	331.6
Quartzite Biface	QBF2_B_1	837050.0	3.12E+07	94.0	37.3	5609.6	331.9	77.8	6622.7	195.0	3.0	103.1	97.8
Quartzite Biface	QBF2_B_2	1157874.9	3.40E+07	85.2	29.4	6097.4	363.2	84.6	10298.7	260.0	2.3	112.2	150.5
Quartzite Biface	QBF2_C_1	593900.0	1.50E+07	70.6	25.2	5270.6	275.4	49.7	3065.5	140.0	1.9	104.4	66.0
Quartzite Biface	QBF2_C_2	2330574.9	5.95E+07	77.0	25.5	16048.5	405.9	67.6	11389.4	390.0	1.7	169.8	310.7
Quartzite Biface	QBF2_D_1	2345899.9	7.41E+07	80.9	31.6	10219.4	511.1	88.1	15936.3	340.0	1.0	125.9	218.0
Quartzite Biface	QBF2_D_2	1168774.9	3.02E+07	71.4	25.8	10589.0	516.9	55.7	5877.6	255.0	2.1	127.6	236.9
Quartzite Biface	QBF2_E_1	1429449.9	3.34E+07	69.4	23.3	10606.2	624.7	51.1	3922.2	260.0	4.3	143.2	275.4
Quartzite Biface	QBF2_E_2	669213.1	2.34E+07	72.7	35.0	4696.4	272.6	63.5	6146.4	250.0	2.4	117.9	160.0
Quartzite Biface	QFB2_E_3	604500.0	1.85E+07	59.5	30.6	4645.8	359.9	48.9	5240.1	270.0	1.8	139.7	248.1
Quartzite Biface	QBF2_F	964125.0	1.56E+07	48.2	16.2	11909.3	271.3	50.6	5295.5	220.0	1.7	130.0	182.9
Quartzite Biface	QBF3_B_1	968700.0	8.36E+06	73.5	8.6	13529.5	290.0	77.5	2970.6	190.0	9.3	111.5	112.4
Quartzite Biface	QBF3_B_2	499200.0	4.68E+06	38.1	9.4	4103.5	298.7	42.2	3535.9	210.0	2.6	143.8	197.1
Quartzite Biface	QBF3_C_1	580875.0	6.19E+06	34.4	10.6	5229.9	293.7	33.9	1765.0	150.0	3.2	132.0	116.4
Quartzite Biface	QBF3_C_2	1204024.9	1.30E+07	72.5	10.8	13485.6	253.4	64.2	2803.4	200.0	5.1	106.8	271.2

Quartzite Flake	QNR1_A_1	826175.0	9.90E+06	52.4	12.0	13821.1	189.8	54.5	4008.9	170.0	3.0	107.4	104.0
Quartzite Flake	QNR1_A_2	392350.0	7.08E+06	113.3	18.0	5304.9	339.3	77.3	6897.0	290.0	4.6	138.5	297.1
Quartzite Flake	QNR1_B_1	416000.0	6.17E+06	67.6	14.8	4452.0	344.8	59.6	4171.9	260.0	4.9	154.5	386.2
Quartzite Flake	QNR1_B_2	160025.0	2.06E+06	35.4	12.9	1689.5	200.0	34.5	1379.1	85.0	0.5	82.9	54.6
Quartzite Flake	QNR1_C	917900.0	2.31E+07	71.8	25.1	5324.5	294.7	77.1	6695.1	195.0	1.2	67.3	89.8
Quartzite Flake	QNR2_A	2204449.9	9.58E+07	106.8	43.4	20965.9	204.3	120.9	4590.5	85.0	6.4	29.1	40.6
Quartzite Flake	QNR2_C	2241824.9	6.53E+07	103.0	29.1	14950.9	335.0	94.9	6049.6	105.0	1.5	51.5	59.5
Quartzite Flake	QNR2_E	1264524.9	5.78E+07	114.3	45.7	6237.8	435.6	114.3	10682.0	260.0	6.4	106.8	134.2
Quartzite Flake	QNR2_F	2918724.9	1.62E+08	162.1	55.6	12080.5	459.6	140.6	11963.6	180.0	3.4	52.9	92.2
Quartzite Flake	QNR2_G	842200.0	4.61E+07	160.5	54.8	8254.4	455.5	140.9	18803.8	360.0	4.8	91.8	141.8
Quartzite Flake	QNR2_H	526950.0	1.95E+07	70.4	37.0	8674.3	137.6	44.3	1420.5	70.0	3.3	44.6	25.8
Quartzite Flake	QNR3_A	446800.0	8.18E+06	63.6	18.3	7852.0	267.0	41.6	4442.9	255.0	2.2	148.2	258.5
Quartzite Flake	QNR3_B	604275.0	1.03E+07	68.1	17.0	6062.7	233.4	64.2	7148.6	220.0	2.3	112.2	120.8
Quartzite Flake	QNR4_A_1	474228.0	3.51E+06	30.0	7.4	6401.7	186.2	31.4	2250.2	170.0	2.3	138.1	253.3
Quartzite Flake	QNR4_A_2	509175.0	9.50E+06	58.7	18.7	3327.1	352.9	55.3	7881.1	340.0	2.6	146.4	801.8
Quartzite Flake	QNR4_B	1674124.9	3.28E+07	70.7	19.6	14787.0	204.4	53.8	5945.5	195.0	2.2	123.4	118.2
Quartzite Flake	QNR4_C_1	998175.0	1.63E+07	51.0	16.3	11728.1	278.5	47.8	3572.2	270.0	1.2	137.4	298.8
Quartzite Flake	QNR4_C_2	1461449.9	2.34E+07	58.4	16.0	11771.3	282.2	52.6	8316.6	270.0	1.6	142.2	244.1
Quartzite Flake	QNR4_C_3	513650.0	7.78E+06	49.1	15.1	5073.4	212.0	48.1	5661.7	210.0	2.0	125.1	162.8
Quartzite Flake	QNR4_D_1	787250.0	1.09E+07	69.3	13.8	5320.1	286.7	53.2	5874.4	200.0	2.1	121.1	120.2
Quartzite Flake	QNR4_D_2	529460.0	7.18E+06	58.6	13.6	6291.8	256.9	39.0	3468.7	190.0	2.5	116.4	188.9
Quartzite Flake	QNR4_E	371100.0	1.12E+07	64.7	16.6	7685.2	235.1	49.2	4326.0	235.0	2.6	140.6	215.2
Quartzite Flake	QNR4_F	830000.0	1.15E+07	47.2	13.8	7316.4	290.5	40.6	4565.9	240.0	1.5	143.2	328.2
Quartzite Flake	QNR4_G	894975.0	1.13E+07	46.5	12.6	7032.7	257.9	45.0	4339.3	250.0	2.7	147.2	245.0
Quartzite Flake	QNR4_H	828500.0	1.43E+07	54.3	17.2	8839.4	225.8	57.7	6995.4	200.0	1.1	119.6	136.7
Basalt Biface	BBF1_A	588100.0	7.05E+06	48.5	12.0	7389.8	475.1	43.5	9627.4	465.0	1.2	152.0	1363.1
Basalt Biface	BBF1_B	632850.0	4.83E+06	32.4	7.6	6411.9	294.9	33.5	1297.4	130.0	2.6	117.6	150.0
Basalt Biface	BBF1_C_1	519150.0	9.02E+06	55.6	17.4	7592.5	500.4	54.0	12224.3	495.0	1.5	157.2	809.0
Basalt Biface	BBF1_C_2	851400.0	1.36E+07	109.2	16.0	13649.6	1311.5	79.8	32115.9	1000.0	1.4	150.6	27140.7
Basalt Biface	BBF1_D_1	593300.0	6.34E+06	39.1	10.7	7366.5	321.1	31.1	4526.9	320.0	1.2	159.8	662.7
Basalt Biface	BBF1_D_2	696425.0	6.20E+06	59.1	8.9	12089.1	381.0	48.7	6200.6	360.0	1.2	154.0	481.8

Basalt Biface	BBF1_E_1	545275.0	6.12E+06	51.1	13.5	7248.8	420.1	41.0	10019.0	420.0	0.7	175.9	19234.1
Basalt Biface	BBF1_E_2	404150.0	4.03E+06	46.5	10.0	7561.6	279.2	39.4	5140.0	220.0	0.5	142.5	182.6
Basalt Biface	BBF1_E_3	147000.0	1.22E+06	31.5	8.3	3807.1	271.3	20.3	1313.4	195.0	1.6	151.9	661.3
Basalt Biface	BBF1_F_1	846047.0	1.16E+07	64.1	13.7	9446.7	492.4	53.5	9109.3	410.0	2.2	148.7	539.2
Basalt Biface	BBF1_F_2	866550.0	1.33E+07	60.7	15.4	9371.8	343.2	52.2	5866.5	270.0	1.8	146.5	289.9
Basalt Biface	BBF1_F_3	230975.0	2.99E+06	60.0	12.9	4699.7	319.9	50.4	9488.1	310.0	1.1	147.7	279.3
Basalt Biface	BBF1_G	762450.0	9.73E+06	61.0	12.8	9003.2	452.8	45.6	8727.2	400.0	0.9	160.7	658.8
Basalt Biface	BBF1_H_1	939700.0	1.85E+07	51.2	19.7	10024.0	280.5	49.0	6508.3	160.0	2.9	110.9	129.1
Basalt Biface	BBF1_H_2	323150.0	4.65E+06	41.9	14.4	2896.0	262.6	36.2	3802.1	250.0	1.9	156.0	363.3
Basalt Biface	BBF1_H_3	606175.0	8.56E+06	40.6	14.1	7392.3	375.9	27.7	3453.4	370.0	1.3	166.6	933.6
Basalt Biface	BBF1_H_4	1499149.9	3.56E+07	91.1	23.7	13264.6	640.3	66.5	21290.5	590.0	0.8	152.6	734.7
Basalt Biface	BBF1_I_1	208725.0	2.78E+06	46.2	13.3	3122.7	164.7	24.8	1393.1	120.0	2.2	107.5	161.3
Basalt Biface	BBF1_I_2	529175.0	1.08E+07	57.8	20.4	7064.1	301.1	40.2	5219.8	265.0	1.5	144.4	243.1
Basalt Biface	BBF1_I_3	640250.0	9.70E+06	47.9	15.2	7773.4	219.9	25.0	2242.0	211.8	0.7	139.8	580.7
Basalt Biface	BBF1_J_1	703275.0	1.60E+07	58.2	22.8	4053.2	275.3	46.8	5612.5	245.0	2.3	139.8	199.1
Basalt Biface	BBF1_J_2	218400.0	4.86E+06	49.8	22.2	2474.1	172.0	61.0	4214.5	145.0	1.9	101.4	69.1
Basalt Biface	BBF1_J_3	484075.0	5.39E+06	53.5	11.1	5773.6	398.2	43.0	7150.1	360.0	1.4	150.0	598.6
Basalt Biface	BBF1_K_1	1024975.0	1.88E+07	65.0	18.4	10093.0	263.2	41.8	2465.3	150.0	2.6	120.2	91.1
Basalt Biface	BBF2_A	1145999.9	1.95E+07	39.1	17.0	9439.3	362.3	37.7	3369.2	280.0	1.6	158.4	769.2
Basalt Biface	BBF2_B	927850.0	1.02E+07	32.4	11.0	4953.2	340.8	32.9	3918.4	280.0	0.9	149.0	967.1
Basalt Biface	BBF3_A	1583049.9	1.03E+07	30.8	6.5	12139.4	289.4	30.5	1452.5	180.0	2.3	157.3	325.4
Basalt Flake	BNR1_A	2589974.9	2.73E+07	50.0	10.5	17067.8	254.1	53.0	2176.7	125.0	2.4	104.4	74.0
Basalt Flake	BNR1_B_1	3304949.9	5.66E+07	76.5	17.1	20371.4	231.1	57.2	4426.0	195.0	2.0	116.0	128.0
Basalt Flake	BNR1_B_2	2534874.9	2.89E+07	46.6	11.4	20490.6	312.1	41.2	6498.6	280.0	1.1	153.5	334.0
Basalt Flake	BNR1_C_1	1366224.9	2.67E+07	62.9	19.6	9390.4	285.3	65.1	7496.5	270.0	1.4	146.0	280.7
Basalt Flake	BNR1_C_2	546850.0	5.57E+06	30.8	10.2	4958.8	254.4	17.2	914.3	105.0	0.7	142.7	106.2
Basalt Flake	BNR1_D	1565524.9	1.56E+07	53.1	10.0	14174.9	425.4	55.8	10383.1	280.0	0.7	148.7	269.9
Basalt Flake	BNR2_A	806200.0	1.50E+07	59.7	18.6	12890.1	206.6	48.2	2999.9	180.0	1.1	126.6	132.1
Basalt Flake	BNR2_B	1139124.9	1.63E+07	51.6	14.3	19883.0	347.2	61.6	5144.2	250.0	2.0	115.9	374.2
Basalt Flake	BNR2_C_1	619675.0	1.12E+07	52.1	18.0	9638.8	186.0	41.6	3044.7	155.0	1.3	125.4	103.0
Basalt Flake	BNR2_D	883850.0	1.15E+07	48.6	13.0	8980.2	232.0	47.2	4773.2	180.0	2.8	107.5	118.1

Basalt Flake	BNR2_E_1	302425.0	3.03E+06	51.1	10.0	8971.1	253.0	38.1	2897.0	195.0	1.8	132.7	357.3
Basalt Flake	BNR2_E_2	632250.0	5.16E+06	50.8	8.2	6051.7	262.1	38.1	3960.2	255.0	0.9	157.2	394.7
Basalt Flake	BNR2_F	1090775.0	1.06E+07	66.6	9.7	6522.5	355.6	56.9	5532.8	240.0	4.1	138.8	209.0
Basalt Flake	BNR3_A_1	3224674.9	3.56E+07	55.1	11.0	23626.3	313.5	63.2	6981.2	300.0	3.0	139.5	322.7
Basalt Flake	BNR3_A_2	548075.0	7.76E+06	46.4	14.2	4240.3	204.3	42.6	4214.4	190.0	2.2	131.7	145.7
Basalt Flake	BNR3_B	2587749.9	3.80E+07	53.3	14.7	24114.3	366.4	47.3	2441.4	150.0	1.8	102.4	87.8
Basalt Flake	BNR3_D	1952024.9	3.00E+07	45.3	15.4	19088.9	362.7	38.8	7637.5	350.0	1.3	158.0	581.1
Basalt Flake	BNR3_E	2262499.9	4.39E+07	59.6	19.4	22382.9	283.1	43.4	5295.3	280.0	1.4	140.1	374.2
Basalt Flake	BNR3_F	2751299.9	3.92E+07	49.6	14.3	27249.4	334.4	38.1	1854.4	185.0	1.9	129.9	550.3
Basalt Flake	BNR3_G_1	877375.0	2.12E+07	100.2	24.2	11693.9	218.8	82.4	4969.2	190.0	5.0	110.6	122.9
Basalt Flake	BNR3_G_2	109675.0	1.72E+06	62.8	15.7	3023.3	91.3	56.0	2191.2	85.0	2.3	67.6	37.0
Basalt Flake	BNR3_H	510125.0	6.78E+06	52.0	13.3	9128.9	167.9	42.1	2544.3	130.0	1.9	106.4	81.1
Basalt Flake	BNR3_I	503225.0	8.26E+06	64.6	16.4	6905.2	168.6	77.8	4072.0	115.0	1.6	62.5	21.1
Basalt Flake	BNR3_J_1	445350.0	9.40E+06	62.2	21.1	6543.2	170.6	53.3	2653.3	105.0	3.6	80.9	55.4
Basalt Flake	BNR3_J_2	404225.0	6.82E+06	55.7	16.9	8763.9	247.8	38.0	816.3	70.0	1.1	77.6	49.7
Basalt Flake	BNR3_K	1603949.9	2.29E+07	52.0	14.3	16219.5	187.5	48.7	3379.6	130.0	1.3	104.8	95.0
Basalt Flake	BNR3_L	745775.0	6.86E+06	51.9	9.2	11641.5	260.7	35.6	6538.2	210.0	2.2	136.6	264.3
Chert Biface	CBF1_A	1183474.9	2.18E+07	42.7	18.4	20541.7	295.6	38.4	2198.7	170.0	1.9	138.0	179.3
Chert Biface	CBF1_F	857775.0	1.38E+07	41.6	16.1	20021.3	440.6	29.7	3007.3	250.0	0.8	157.8	443.2
Chert Biface	CBF1_G	238575.0	3.85E+06	52.7	16.1	3277.3	186.7	43.9	1853.0	140.0	4.3	114.3	107.4
Chert Biface	CBF1_H	416775.0	6.98E+06	52.1	16.7	4373.0	233.0	46.2	3221.2	170.0	2.6	122.1	176.0
Chert Biface	CBF2_A	1113300.0	1.84E+07	75.9	16.6	17207.7	276.3	80.2	7321.7	210.0	2.2	111.7	102.3
Chert Biface	CBF2_B	547900.0	7.13E+06	134.8	13.0	15151.0	283.9	131.6	18064.8	280.0	2.6	89.9	127.6
Chert Biface	CBF2_C	494350.0	6.56E+06	43.2	13.3	5763.8	255.9	36.3	4035.0	250.0	0.9	145.7	308.9
Chert Biface	CBF2_E	1272424.9	2.32E+07	73.3	18.3	16258.5	270.7	68.4	3875.8	240.0	3.5	136.9	222.0
Chert Biface	CBF2_1	189400.0	5.57E+06	78.8	29.4	1387.2	299.2	78.8	4856.1	180.0	4.2	95.7	79.9
Chert Biface	CBF2_2	137200.0	2.31E+06	69.4	16.8	1789.8	206.6	68.9	1718.6	100.0	4.4	73.1	46.5
Chert Biface	CBF2_G	3341749.9	1.37E+08	126.3	41.0	26236.4	501.6	103.3	23527.2	480.0	2.1	113.4	542.4
Chert Biface	CBF2_H	3725974.8	1.65E+08	107.2	44.4	18697.9	691.9	85.8	19560.7	630.0	0.9	148.1	729.9
Chert Biface	CBF2_I	392550.0	7.38E+06	58.2	18.8	4824.2	152.0	50.5	3126.9	145.0	1.8	109.0	71.9
Chert Biface	CBF3_A	579450.0	7.62E+06	42.3	13.1	7787.9	223.3	35.3	2234.7	170.0	2.2	146.7	149.4

Chert Biface	CBF3_B	1017150.0	1.87E+07	47.8	18.4	13226.1	280.3	46.8	4279.8	210.0	1.5	139.0	176.1
Chert Biface	CBF3_C	602025.0	8.67E+06	47.1	14.4	12447.4	293.5	46.3	1085.6	70.0	2.0	78.0	34.2
Chert Biface	CBF3_D	556750.0	1.32E+07	68.0	23.7	6519.7	235.8	55.1	4327.7	200.0	2.3	116.9	135.0
Chert Biface	CBF3_E	82675.0	1.21E+06	44.0	14.6	1179.3	172.2	36.4	2300.3	160.0	1.9	104.1	766.9
Chert Biface	CBF3_G	589625.0	8.28E+06	40.9	14.1	8539.8	227.5	40.9	2997.4	200.0	3.2	151.8	248.5
Chert Biface	CBF3_H	728625.0	1.47E+07	63.8	20.1	11045.4	446.5	47.0	6479.8	380.0	1.7	149.8	382.8
Chert Biface	CBF3_I_1	573200.0	1.96E+07	84.2	34.2	8191.3	596.0	80.9	24017.5	580.0	2.2	126.0	1036.3
Chert Biface	CBF3_I_2	401325.0	1.15E+07	69.5	28.6	4653.8	230.8	57.9	4572.8	230.0	3.1	130.9	173.8
Chert Biface	CBF3_J	481150.0	7.52E+06	47.0	15.6	8291.6	303.0	37.0	928.7	80.0	2.5	89.3	36.9
Chert Biface	CBF3_K	271500.0	3.16E+06	41.3	11.6	4957.4	260.5	38.9	2467.1	190.0	1.2	110.7	3496.4
Chert Biface	CBF3_L	553750.0	8.00E+06	41.0	14.4	9464.3	275.1	33.8	2921.9	230.0	2.7	145.2	535.3
Chert Flake	CNR1_A	1067800.0	1.44E+07	51.8	13.5	13613.8	208.6	55.7	1628.1	130.0	2.3	94.6	238.4
Chert Flake	CNR1_B	772350.0	1.15E+07	56.0	14.9	6969.7	274.4	52.8	1615.7	120.0	4.4	122.3	114.3
Chert Flake	CNR1_C	690100.0	6.88E+06	40.8	10.0	14450.6	275.5	30.6	1083.6	90.0	1.9	104.4	50.8
Chert Flake	CNR1_D	954325.0	1.29E+07	44.2	13.5	15412.7	369.6	34.9	4178.0	360.0	0.9	166.5	881.4
Chert Flake	CNR1_E	610575.0	1.23E+07	66.9	20.2	6930.3	240.7	67.8	5357.7	200.0	2.1	114.1	110.4
Chert Flake	CNR1_F_1	578250.0	1.22E+07	86.4	21.1	9476.8	310.9	70.0	10289.4	280.0	1.4	125.6	208.6
Chert Flake	CNR1_F_2	370125.0	8.65E+06	81.1	23.4	9251.0	470.1	83.4	14872.7	420.0	0.9	133.6	506.7
Chert Flake	CNR2_A_1	712325.0	1.43E+07	59.6	20.1	7922.5	199.8	51.0	4318.4	160.0	2.3	121.5	90.3
Chert Flake	CNR2_A_2	455675.0	9.92E+06	59.8	21.8	6403.6	159.9	63.7	4186.4	140.0	2.7	89.7	59.6
Chert Flake	CNR2_B_1	825975.0	1.78E+07	53.3	21.6	7293.0	301.1	48.4	6233.9	295.0	1.4	146.5	355.8
Chert Flake	CNR2_B_2	571625.0	5.57E+06	30.2	9.7	12634.1	185.3	23.5	1313.2	140.0	1.0	122.1	563.6
Chert Flake	CNR2_C_1	1098125.0	2.54E+07	56.3	23.2	10546.3	516.6	44.6	4672.3	480.0	1.1	158.5	1928.0
Chert Flake	CNR2_C_2	453900.0	5.41E+06	40.8	11.9	9547.3	173.7	31.6	1436.9	100.0	1.3	109.5	61.3
Chert Flake	CNR2_D	861600.0	1.12E+07	40.2	13.0	13151.3	207.4	43.6	3340.2	150.0	1.5	123.7	119.2
Chert Flake	CNR2_E	488050.0	5.11E+06	43.1	10.5	9671.8	345.5	39.6	3631.9	260.0	1.2	134.4	541.5
Chert Flake	CNR2_F	698975.0	1.11E+07	62.9	16.9	12562.9	488.4	61.9	13122.3	450.0	1.4	144.3	938.0
Chert Flake	CNR2_G	431950.0	4.88E+06	44.8	11.3	12246.2	234.6	45.1	3909.9	210.0	2.4	135.3	185.0
Chert Flake	CNR3_A	1222049.9	3.26E+07	66.7	26.7	15276.5	391.0	49.4	9523.1	360.0	0.8	146.2	382.9
Chert Flake	CNR3_B	645525.0	1.16E+07	62.6	20.0	8212.9	155.6	60.8	4648.4	150.0	4.7	107.1	100.9
Chert Flake	CNR3_C	1563924.9	5.29E+07	81.3	33.9	20252.5	319.4	66.4	4507.1	150.0	5.9	98.9	71.3

Chert Flake	CNR3_D_1	917050.0	4.00E+07	123.2	43.6	13559.3	201.8	90.6	6439.8	160.0	4.6	88.9	72.5
Chert Flake	CNR3_D_2	213850.0	5.49E+06	64.3	25.7	4261.5	182.9	45.2	2026.9	110.0	1.5	82.3	53.5
Chert Flake	CNR3_E	1020650.0	4.33E+07	118.4	42.4	12950.7	266.3	91.8	7822.1	255.0	1.8	106.9	181.2
Chert Flake	CNR3_F	1852399.9	6.26E+07	100.2	33.8	15995.9	439.1	91.6	5728.0	160.0	3.0	87.5	71.4
Chert Flake	CNR3_G	1098900.0	4.54E+07	100.2	41.3	13389.9	343.4	75.5	6982.5	300.0	1.5	117.3	430.2
Chert Flake	CNR3_H	401275.0	7.50E+06	52.1	18.7	6913.4	177.7	45.7	1708.6	100.0	3.3	100.3	60.3
Phonolite Biface	PBF1_A	1555499.9	3.17E+07	52.2	20.4	11151.0	282.1	55.0	6846.3	260.0	1.4	139.1	252.1
Phonolite Biface	PBF1_B_1	1231899.9	1.92E+07	56.7	15.6	10612.6	314.4	40.6	3523.0	210.0	1.7	142.9	246.1
Phonolite Biface	PBF1_B_2	116775.0	2.10E+06	46.1	18.0	1834.3	180.5	33.3	1678.3	100.0	1.8	115.0	73.2
Phonolite Biface	PBF1_C	1928199.9	3.07E+07	43.2	15.9	13240.4	245.4	39.0	4411.8	230.0	1.0	158.4	287.1
Phonolite Biface	PBF1_D	1678374.9	2.80E+07	64.8	16.7	12134.2	665.4	63.4	19363.4	640.0	1.8	163.0	1209.2
Phonolite Biface	PBF1_E	1415899.9	2.79E+07	46.6	19.7	9450.5	283.9	50.1	2821.0	110.0	1.8	94.6	50.1
Phonolite Biface	PBF1_H	423975.0	1.14E+07	69.2	26.8	6371.2	255.4	55.3	3438.8	190.0	2.6	126.2	159.2
Phonolite Biface	PBF1_I	977725.0	1.29E+07	44.6	13.2	7109.8	401.6	39.4	4512.0	380.0	0.9	162.7	1013.8
Phonolite Biface	PBF1_J	1090400.0	2.10E+07	64.2	19.3	8318.9	412.3	58.1	10048.8	380.0	2.4	150.6	421.3
Phonolite Biface	PBF1_K	875600.0	1.76E+07	52.7	20.1	5895.8	447.7	41.4	7298.4	400.0	0.8	158.9	689.1
Phonolite Biface	PBF1_L_1	1314724.9	1.82E+07	55.7	13.8	16051.5	464.1	50.0	7079.3	420.0	1.0	160.5	770.0
Phonolite Biface	PBF1_L_2	497325.0	5.15E+06	42.8	10.4	8994.1	251.0	38.8	4884.5	240.0	0.6	140.0	225.0
Phonolite Biface	PBF1_L_3	121425.0	2.24E+06	53.7	18.4	1195.2	171.6	54.6	3861.2	170.0	2.0	115.1	108.8
Phonolite Biface	PBF2_A	826250.0	1.02E+07	46.5	12.3	9566.3	280.5	38.7	4672.9	280.0	1.3	157.5	394.6
Phonolite Biface	PBF2_B_1	806825.0	1.29E+07	45.3	16.0	5606.2	269.1	43.0	3505.5	170.0	1.5	142.5	152.7
Phonolite Biface	PBF2_B_2	900125.0	1.30E+07	69.6	14.5	9668.3	360.9	57.8	5111.7	230.0	3.2	136.1	222.3
Phonolite Biface	PBF2_B_3	283350.0	6.36E+06	54.0	22.5	2114.5	228.5	50.7	5622.8	200.0	0.9	116.2	140.0
Phonolite Biface	PBF2_C_1	447875.0	4.98E+06	44.6	11.1	7435.7	218.9	33.5	2617.1	180.0	1.8	140.8	150.2
Phonolite Biface	PBF2_C_2	523725.0	5.78E+06	43.6	11.0	8823.6	195.3	36.7	1913.8	160.0	2.0	129.4	765.1
Phonolite Biface	PBF2_D	713725.0	1.93E+07	61.9	27.0	5134.8	321.5	62.9	6666.5	210.0	2.4	112.0	110.3
Phonolite Biface	PBF2_E_1	1095322.0	2.44E+07	67.7	22.2	5637.4	609.2	57.3	15414.3	590.0	1.6	163.1	1145.2
Phonolite Biface	PBF2_E_2	686125.0	1.96E+07	66.1	28.6	5147.3	387.1	51.9	8052.9	300.0	3.5	154.6	387.0
Phonolite Biface	PBF2_F	2030099.9	3.94E+07	49.3	19.4	9634.6	566.6	42.6	2773.1	180.0	2.5	134.8	180.8
Phonolite Biface	PBF2_G_1	1574099.9	2.90E+07	77.1	18.4	13091.2	434.2	66.9	5901.8	270.0	3.3	139.4	333.7
Phonolite Biface	PBF2_G_2	381625.0	6.91E+06	55.4	18.1	3683.4	337.2	40.4	4866.1	280.0	2.0	132.4	577.5

Phonolite Flake	PNR1_A_1	898875.0	9.23E+06	69.7	10.3	10620.5	203.3	52.3	2543.2	110.0	2.4	90.0	54.2
Phonolite Flake	PNR1_A_2	521625.0	8.18E+06	51.5	15.7	6364.7	229.6	51.8	2077.5	90.0	3.4	82.6	36.2
Phonolite Flake	PNR1_B	583750.0	8.47E+06	45.7	14.5	6981.0	208.5	37.9	2602.3	170.0	1.4	112.3	230.0
Phonolite Flake	PNR1_C_1	1920199.9	3.35E+07	45.1	17.4	15958.2	392.8	43.8	5907.5	330.0	1.0	152.8	792.9
Phonolite Flake	PNR1_C_2	665075.0	7.92E+06	38.1	11.9	8816.3	299.5	37.2	2738.7	170.0	2.1	146.0	160.9
Phonolite Flake	PNR1_D	1373674.9	2.49E+07	69.2	18.1	15391.7	284.7	54.9	3018.2	200.0	3.2	139.4	200.1
Phonolite Flake	PNR1_E_1	2643924.9	4.61E+07	75.1	17.4	20222.6	239.6	66.6	2761.6	140.0	3.2	92.3	85.2
Phonolite Flake	PNR1_E_2	186075.0	2.44E+06	32.3	13.1	3470.7	175.0	32.1	2097.8	170.0	1.5	149.2	201.6
Phonolite Flake	PNR1_G_1	732075.0	1.06E+07	32.9	14.4	6307.8	237.0	28.9	2339.3	200.0	1.0	158.5	371.4
Phonolite Flake	PNR1_G_2	1360299.9	1.46E+07	76.0	10.8	14449.7	419.3	70.2	8542.7	410.0	2.3	149.0	860.4
Phonolite Flake	PNR1_H	1484399.9	1.90E+07	40.0	12.8	13288.7	218.8	38.4	1465.2	130.0	1.1	98.8	246.0
Phonolite Flake	PNR2_C	1570849.9	3.41E+07	97.6	21.7	10854.1	364.7	79.9	4256.2	150.0	2.4	76.7	106.1
Phonolite Flake	PNR2_D_1	982900.0	1.75E+07	63.2	17.8	5786.3	356.0	56.9	7399.8	350.0	1.2	139.2	385.2
Phonolite Flake	PNR2_D_2	339525.0	4.10E+06	41.3	12.1	4423.3	140.0	39.6	1951.6	110.0	1.3	110.8	76.1
Phonolite Flake	PNR2_F	1063525.0	2.27E+07	76.4	21.3	11405.0	235.6	49.1	5264.4	180.0	1.6	108.7	129.0
Phonolite Flake	PNR2_H	686525.0	1.56E+07	69.8	22.7	6522.7	251.2	46.9	3332.2	140.0	2.6	110.7	70.4
Phonolite Flake	PNR3_A	3138124.9	5.27E+07	58.8	16.8	19082.0	300.9	54.7	3907.5	200.0	2.6	137.8	222.6
Phonolite Flake	PNR3_B_1	1189974.9	1.86E+07	47.2	15.6	14777.1	370.4	46.5	4132.6	190.0	3.4	133.1	163.2
Phonolite Flake	PNR3_B_2	975150.0	1.87E+07	51.7	19.2	15709.7	249.6	37.0	1660.4	130.0	2.4	128.5	104.5
Phonolite Flake	PNR3_C	1452649.9	2.32E+07	58.9	16.0	18029.5	312.4	52.2	4728.6	280.0	2.0	139.8	443.9
Phonolite Flake	PNR3_E	1210424.9	1.74E+07	86.5	14.4	17011.6	202.7	90.8	3798.5	110.0	10.4	61.2	45.4
Phonolite Flake	PNR3_F	1178624.9	1.36E+07	79.4	11.5	15460.4	215.9	81.9	3024.5	150.0	3.5	97.8	84.0
Phonolite Flake	PNR3_G	577050.0	1.05E+07	51.5	18.2	7159.8	196.2	38.3	2285.4	190.0	2.4	114.5	552.9
Phonolite Flake	PNR3_H	534450.0	7.93E+06	63.7	14.8	8369.3	199.8	55.3	3307.8	180.0	3.7	111.1	159.5
Phonolite Flake	PNR3_I	1561699.9	3.55E+07	66.6	22.7	11851.2	325.5	57.5	4243.6	280.0	2.0	157.1	670.6

APPENDIX C - MEASUREMENTS FROM RAW ARCHAEOLOGICAL CUT MARKS

ID	Surface Area (3-D)	Volume (3-D)	Maximum Depth (3-D)	Mean Depth (3-D)	Maximum Length (3-D)	Maximum Width (3-D)	Maximum Depth (Profile)	Area (Profile)	Width (Profile)	Roughness (Profile)	Angle (Profile)	Radius (Profile)
T5_L10_119	2965474.9	1.31E+08	110.6	44.3	9396.9	330.9	81.7	15270.1	320.0	1.6	124.0	215.7
T5_L10_928_A	250675.0	3.97E+06	60.1	15.8	3947.6	213.0	56.1	4795.7	180.0	2.2	123.8	111.9
T5_L10_928_B	394225.0	5.67E+06	55.3	14.4	3765.2	361.3	43.6	5356.6	230.0	2.1	148.9	247.0
T5_L10_952_A	6484574.7	5.75E+08	235.0	88.7	16243.3	602.9	143.7	25044.5	300.0	2.4	83.3	149.3
T5_L10_952_B	7491649.7	9.23E+08	344.3	123.3	16578.9	932.9	294.9	109625.4	700.0	3.2	102.3	855.7
T5_L10_1062	1968624.9	4.01E+07	90.3	20.4	10697.5	684.2	80.2	10608.2	310.0	2.8	121.6	299.2
T5_L10_1300	1322424.9	5.44E+07	95.0	41.2	7176.7	441.1	88.3	16793.0	370.0	2.9	125.3	328.7
T5_L10_1418	3397774.8	1.98E+08	193.7	58.2	11860.8	410.0	131.5	21749.4	350.0	5.1	99.4	262.8
T5_L10_1601	1356374.9	9.06E+07	142.7	66.8	5541.1	604.0	154.9	42187.3	600.0	2.4	110.5	530.6
T5_L10_1751	3051774.9	1.06E+08	74.2	34.6	8447.6	713.6	75.0	29773.2	620.0	1.6	153.7	767.4
T5_L10_2135_A	692475.0	5.37E+06	32.1	7.8	11568.5	207.0	30.6	3071.9	200.0	1.6	151.9	228.8
T5_L10_2135_B	1191749.9	1.74E+07	45.6	14.6	19307.5	197.8	46.4	2586.1	130.0	3.2	122.4	78.1
T5_L10_2135_C	384425.0	3.11E+06	37.8	8.1	5657.9	257.8	34.1	1803.8	110.0	2.4	119.0	81.6
T5_L10_2135_D	629900.0	6.28E+06	36.4	10.0	7417.1	354.6	36.9	2900.6	190.0	1.2	114.3	318.1
T5_L10_2226_A	1479374.9	4.96E+07	89.4	33.5	6085.7	501.1	83.8	17221.0	420.0	1.9	132.9	338.9
T5_L10_2226_B	1287549.9	6.49E+07	123.8	50.4	5925.6	413.2	119.0	17839.2	350.0	2.7	99.8	177.1
T5_L10_2537	4378524.8	1.30E+08	82.8	29.6	13882.0	515.2	42.3	2773.3	100.0	2.6	93.3	53.3
T5_L10_2784_A	5061899.8	3.40E+08	198.3	67.1	15026.9	1025.7	184.2	69503.2	930.0	2.6	105.8	1197.6
T5_L10_2784_B	1009700.0	2.88E+07	124.2	28.5	6823.2	538.5	122.1	3829.7	100.0	11.0	39.7	N/A
T5_L10_3025_A	2572074.9	9.65E+07	127.9	37.5	19385.1	490.4	75.1	11970.3	280.0	2.3	137.9	245.1
T5_L10_3025_B	1178949.9	3.78E+07	85.6	32.0	8404.7	252.2	65.5	6017.6	180.0	3.5	106.2	91.6
T5_L10_3132	1495749.9	4.33E+07	72.7	29.0	5398.4	475.1	72.7	18971.5	460.0	2.7	154.3	533.7

APPENDIX D – MISCLASSIFIED CUT MARK DATA POINTS BY QUADRATIC DISCRIMINANT MODEL

Cut Mark ID	Tool Technology	Raw Material	Tool Technology and Raw Material	Quartzite Tools	Basalt Tools	Chert Tools	Phonolite Tools	Biface Tools	Flake Tools	Count
QBF1_D_1		M								**1**
QBF1_E		M								**1**
QBF2_A_1		M								**1**
QBF2_B_1	M									**1**
QBF2_C_1	M									**1**
QBF2_C_2		M								**1**
QBF2_D_2		M								**1**
QBF3_C_1		M								**1**
QBF3_C_2		M								**1**
QNR3_B		M								**1**
QNR4_C_3		M								**1**
QNR4_D_1		M								**1**
QNR4_G	M									**1**
BBF1_E_2	M									**1**
BBF1_H_1	M									**1**
BBF1_H_2		M								**1**
BBF1_I_2		M								**1**
BBF1_I_3	M									**1**
BBF1_K_1	M									**1**
BBF2_B		M								**1**
BNR1_C_1	M									**1**
BNR2_A		M								**1**
BNR2_E_1	M									**1**
BNR2_F		M								**1**

BNR3_A_1		M								**1**
BNR3_G_1		M								**1**
BNR3_J_2		M								**1**
CBF1_A	M									**1**
CBF2_A	M									**1**
CBF2_B		M								**1**
CBF2_G	M									**1**
CBF3_C	M									**1**
CNR1_A		M								**1**
CNR1_D	M									**1**
CNR1_E			M							**1**
CNR1_F_2	M									**1**
CNR2_A_1		M								**1**
CNR2_D		M								**1**
CNR2_E	M									**1**
CNR2_F	M									**1**
CNR2_G	M									**1**
CNR3_A	M									**1**
CNR3_D_1		M								**1**
CNR3_F		M								**1**
PBF1_I	M									**1**
PBF1_L_1		M								**1**
PBF1_L_3		M								**1**
PBF2_B_2	M									**1**
PBF2_C_2		M								**1**
PBF2_E_2	M									**1**
PNR1_C_2	M									**1**
PNR1_G_1	M									**1**
PNR1_G_2	M									**1**
PNR2_C		M								**1**
PNR3_B_2		M								**1**
PNR3_G	M									**1**

QBF2_A_2	M	M								**2**
QBF2_F	M	M								**2**
QNR2_H			M						M	**2**
BBF1_J_2			M					M		**2**
BBF2_A		M	M							**2**
BNR3_A_2			M						M	**2**
BNR3_K			M						M	**2**
CBF3_G		M	M							**2**
CNR1_F_1	M	M								**2**
CNR3_H			M						M	**2**
PBF1_L_2	M	M								**2**
PNR1_E_1			M						M	**2**
QBF3_B_2		M	M					M		**3**
QNR3_A	M	M	M							**3**
QNR4_A_2	M	M	M							**3**
QNR4_B		M	M						M	**3**
QNR4_C_1		M	M						M	**3**
QNR4_C_2		M	M						M	**3**
QNR4_D_2	M	M	M							**3**
BBF1_F_1		M	M					M		**3**
BBF1_F_2		M	M					M		**3**
BBF1_J_1		M	M					M		**3**
BNR2_C_1		M	M						M	**3**
BNR3_H		M	M						M	**3**
BNR3_J_1		M	M						M	**3**
CBF1_H		M	M					M		**3**
CBF2_E	M	M	M							**3**
CBF2_I	M		M			M				**3**
CBF3_D	M		M			M				**3**
CBF3_I_2	M		M					M		**3**
CNR2_A_2		M	M						M	**3**
CNR3_D_2		M	M						M	**3**

PBF2_D		M	M					M		**3**
PBF2_G_1	M		M				M			**3**
PNR2_D_1	M		M						M	**3**
PNR2_F		M	M						M	**3**
QNR4_F	M	M	M						M	**4**
CBF2_C		M	M			M		M		**4**
CNR2_B_1	M	M	M			M				**4**
PBF1_B_1	M		M				M	M		**4**
PBF1_H	M	M	M					M		**4**
PBF2_C_1	M	M	M					M		**4**